The Thesis Committee for Fei Ho
Certifies that this is the approved version of the following thesis:

The use of a pH-triggered polymer gelant to seal cement fractures in wells

APPROVED BY
SUPERVISING COMMITTEE:

Supervisor: _____
Matthew T. Balhoff

Co-Supervisor: _____
Chun Huh

The use of a pH-triggered polymer gelant to seal cement fractures in wells

by

Fei Ho, B.S.

Thesis

Presented to the Faculty of the Graduate School of

The University of Texas at Austin

in Partial Fulfillment

of the Requirements

for the Degree of

Master of Science in Engineering

The University of Texas at Austin

December 2015

Dedication

To my family, my friends, and my cats.

Acknowledgements

Foremost, I cannot express enough gratitude to my supervisor Dr. Matthew Balhoff for his continuous guidance and support. His motivation has helped me grasp many opportunities to present and publish my research during my graduate studies. I could not have had the invaluable experience and have completed my thesis without his patience and encouragement.

I would also like to express my sincere gratitude to Dr. Chun Huh for his invaluable advice and encouragement throughout my graduate studies. Special thanks must be given to Dr. Steven Bryant for his insight and immense knowledge that had brought me to this research project. Special thanks must also go to Dr. Paul Bommer for his vast experience in oilfield operations and practical approach in solving problems. Thanks must also be given to Dr. Quoc Nguyen for his generosity in lending me a Hassler coreholder which allowed me to produce some of my best experiments.

In addition, I want to thank my research teammates, James Patterson, for teaching me everything he knew; Mohammadreza Shafiei, for always providing me with up-to-date rheology data; and Shayan Tavassoli, for useful materials and recommendations. Also, thanks to Dr. Ijung Kim for sharing his CO_2 equipment and always being helpful. And, thanks to Pengpeng Qi for letting me borrow his pressure transducers.

Thanks to Glen Baum for finding me equipment and helping me set up my experiments; and to Gary Miscoe for preparing numerous cement cores during my research. Thanks to all my undergraduate assistants, Paulami Das, Lucas Mejia, and Valeriy Shakenov, who helped run many experiments. And special thanks to Nicholas Lavender, who has supported me through everything.

This research was funded by the Department of Energy (grant DE-FE0009299 "AREA 2: Novel Materials for Robust Repair of Leaky Wellbores in CO2 Storage Formations").

Abstract

The use of a pH-triggered polymer gelant to seal cement fractures in wells

Fei Ho, M.S.E.

The University of Texas at Austin, 2015

Supervisor: Matthew T. Balhoff

Co-Supervisor: Chun Huh

The potential leakage of hydrocarbon fluids or CO_2 out of subsurface formations through wells with fractured cement or debonded microannuli is a primary concern in oil and gas production and CO_2 storage. A novel application using pH-sensitive microgel dispersion is introduced as a solution to remediation workovers using oilfield cement, which often fails to provide effective seal in smaller fractures. The application is based on the reaction of a low-pH poly(acrylic acid) polymer that can develop substantial yield stress when passing through strongly alkaline cement fractures. While the pH–trigger mechanism and rheology show promising results, an unexpected phenomenon, known as polymer syneresis, produced a byproduct that was proven to compromise the seal of the injected gel in place.

This study focuses on understanding the development of polymer viscosity and identifying the main components of syneresis. Several chemicals were studied to inhibit syneresis and tested as either polymer additives or cement pre-treatment in cement

fracture corefloods. The chemical inhibitors and its applications were then selected based on not only their ability to eliminate syneresis, but also their reaction with polymer during injection and subsequent development of gel yield stress in cement fractures. Cores pre-treated with a chelating agent, known as sodium triphosphate ($Na_5P_3O_{10}$), showed good injectivity during polymer placement and significant improved sealing performance during water breakthrough tests.

The resulting gel-in-place provided longer periods of effective seal and held pressure gradients orders of magnitude higher than just a few psi/ft from gel placed in un-treated cores. Furthermore, the comparison of holdback pressure gradients between designed corefloods indicated improvement in gel strength as fracture aperture is decreased and polymer shut-in time is increased. With proper cement pretreatment, the pH-triggered polymer-gel system has been seen to effectively plug small fractures and have valuable applications for long-term robust seal in leaky wellbores.

Table of Contents

List of Tables

List of Figures

Chapter 1: Introduction and Literature Review[1]

The potential leakage of hydrocarbon fluids or CO_2 out of subsurface formations through wells with fractured cement or debonded microannuli is a primary concern in oil and gas production and CO_2 storage. Typically, these leaky wells are subjected to remediation workovers using conventional oilfield cement, yet leakage pathways with small apertures are often difficult to repair with the existing technology. Therefore, a sealant that can be placed into these fractures easily while providing a long-term robust seal is desired. The use of inexpensive, pH-triggered polymer sealants could potentially be the solution to plugging these fractures.

The application is based on the transport and reaction of a low-pH poly(acrylic acid) polymer through strongly alkaline cement fractures. pH-sensitive microgels viscosify upon neutralization with cement to become highly swollen gels with substantial yield stress that can block fluid flow. Although the pH-triggered gelling mechanism and rheology measurements of the polymer gel show promising results, previous experiments in a cement fracture have found that the polymer solution undergoes a reaction caused by the release of calcium cation from cement that collapses the polymer network; an effect known as "syneresis" in chemistry. The syneresis produces an undesirable calcium-

[1] Ho, J.F., Patterson, J.W., Tavassoli, S., Shafiei, M., Balhoff, M.T., Huh, C., Bommer, P.M., and Bryant, S.L., 2015. The use of a pH-triggered polymer gelant to seal cement fractures in wells. Presented at the Society of Petroleum Engineers (SPE) Annual Technical Conference and Exhibition (ATCE), Houston, Texas, U.S.A., 28-30 September. SPE-174940-MS

Contributions: J.F.Ho and J.W.Patterson were involved in the design and performance of laboratory experiments. M.Shafiei was involved in the acquisition of rheological data. J.F.Ho, J.W.Patterson, M.T.Balhoff, C.Huh, P.M.Bommer, and S.L.Bryant were involved in the conception and analysis of the work. J.F.Ho, J.W.Patterson, and S.Tavassoli were involved in the drafting and revision of the manuscript.

precipitation byproduct that is detrimental to the strength and stability of the gel in place. As a result, gel-sealed leakage pathways that are subjected to various degrees of syneresis often fail to holdback pressure.

A key challenge for the polymer application focuses on the removal of the calcium content in existing cement to inhibit syneresis. Multiple chemicals are investigated and tested for pre-treatment of cement cores to remove calcium from the cement surface zone before polymer placement. A desirable pre-treatment procedure could successfully eliminate syneresis without compromising the injectivity of polymer solution during placement. The performance of pH-triggered polymer gel in cement, in the absence of calcium, can then be determined by measuring the resistance of gel-in-place during a liquid breakthrough test.

1.1 CARBON CAPTURE & STORAGE (CCS)

Carbon dioxide (CO_2) is a primary greenhouse gas (GHG) naturally present in the atmosphere. Like other greenhouse gases, CO_2 is a heat-trapping gas that has the ability to absorb part of the solar energy reaching Earth's surface and maintain global temperature. The concentration of CO_2 in the atmosphere has been primarily controlled by the rate of the Earth's carbon cycle in which CO_2 is emitted to the atmosphere through natural sources and recycled back to the Earth through geological processes. However, CO_2 concentrations in the atmosphere have increased nearly 30% due to human activities since the industrial revolution (NRC, 2010). Some of the major sources of human-related CO_2 emission include the combustion of fossil fuels for electricity and transportation, and certain processes in cement and steel industries. These activities contribute to the overload of carbon dioxide in the atmosphere.

Carbon dioxide capture and storage (CCS) is considered as one of the options for reducing CO_2 emissions from human activities, specifically targeting stationary industrial-scale emissions, by capturing and storing anthropogenic CO_2 in underground geological formations. The technologies of CCS can be categorized into three sequential processes: (1) capture of CO_2 from power plants or industrial processes, (2) transport of captured and compressed CO_2, and (3) injection/geological storage of CO_2 in subsurface formations (EPA, 2012). Much research in recent years has focused on improving CO_2 capture and separation. As a result, power plants equipped with CCS system using available technology can eliminate about 90% of its CO_2 emissions (IPCC, 2005).

The focus of this research is on the third process in which CO_2 is stored in underground geological formations. The storage system requires a physical trapping mechanism, overlying formation with low permeability, to prevent the injected CO_2 from migrating to the surface. These geological systems can be found in the following:

- *Deep saline formations*: non-potable saline water-bearing formation is usually sealed by a caprock that can be used for permanent storage.
- *Coal-bed methane:* CO_2 can exchange with methane and bind to coal when injected into coalbeds where will be stored permanently. This type of storage is said to be in research phase in which there are no operational projects.
- *Application of CO_2 in enhanced oil recovery:* EOR procedure that involves injecting CO_2 to increase oil production from mature oil fields.
- *Depleted oil and gas reservoirs* that are no longer economic for oil or gas production, but have established trapping and storage characteristics.

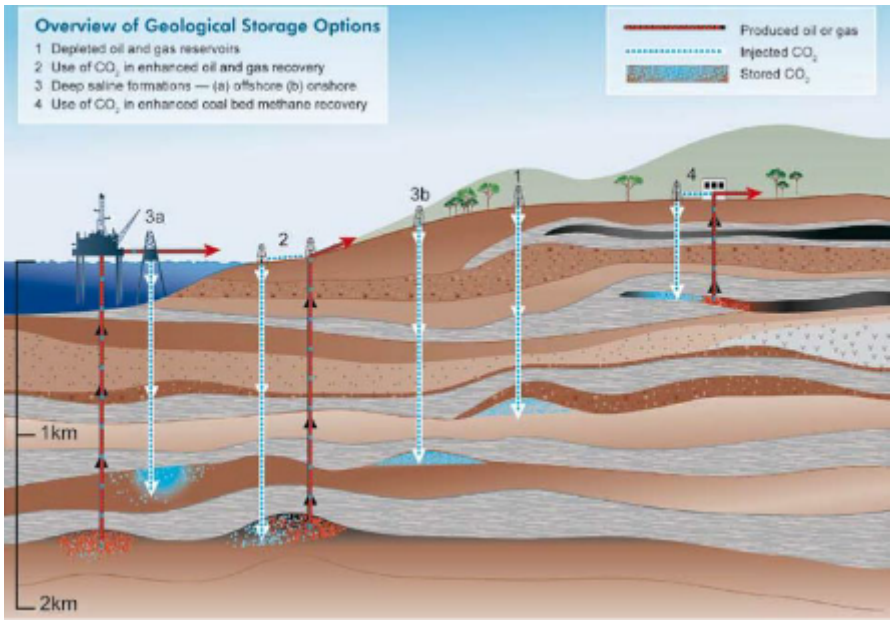

Figure 1.1: Options for storing CO_2 in deep underground geological formations (IPCC, 2005)

Figure 1.1 illustrates the various geological storage options. Of the above options, depleted hydrocarbon reservoirs and deep saline formations with sedimentary basins are considered the most ideal candidates for storage due to the abundant knowledge of the existing reservoirs, and the depth and high concentrations in dissolved solids of saline formations (Bruant et al., 2002). Sealing efficiency of the trapping barrier and of the wellbore cement plays a major role in determining the overall effectiveness of geological CO_2 storage projects. When successfully sealed and stored, some supercritical CO_2 will dissolve into the formation brine or precipitate as carbonate minerals as shown in Figure 1.2. These processes are known to further enhance the security of geological CO_2 storage (Bruant et al., 2002).

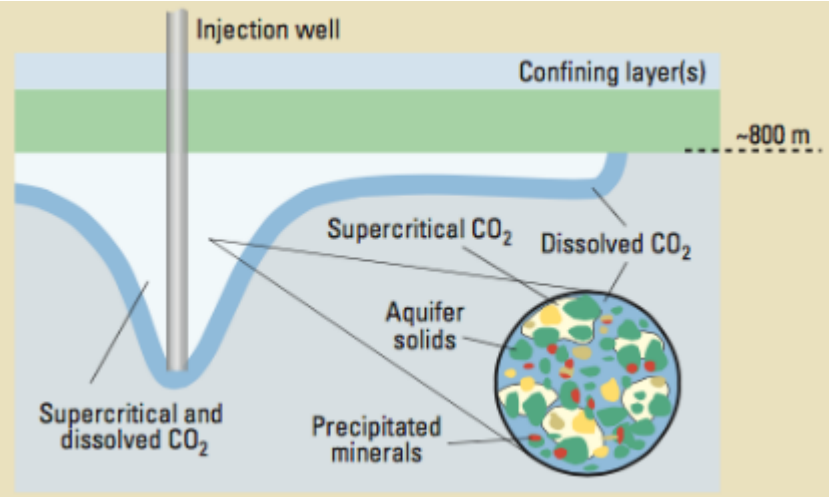

Figure 1.2: CO_2 is injected as a supercritical fluid, some of which dissolves in the brine and some of which is trapped in precipitated mineral phases (Bruant et al., 2002).

The long-term containment of carbon dioxide, in terms of geological time, is crucial to the success of these projects. Many studies have offered useful estimates to evaluate the performance of current storage technologies. The commonly accepted proposal suggested that the fraction of CO_2 retained should be at least 90-99% over 100 years, or 60-95% over 500 years for mitigation to be deemed successful (IPCC, 2005). Another study suggested that leakage rates below 0.01%/year, meaning 99% retention rate over 100 years, would meet the requirement of geological CO_2 storage (Hepple and Benson, 2002). However, more work is needed to establish a baseline for CO_2 retention to ensure long-term security, as on going monitoring is required throughout the project life.

1.2 CO_2 Leakage Conditions

It is recommended to store CO_2 at depths greater than 2600 ft where it will be in supercritical state, which can be maintained because many suitable storage systems are known to be at depths up to 6500-9800 ft (IPCC, 2005). Typical geological storage

conditions can be estimated at 4300 psi and 100-150°C under normal pressure and temperature gradients. The pressure in storage formations can be assumed to be near hydrostatic condition at pressure gradients of 0.433-0.465 psi/ft. In-situ CO_2 storage pressure can be estimated by:

$$P_{storage} = \rho g_{hydrostatic} \cdot D, \tag{1.1}$$

where $P_{storage}$ is the CO_2 pressure in the storage formation $\varrho g_{hydrostatic}$ is the hydrostatic pressure gradient, and D is the depth of the storage formation. The CO_2 storage temperature can be estimated by:

$$T_{storage} = \alpha_T \cdot D, \tag{1.2}$$

where $T_{storage}$ is the CO_2 temperature in the storage formation, and α_T is the geothermal gradient which is typically 0.015 °F/ft.

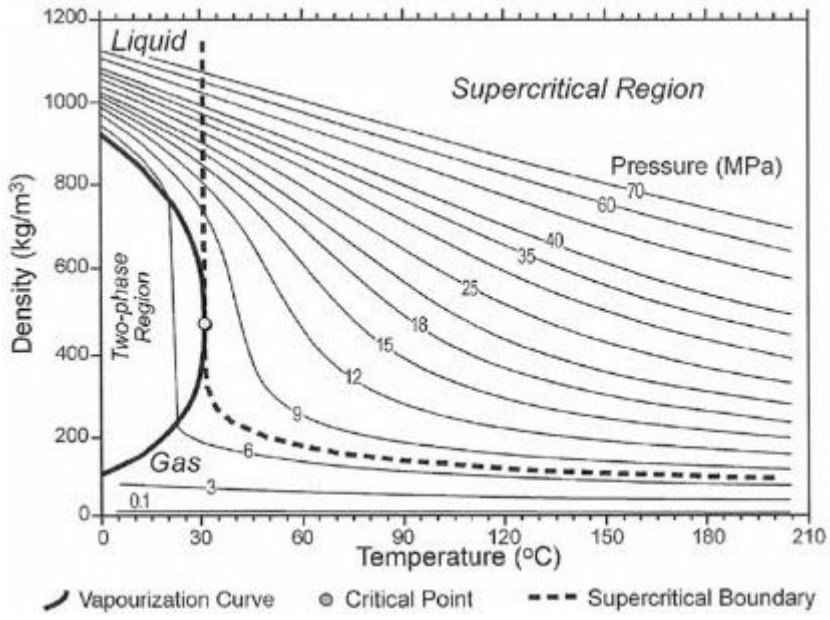

Figure 1.3: Variation of CO_2 density as a function of temperature and pressure (IPCC, 2005).

The density of stored supercritical CO_2 can be estimated using Figure 1.3. For storage wells that have developed leakage pathways, the density difference in CO_2 and brine could result in buoyant forces that will drive the stored CO_2 upwards into shallower formations, aquifers, or the surface. Thus the CO_2 leakage pressure gradient due to buoyancy can be calculated by equation 1.3,

$$\nabla P_{CO_2} = \rho_{CO_2} \cdot g \,, \tag{1.3}$$

where ∇P_{CO2} is the CO_2 leakage pressure gradient, ϱ_{CO2} is the density of CO_2., and g is the gravitational constant.

The buoyant forces of a rising CO_2 plume can result in a leakage pressure gradient between 0.2 psi/ft to 0.4 psi/ft depending on the storage depth. Even during the CO_2 injection process, leakage pressure gradient is expected to be in the order of only 1.0-10 psi/ft. Because pressure increase within a CO_2 storage reservoir during injection is

unlikely to exceed ~1000 psi above hydrostatic, and that the thickness of the caprock is usually required to be at least 10-100 ft. Therefore, sealant material that can hold back just a few psi/ft of pressure gradient is sufficient to stop CO_2 and fluids from flowing in the vertical direction along the wellbore.

1.3 WELLBORE INTEGRITY

Wellbore integrity can be defined as the ability of the wellbore cement to maintain isolation between permeable reservoirs and impermeable layers in geological formations. Wellbore cement often develops leaks during the life of the well if not properly completed and abandoned (Watson and Bachu, 2009). When wellbore integrity is compromised, leakage occurs and pressurized fluids are allowed to migrate vertically to the surface. Leakage of gases and hydrocarbon fluids through wellbore cement can occur during drilling, hydraulic fracturing, production, or after abandonment that may endanger the health and safety of field workers and our environment (Davies et al., 2014). Specifically, the highest probabilities of leakage are associated with decommissioned wellbores in comparison to wells associated with producing or injecting.

The potential leakage of fluids along the interface between a wellbore and earth formations is a primary concern in hydrocarbon recovery (Dusseault et al., 2000) and carbon sequestration (van der Tuuk Opedal et al., 2013). Leakage pathways in the cement annulus can be generated due to either mechanical well failures from cyclic pressure and temperature changes, or chemical degradation from formation fluids (Zhang and Bachu, 2010). In the case of anthropogenic carbon dioxide storage, CO_2 plumes can potentially leak through the fractures developed in the cement or debonded microannuli formed between cement and surrounding materials (Watson et al., 2007). Figure 1.4 is an

illustration of the leakage problem commonly seen in old cement wellbores and a remedial procedure using the pH-triggered polymer gel.

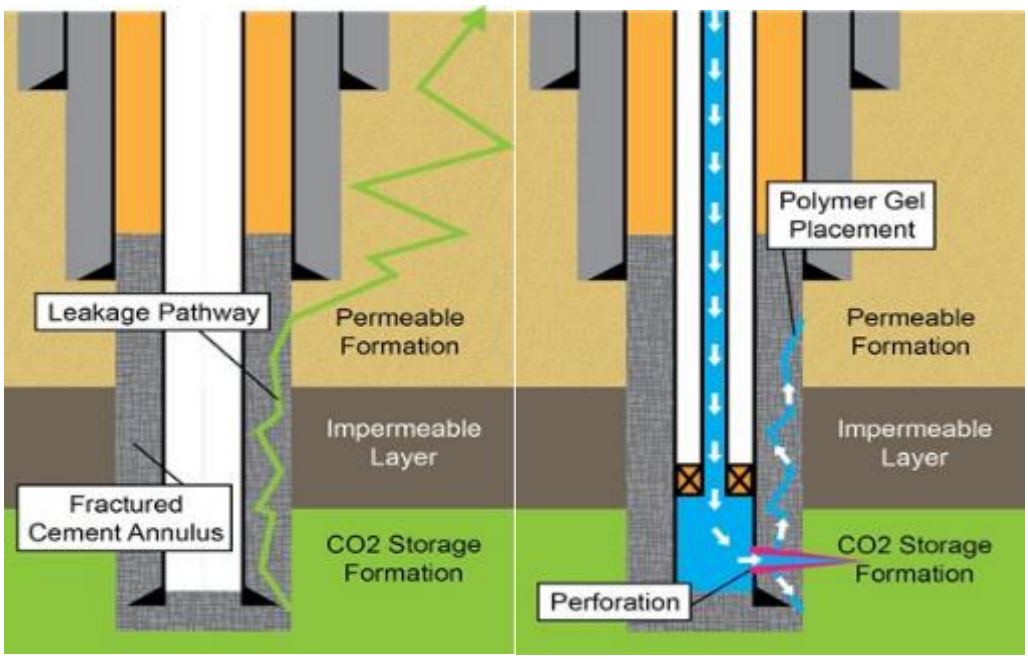

Figure 1.4: Leakage pathway in fractured cement annulus (left) and polymer gel placement through perforation to seal leakage (right).

1.4 SEALANT TECHNOLOGY

Typically, wells with poor primary cementing jobs or suspected leaks are repaired with cement squeeze operations, in which new cement is injected through perforations created in the casing near the suspected source of leakage to achieve proper zonal isolation. Squeeze cementing is a remedial process that involves the application of differential pressure across the cement slurry to accomplish the process of cement dehydration (Goodwin, 1984). In principle, the slurry is designed specifically to reach and fill the problem area, and create immobility until some compressive strength can be developed. However, cement slurry is often improperly placed or poorly designed due to

the misjudgment of the leakage problem at hand. The presence of an annular gap and/or fractures with apertures on the order of 0.01–0.3 mm can still have a significant increase in effective permeability in the range of 0.1–1 mD (Um et al., 2014). Particularly, fractures or leakage pathways with small apertures are often difficult for oilfield cement to repair, as the cement slurry is potentially screened out from dispersing fluid and cannot enter the fracture. Therefore, squeeze cementing is often unsuccessful, and can result in a waste of rig time and escalation of costs.

The main factor limiting the sealing performance of traditional oilfield cement is the particle size in the slurry. The commonly used Class G oilwell cement contains large particles in the 100-150 μm range which makes it difficult to access narrow channels, micro-annuli, or narrow mud channels and often lead to unsatisfactory results. In addition, bridging and cement dehydration will occur when the slurry is squeezed to penetrate fractures narrower than 400 μm. Ultra-fine cement technologies, such as Halliburton's Micro Matrix cement and Schlumberger's SqueezeCRETE, have been developed to significantly reduce the particle size of the cement slurries. These new slurries are said have improved penetration capabilities through narrow slots. Table 1.1 compares a few key advantages and disadvantages of oilfield Portland cement and Ultra-fine cement in sealing off narrow fractures. Penetration capability through a narrow slit is an indication of slurry viscosity and set time is an indication of the duration the slurry could remain pump-able.

Table 1.1: Comparison of cement for sealing narrow fractures (penetration capability through slit width = 150μm, data from Halliburton Micro Matrix cement).

	Conventional Cement Slurry	Ultra-fine Cement Slurry
Particle Size	10-150 μm	0.5-10 μm
Penetration Capability	0	90%
Set Time	Long	Short
Price	1X	5-10X

Alternative technologies have been developed to address issues outside the capabilities of either conventional or ultrafine cement. New sealants have eliminated the use of solid particles to prevent screen-out during squeeze off:

- *Injectrol®:* a sodium silicate gel system, when in a solution form particulate solids whenever they come into contact with such divalent ions as those found in calcium chloride or cement. As the water phase is squeezed into the solution, these particulate solids accumulate to form a paste-like material that continues to grow during the squeeze process until it becomes a permanent solid (product of Halliburton Energy Services).
- *PermSeal:* a monomer solution that polymerizes in-situ. When injected, these monomers are transformed into right-angle-set polymers that allow the solution to generate an extremely resilient material resistant to high extrusion pressures (product of Halliburton Energy Services).
- *BrightWater®:* a temperature-controlled agent that can be used to develop fluid viscosity. These tightly bounded particles are designed to thermally pop at a pre-

determined location within the target zone. New cold-activating BrightWater technology can be activated at less than 50°C.

- *Biomineral technology*: uses low viscosity fluids to carry naturally occurring mircoorganisms to seal fractures ranging in size from 2 microns to 1 mm. The biomineralization results in the formation of carbonates and phosphates that are stronger than surrounding formation. This technology is designed to seal hydrocarbons and CO_2 in sandstone, shale, and other formations.
- *CSI epoxy resin: is* a system of resin and chemical hardener that is designed to address issues with remedial cementing. The resin is formulated to solidify after a set time with no shrinking and provided long- term durability.
- *Other polymer microgels* are often used in conjunction with crosslinkers that develop large viscosities after a characteristic reaction time (Sydansk, 1993), and resins are also formulated to solidify after a set time (Morris et al., 2012).

Table 1.2 is a comparison of some of these alternative technologies based on factors regarding cement fracture application.

Table 1.2: Comparison of commercialized solids-free sealant technologies.

	CSI Resin	Injectrol	PermSeal	BrightWater	Biomineral
Mechanism	Epoxy resin and chemical hardener	Internally-catalyzed silicate	High temperature controlled polymer	Cold temperature controlled polymer	Calcite carbonate-forming microorganism
Working Temperature	5 - 150°C	Above 50°C	10 - 150°C	Below 90°C	
Thickening Time	Below 12 hr	~48 hr	Depends on temperature and concentration	Depends on temperature	Long
Strength	High mechanical strength and longevity		H_2S, CO2 and formation brine resistant		
Weakness		Strong acids		Not good for fractures	
Environmental friendly			Yes		Yes

1.5 pH-Triggered Mechanism

Polyacrylic acid microgels can swell a thousand fold as the pH of the environment changes. The microgel dispersion is not viscous in low pH environments but if pH increases, its viscosity can increase by several orders of magnitude (Choi et al., 2006). The viscosity of the microgel dispersion depends strongly on pH and also concentration

and salinity (Lalehrokh, 2008). This characteristic makes pH-sensitive polymer gelant easy to use in sealing leakage pathways associated with existing wellbores. Because the main hydration product of interest in cement is calcium hydroxide, $Ca(OH)_2$. The hydrated cement is highly alkaline which has sufficient neutralization capacity to induce the pH transition for gel formation.

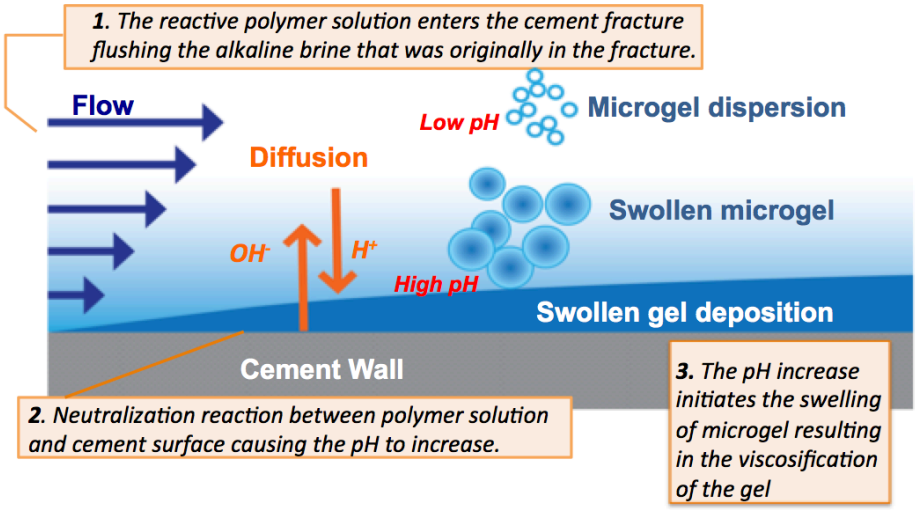

Figure 1.5: An illustration of the reaction between the pH-triggered microgel dispersion and the cement fracture. The microgel dispersion can be injected easily, much like water, into cement fracture starting at low pH. The pH and volume of the microgel dispersion increases while OH^- ions leach out of the alkaline cement walls to neutralize the solution resulting in the viscosification of the gel. Swollen gel is then deposited in the cement.

A schematic of pH-triggered gelling mechanism with injection of the polymer into a cement fracture is illustrated in Figure 1.5. After injection, a shut-in time allows polymer to further react with cement and results in an increase in the pH. The relatively narrow transition zone from low viscosity to high viscosity value occurs at a pH around 4 (Choi et al., 2006). This triggers the gelling mechanism of polymer which will develop sufficient mechanical strength (yield stress) to block flow. The pH-triggered application

is convenient and differs from other viscosification systems because additives are not required and treatment design would not need to account for the complexity of time/temperature/composition sensitive agents for gellation, such as polymer crosslinkers. One benefit to end-users is that this material is well studied, inexpensive, and commercially available in quantity. Another benefit is that such yield stress fluids become more effective as the fracture they occupy becomes narrower. This is because the pressure gradient that the gel will withstand is inversely proportional to fracture aperture. Hence this polymer is potentially useful for repairing leakage pathways in oilfield cement, especially those that are too narrow to be easily treated by squeeze cementing.

1.6 POLYMER RHEOLOGY

Any fluid moving on a surface will experience friction along the path of flow, this friction force is commonly known as shear stress. It is defined as the stress applied to a body of fluid in order for it to flow. Shear stresses applied can be translated to specific shear rates depending on the characteristic of the fluid, for instance, the mechanical work required to set a pump at a certain injection rate. One concept of fluid characteristic is viscosity, informally referred to as thickness; it simply describes the fluid's resistance to flow. To characterize the flow of polymers, it is necessary to understand the basic models that describe simple flow behaviors. These models can be very useful in describing the behaviors of materials; however, most materials will exhibit a combination of these simple relationships over a sufficiently large range of shear rate.

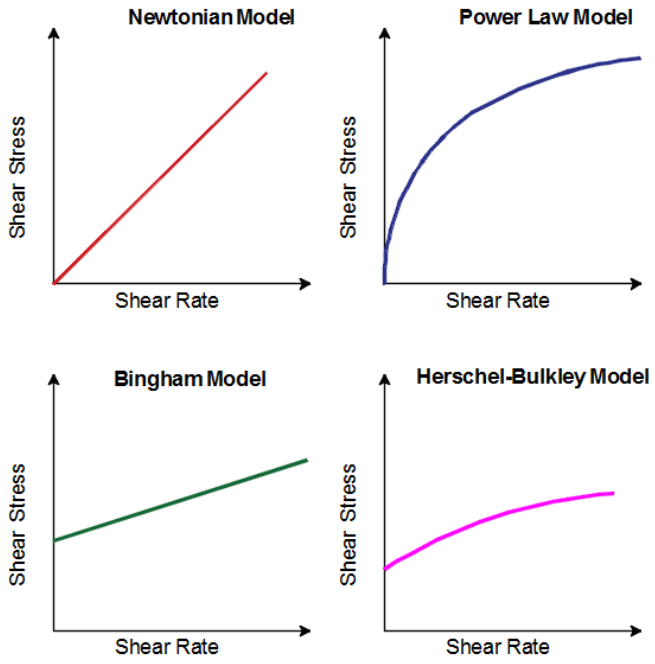

Figure 1.6: Rheological models (Schlumberger Oilfield Dictionary).

The complexity of the Herschel-Bulkley model makes it the most versatile of the four basic fluid models (Figure 1.6) and can accurately characterize many industrial fluids. The equation for the this model is given as:

$$\sigma = \sigma_y + K\dot{\gamma}^n \tag{1.4}$$

where σ is the shear stress, σ_y is the yield stress, K is the consistency index, $\dot{\gamma}$ is the shear rate, and n is the power law index. This model incorporates the elements from the two of the basic fluid models where the first term describes a yield stress and second term follows the power law behavior. The Herschel Bulkley model can be simplified to other basic flow models as special cases:

1. Newtonian flow ($\sigma_y = 0, n = 0$):

$$\sigma = \mu\dot{\gamma} \tag{1.5}$$

where μ is the viscosity. This is the simplest type of flow where the fluid viscosity is constant and independent of the shear rate. It can be used to describe fluids such as water, oils or dilute polymer solutions.

2. Power law flow ($\sigma_y = 0$):

$$\sigma = K\dot{\gamma}^n \tag{1.6}$$

For non-Newtonian fluids, K and n are constant while the apparent viscosity depends on the shear rate:

$$\mu_{apparent} = \frac{\sigma}{\dot{\gamma}} \tag{1.7}$$

$$\mu_{apparent} = K\dot{\gamma}^{(n-1)} \tag{1.8}$$

where μ_{apparent} is the apparent viscosity. Power law flow is a non-Newtonian flow where viscosity increases or decreases as the shear rate is increased. The power law model is a non-linear relationship between shear stress and shear rate and can seen over a small range of shear rates for some fluids. Shear thinning and shear thickening are two types of fluid behaviors that can be described using the power law model. If the viscosity decreases as the shear rate is increased the fluid is said to be shear thinning and *n* will be positive ($n > 1$); for example, some polymer solutions and melts. If the viscosity increases as shear rate is increased the fluid is said to be shear thickening and *n* will be negative ($n < 1$); for example, when cornstarch is mixed with water.

3. Bingham flow (n =0):

$$\sigma = \sigma_y + \mu\dot{\gamma} \tag{1.9}$$

Bingham fluids require a sufficient shear stress be applied to initiate flow while above this shear stress it behaves as Newtonian flow (viscosity is constant). The shear stress that is required to initiate flow is defined as the yield stress and can be seen in many

concentrated suspension and colloidal systems. These models can be utilized under a small range of shear rates an often combined for larger shear rates to describe most behaviors of fluids. In addition, empirical models for complex fluid behavior are often developed by fitting rheological data.

The injection of pH-triggered polymer gel into cement fractures exhibits both viscosification and depositional effects that influence the flow rate or injection pressure during flow; these phenomena have been observed in past laboratory experiments (Patterson, 2014). The polymer is seen to have a yield stress and shear thinning behavior. The yield stress exhibited is analogous to that of a solid material meaning that it does not flow below a critical applied stress (Barnes, 1999). Shear thinning is seen in injection experiments where viscosity decreases when injection rate is increased. When a shear thinning fluid also possesses a yield stress, the low flow regions in which the shear stress is less than the yield stress will either exhibit plug flow or no flow.

Sealant exhibiting behaviors of a semi-solid that can be used to seal leakage pathways in cement fracture are ideal candidates. A class of poly(acrylic acid) polymers known commercially as Carbopol® are pH-sensitive microgels and swell/thicken upon neutralization to become bulk gels with substantial yield stress of over 100 Pa (Huh et al., 2005). Carbopol® 934 has been one of the most widely used thickening and gelling agents for various commercial applications for the last fifty years. This polymer is commonly used by rheologists and chemical engineers because of its versatility in imparting extreme non-Newtonian properties without excessive elasticity but highly shear thinning (Roberts and Barnes, 2001; Shafiei et al., 2015).

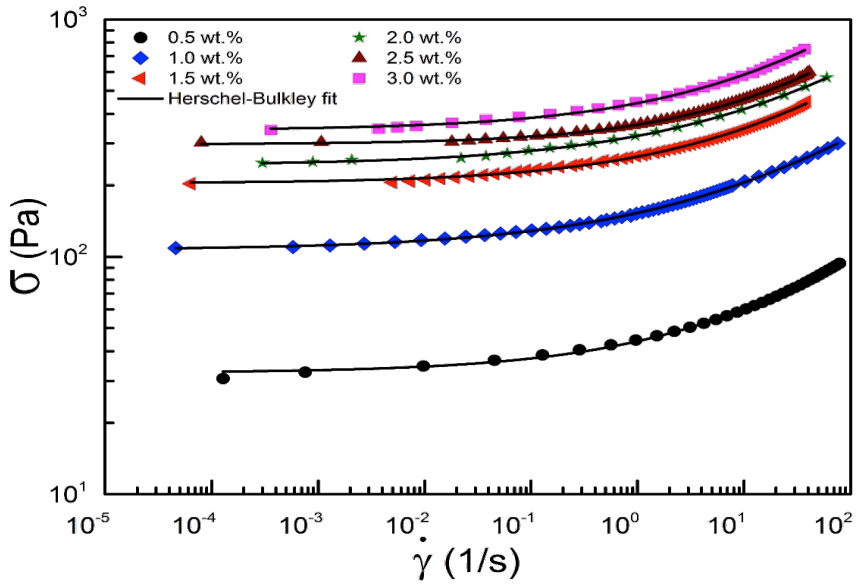

Figure 1.7: An AR-G2 Magnetic Bearing Rheometer was used to determine the rheology of the 3 wt% Carbopol 934 polymer dispersion at pH 3.96. The polymer dispersion was classified as a Herschel-Bulkley (HB) fluid (Shafiei, 2015).

The polymer dispersion is found to have good fit with the Herschel-Bulkley model (Figure 1.7), which exhibits both shear-thinning (power law) behavior and a yield stress. Yield stress is measured dynamically in a rheometer by extrapolation to the y-intercept of a stress versus shear rate curve or static tests (Cloitre et al., 2003; Balhoff et al., 2011) such as creep or vane. At a given pH and concentration, the polymer behavior can be described by the Herschel Bulkley equation (1.4) where the apparent viscosity can be expressed as:

$$\mu_{apparent} = \frac{\sigma_y}{\dot{\gamma}} + K\dot{\gamma}^{(n-1)} \tag{1.10}$$

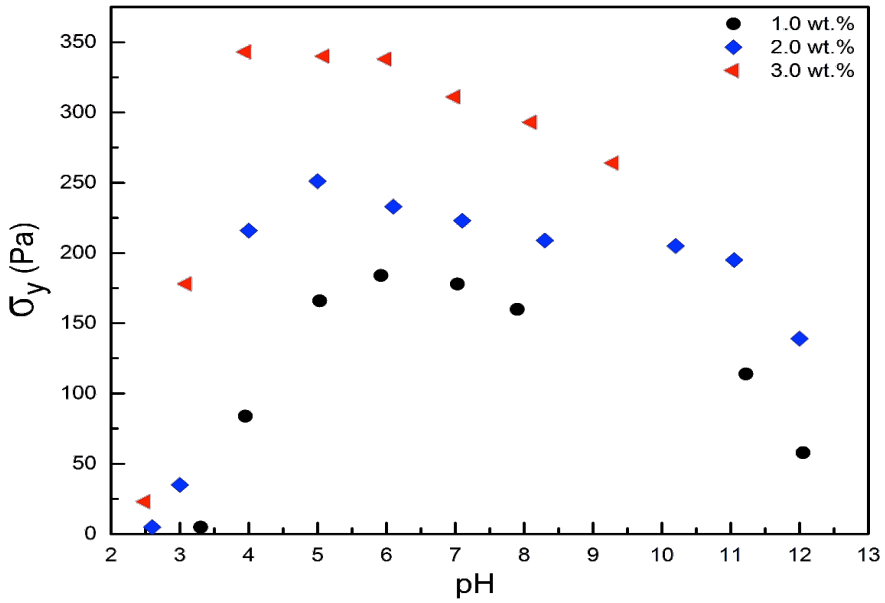

Figure 1.8: Yield stress measurement at various pH for 1-3 wt % Carbopol 934 (Shafiei, 2015).

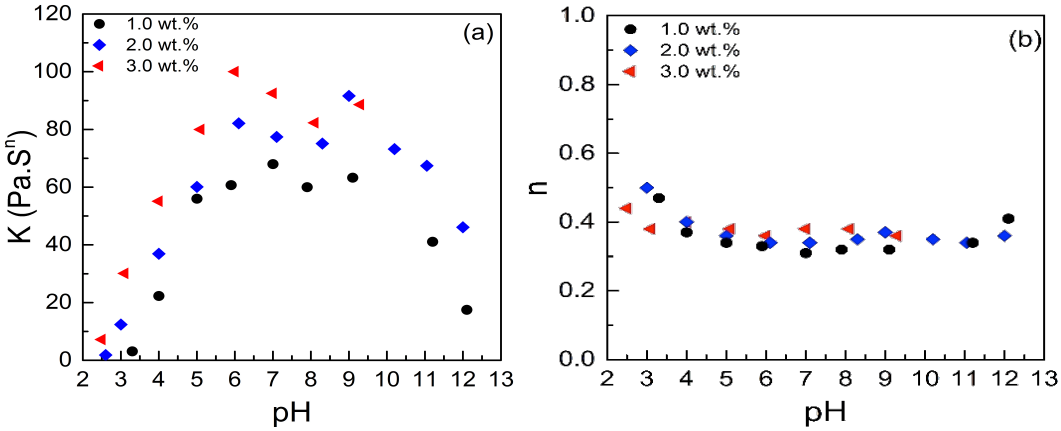

Figure 1.9: Consistency index, *K*, and power law index, *n*, measurements at various pH for 1-3 wt % Carbopol 934 (Shafiei, 2015).

The apparent viscosity is dependent upon those Herschel-Bulkley parameters and the shear rate of the fluid. Since the polymer dispersion can change in viscosity based on pH, these Herschel-Bulkley parameters are in turn a strong function of the solution's pH

among other parameters. Figure 1.8 shows the polymer yield stress significantly increases over pH values from 3 to 5 and remains relatively high at pH value between 5 and 10. Figure 1.9 is the measurement of consistency index, K, and power law index, n, measurements for various pH. Note that the trend in K very much resembles that of in the previous figure and n is seen to remain relatively constant over various pH and concentration.

Huh et al. (2005) developed a comprehensive rheological model for pH-triggered polymer solutions that can predict polymer viscosity based on pH, salinity, concentration and shear rate. The model couples the ionic hydrogel swelling theory (Brannon- Peppas and Peppas, 1988) with several viscosity equations that relates to polymer concentration, molecular size and shear rate. Their viscosity simulations are successfully verified with experimental data. The following are the four parameters that contribute to the viscosity of such pH-triggered polymer:

1. Shear rate (γ): At low pH, the polymer exhibits a Newtonian behavior where the apparent viscosity is almost constant. As pH increases, the shear thinning behavior becomes more increasingly evident as shown in Figure 1.10.

2. pH: For a given shear rate, the apparent viscosity can be seen to increase with pH as seen in Figure 1.10. The polymer viscosity exhibits a sudden increase around pH 4. This sharp transition explains the pH-trigger mechanism.

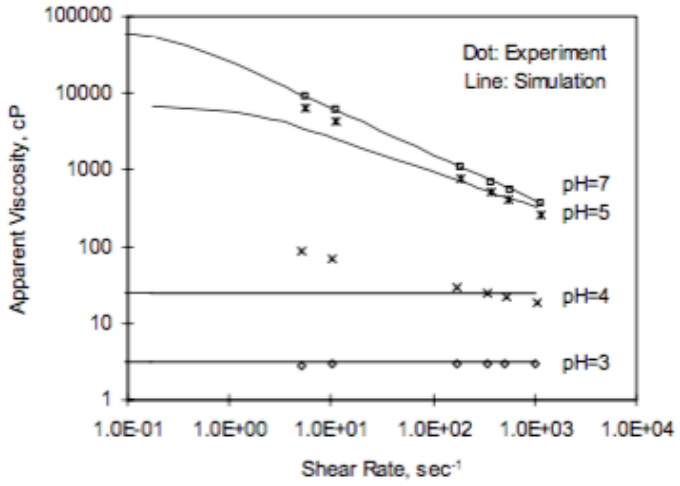

Figure 1.10: Apparent viscosity dependence on shear rate shows polymer solution transformation from Newtonian flow to shear thinning as pH increases (Huh et al., 2005).

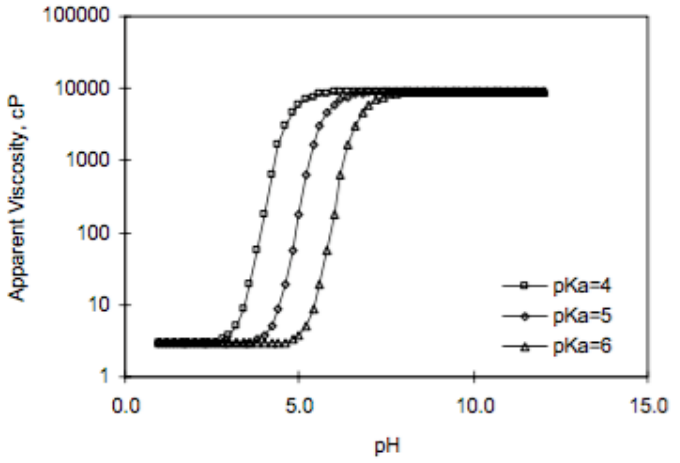

Figure 1.11: Apparent viscosity dependence on K_a (dissociation constant of ionizable groups on polymer) under various pH (Huh et al., 2005).

3. Salinity: For a given pH value, the apparent viscosity can be seen to decrease exponentially as the dissociation constant, K_a, increases (Figure 1.11). The Na^+ associated with salinity drives the dissociation of the crosslinking polymer structure. The polymer is seen to lose viscosity as salinity increases.

4. Concentration: For a given salinity and shear rate, the apparent viscosity increases exponentially with polymer concentration at higher pH as seen in Figure 1.12.

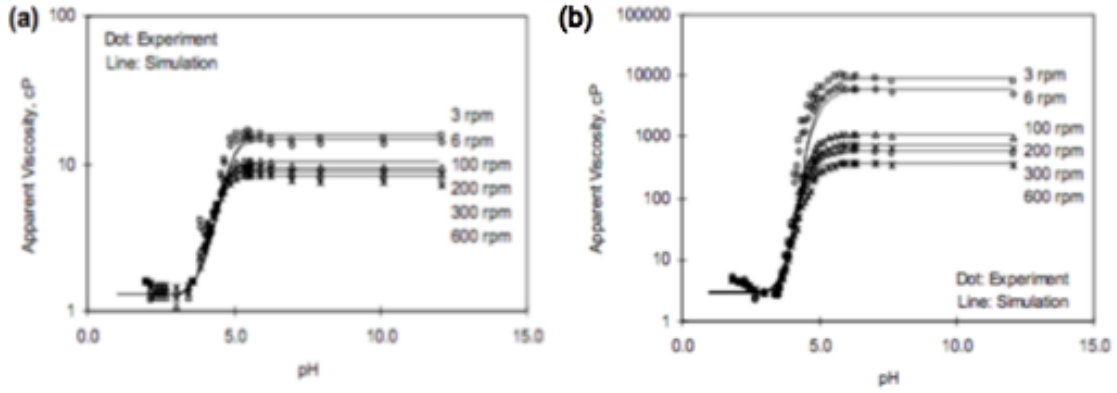

Figure 1.12: Apparent Viscosity dependence on polymer concentration (Carbopol EZ-2) as pH changes in (a) 1 wt% EZ-2 in 3 wt% NaCl, (b) 3 wt% EZ-2 in 3 wt% NaCl (Huh et al., 2005).

The intensive experiments show that polymer viscosity is strongly dependent on shear rate, pH, concentration and salinity and the comprehensive model can predict viscosity based on those parameters very accurately. In addition, thickening properties of Carbopols are known to decrease as temperature increases. Thermal stability of Carbopol ® 934, 941, 940 are higher at up to 70°C than other pH-sensitive polymers as shown in Figure 1.13, however it is important to investigate their properties at temperatures greater than 100°C that is suitable for geological storage conditions.

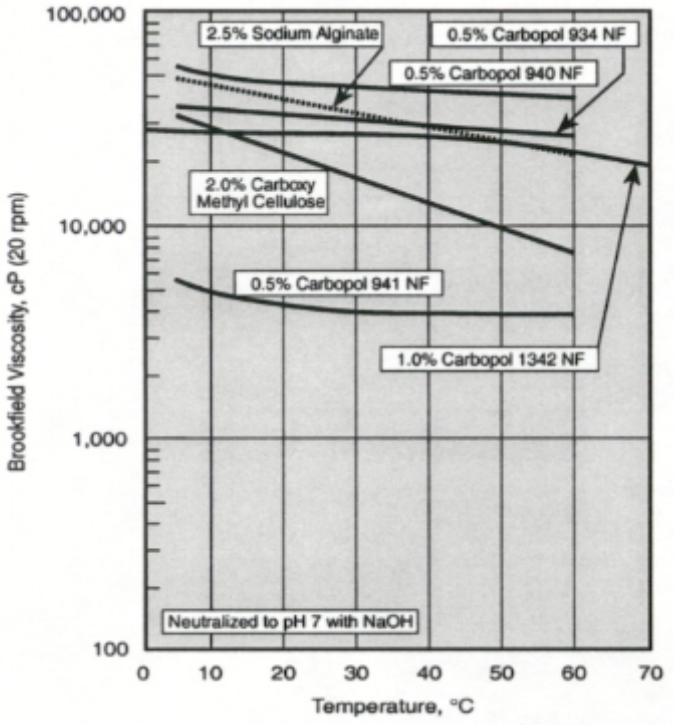

Figure 1.13: Effect of temperature on viscosity of water solutions of Carbopol® polymers (Lubrozol Pharmaceutical Bulletin, 2011)

1.7 DIFFUSION COEFFICIENTS

Hydroxide and proton concentrations are key sources for pH in the reacting polymer solution. The pH can then be used with polymer concentration to predict the Herschel Bulkley parameters (σ_y, K, n) to accurately characterize viscosity. To calculate the concentrations of hydroxide, proton and polymer in the cement fracture, it is necessary to determine the diffusion coefficient that describes the relative movement and distribution of these molecules.

The Stokes-Einstein equation estimates the diffusion coefficient of a macroscopic particle of radius, r, undergoing a Brownian motion to the viscosity of the fluid in which it is immersed. With significant difference the molecular size of hydroxide and swollen

gel, one can assume no-slip condition at the interface of both species. The diffusion coefficient of hydroxide ion and swollen gel can be expressed as:

$$D_{OH^-,gel} = \frac{k_B T}{6\pi r} \frac{1}{\mu_{gel}}, \tag{1.11}$$

$$r = \left[\frac{3(MW)}{4\pi N \rho} \right]^{1/3}, \tag{1.12}$$

where D_{OH^-}, gel is the diffusion coefficient of OH- ion and swollen gel, μ_{gel} is the swollen gel viscosity, r is the hydrodynamic radius of hydroxide ion, k_B is the Boltzmann constant, and T is the temperature of the solution environment. The diffusion coefficient of OH^- is inversely proportional to gel viscosity, which means that as polymer gels up it becomes difficult for more OH^- to diffuse and increase the pH above optimal pH. In addition, an empirical diffusivity equation was developed and correlated with lab results for Carbopol 940 (A-sasutjarit et al., 2005):

$$D_{ion-gel} = 0.0659 / \mu_{apparent} + 9 \times 10^{-5}, \tag{1.13}$$

where $D_{ion,gel}$ is the diffusion coefficient of between ion and gel. This equations also suggests the inverse relationship between diffusivity and gel viscosity, but showed that diffusivity will asymptote to a constant value at higher viscosities due to the reduction of free volume and the impediment of ion mobility.

For sealing micro-fractures in cement, only a small concentration of polymer is required to achieve significant yield stress. Studies have shown that the diffusivity has an inverse dependence on polymer molecular weight for solutions with low concentration of

solid microgel particles (Bird et al., 1987). The diffusion coefficient for polymer solution can be expressed as:

$$D_{polymer-solution} = \frac{1}{MW_{polymer}}, \tag{1.14}$$

where $D_{\text{polymer-solution}}$ is the diffusion coefficient of polymer microgel dispersion, and MW_{polymer} is the molecular weight of microgel particles.

1.8 MODEL DEVELOPMENT

The sealing dynamics, namely flow field and concentrations, of pH-triggered polymer gel in cement fractures can be modeled using the Herschel Bulkley model, continuity equation, Navier-Stokes equation, convective-diffusion equation and diffusion coefficient models. A 2D slit geometry can be assumed when modeling the injection of polymer through a micro-fracture pathway. The reactive transport of polymer solution is assumed to take place between two parallel cement plates with constant aperture. When the acidic microgel dispersion enters the fracture the neutralization will happen instantly as hydroxide ions diffuse out from the cement surface. The sudden increase in pH will cause the solid microgel particles to swell and deposit as gel on the cement surface while the rest of the dispersion is carried along in the longitudinal direction by flow. As the swollen gels deposit on the surface, the aperture of the flow region will decrease and eventually block up the entire fracture. The modeling of the concentrations of key species and flow behavior can be simplified by making the following assumptions:

1. The swelling of microgel particles occur instantly upon neutralization with OH^- ions and is irreversible.
2. Cement surface in the fracture are assumed to be smooth and has a no-slip condition for fluid flow.

3. The diffusion of OH^- and H^+ only occurs in the traverse direction (*y*) in to the dispersion while OH^- diffuses into the solution and H^+ diffuses towards the cement wall.
4. The flow velocity of polymer solution only occurs in the in the longitudinal direction (*x*).

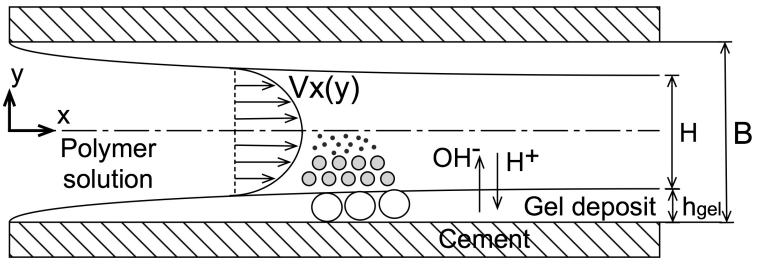

Figure 1.14: Schematic of 2D reactive transport model for polymer, hydroxide and proton concentration. The blockage of the cement fracture aperture (B) will depend on the increasing gel deposit on the cement surface (h_{gel}), the changing flow field of polymer solution (v_x) and diffusion of species in the depositional gel layer.

The swollen gel will at some point deposit on the cement surface forming a solid gel layer that causes the narrowing of the aperture as illustrated in Figure 1.14. The thickening of deposited gel layer is yet to be developed and time-dependent. To simplify the problem, preliminary kinetic equations can be assumed and the reactive transport of microgel dispersion can be modeled in quasi-steady state as time is analogous to distance particles traveled longitudinally (*x*). Key theories and equations required characterizing the pH-gelling phenomena is explained in the following:

1. Momentum equations:

The flow field can be calculated by using the continuity equation and Navier-Stokes equation. The continuity equation describes a transport of conserved quantity, meaning that the energy of the specie is locally conserved and can only move by continuous flow. The differential form of the equation can be defined as:

$$\frac{\partial \rho}{\partial t} + \nabla \cdot (\rho \boldsymbol{u}) = 0 \tag{1.15}$$

This is true for all the species considered in polymer solution. For a single-phase incompressible flow, it can further simplify the equation to:

$$\nabla \cdot \mathbf{u} = 0 \tag{1.16}$$

The Navier-Stokes equation is a balance equation used to describe the motion of viscous fluids and is given in a simplified form as:

$$\rho \frac{\partial \boldsymbol{u}}{\partial t} = \mu \nabla^2 \mathbf{u} - \nabla p \tag{1.17}$$

These two equations can be used with boundary conditions and initial condition for flow through a slit of constant aperture. In this geometry, pressure changes in the *y* direction can be ignored. The injection of polymer will cause shearing of the solution, in the direction of the flow path, relative to the stationary cement wall ($v_x = 0$ when $y = H/2$); therefore, velocity of the fluid will only change in the transverse direction (*y*). The equation can be simplified to:

$$\frac{\partial p}{\partial x} + \mu \frac{\partial^2 v_x}{\partial y^2} = 0 \tag{1.18}$$

This is a partial differential equation that can be used calculate flow field and pressure distribution in the cement fracture based on fluid behavior of gel. In addition, the velocity

and pressure distribution will change due to the thickening of the gel based on its pH over time.

2. Herchel Bulkley model:

Since rheology data (Shafiei, 2015) indicate that the polymer solution behavior best fit the Herschel Bulkley model, we can use the measurements of yield stress, consistency index and power-law index based on pH to calculate the flow field. At a given injection rate, Q, fracture aperture, B, and pH, the viscosity can be substituted using the apparent viscosity calculated from the Herschel Bulkley parameters. While injection rate is constant, the flow field will change in the x direction as the fluid thickens (parameters K, σ_y *and* n) and aperture narrows.

3. Convective-diffusion equation:

The equation is used to describe the diffusion and convection of microgel particles, hydroxide ions and protons in the polymer solution in terms of concentration. The convective-diffusion equation is given by:

$$\frac{\partial c}{\partial t} + \underbrace{\boldsymbol{u}\cdot\nabla c}_{convective} = \underbrace{\nabla\cdot\left(D\nabla c\right)}_{diffusion} + \underbrace{R}_{\substack{chemical\\reaction}} \tag{1.19}$$

As previously stated, the concentration will not change in quasi-steady state. Thus the equation can be further simplified to:

$$\boldsymbol{u}\cdot\nabla c = \nabla\cdot\left(D\nabla c\right) + R \tag{1.20}$$

where movement of these molecules can be calculated based on its diffusion and the flow field that carries it. In addition, it is necessary to include the source term as neutralization of OH^- and H^+ is a chemical reaction and causes the disappearance of the molecules.

4. Boundary conditions:

The concentration of species can be solved with the mathematical equations mentioned using key initial and boundary conditions specific to the pH-trigger mechanism. The initial conditions for the reactive transport of polymer concentration, hydroxide and proton are listed as follows:

$$c_{polymer} = c_{inlet} \quad \text{at} \quad t = 0\,, \tag{1.21}$$

$$c_{H^+} = 10^{-pH_{inlet}} \quad \text{at} \quad t = 0\,, \tag{1.22}$$

$$c_{OH^-} = 10^{-(14-pH_{inlet})} \quad \text{at} \quad t = 0\,, \tag{1.23}$$

where c_{polymer} is the concentration of polymer, $c_{\text{H+}}$ is the concentration of protons, $c_{\text{OH-}}$ is the concentration of hydroxide ions, c_{inlet} is the concentration of the original polymer injected, and pH_{inlet} is the pH of the original polymer injected at $t = 0$, the time when injection started; for example, the initial 3 wt % Carbopol solution has a pH around 2.5. With the boundary conditions listed as:

$$c_{polymer} = c_{inlet} \quad \text{at} \quad x = 0\,, \qquad \frac{\partial c_{polymer}}{\partial x} = 0 \quad \text{at} \quad x = L\,; \tag{1.24}$$

$$c_{H^+} = 0 \quad \text{at} \quad y = B/2\,, \qquad \frac{\partial c_{H^+}}{\partial y} = 0 \quad \text{at} \quad y = 0\,; \tag{1.25}$$

$$c_{OH^-} = 1 \quad \text{at} \quad y = B/2\,, \qquad \frac{\partial c_{OH^-}}{\partial y} = 0 \quad \text{at} \quad y = 0\,; \tag{1.26}$$

where L is the length of the fracture, and B is the original aperture of the fracture. Meaning that polymer concentration is the same as the original polymer injected at the fracture inlet and consumption of polymer is ceases as the solution exits the fracture; concentration of protons is zero at the cement wall and there is no penetration of the protons at the center of the fracture; concentration of hydroxide ions will be at its

maximum at the cement wall and there is no penetration of ions at the center of the fracture.

The initial conditions describe the concentration before injection as a starting point for calculations before moving on to the next time step ($t=t+\Delta t$). Within each time step, the model assumes quasi-steady state and the concentrations can be calculated base on the boundary conditions. These constant boundary conditions hold true in each quasi-steady state as flow region gets smaller with time. In order for the calculation to march forward in time, it is required to assume a kinetic relationship for gel deposition as a function of time.

5. Gel thickening kinetics equation:

A preliminary gel layer thickness equation was proposed in order to develop the model. The time-dependent gel layer thickness can be described by:

$$\frac{\partial(h_{gel})}{\partial t} = k_h \frac{(c_h - c_c)}{(\gamma_h)^m} \quad \text{at} \quad y = h_{gel}, \tag{1.27}$$

where h_{gel} is the thickness of the immobile gel layer on the cement surface, k_h is a kinetics constant, γ_h is the shear rate at the gel layer surface, c_h is the OH^- concentrations at the gel layer surface, and c_c is the critical swelling concentration. It assumes that swelling of microgel particles occur instantly and only depend on the OH^- concentration. The assumption could be simplified by setting a critical swelling OH^- concentration, c_c, above which the microgel particles have a uniform swollen size; below which they have a uniform solid size. In addition, high shear rate, γ_h, felt at the gel surface discourages the deposition of swollen microgel particles.

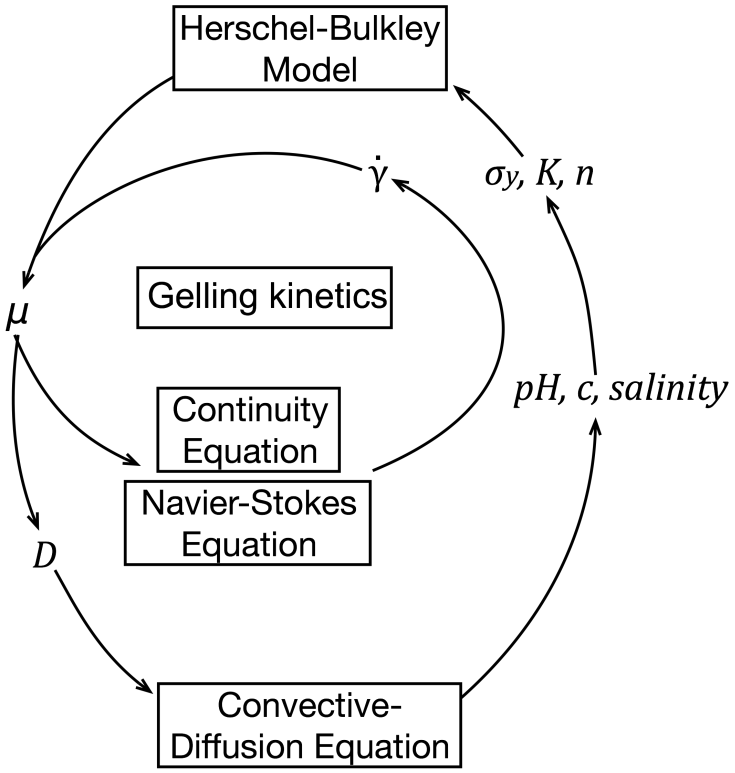

Figure 1.15: Reactive transport model development of pH-triggered polymer.

Together with the kinetics of gel deposition, this 2D model can be used to predict the pH condition as the composition of polymer solution changes with time and location; subsequently when the gel deposit will completely block flow. Figure 1.15 illustrates the equations and steps needed to calculate key parameters a time step.

1.9 POLYMER SYNERESIS

Polymer syneresis is the shrinkage of gel volume due to the expulsion of liquid. It results from excessive chemical attractive forces within the gel structure. Syneresis of polymer gel can result not only from excessive cross-linking within, but also from chemical modification by the environment over time. Polymer gels undergoing syneresis have difficulty of maintaining gel stability, and can shrink up to 95% of its initial volume

(Bryant et al., 1996). As a result, syneresis is often considered undesirable and unacceptable in the application of polymer gels for reducing permeability of a porous medium or sealing fluid flow in fractures.

Divalent ion-induced syneresis is commonly seen in polymer gel treatments done at high temperatures or in the presence of hard formation brines (Albonico and Lockhart, 1997; Bryant et al., 1996). A previous study (Patterson, 2014) has found that Carbopol 934 polymer would undergo syneresis after placed in cement fractures. In the application of sealing cement fractures, the presence of divalent cations in cement can destabilize gel structure and greatly compromise the gelant's mechanical strength to block fluid flow. This phenomenon can be explained in Figure 1.16. When polymer is in contact with a cement fracture, hydroxide ions quickly leach out and neutralize the solution; the repellence of negative charges along polymer chain causes the structure to extend to a swollen microgel particle. As the calcium cations ooze out from cement into the developed gel, the negative carboxylate anions will easily bind with the cation and result in the collapse of the polymer structure. This contraction of the polymer chain can be seen from shrinkage in the volume of gel and expulsion of the absorbed water.

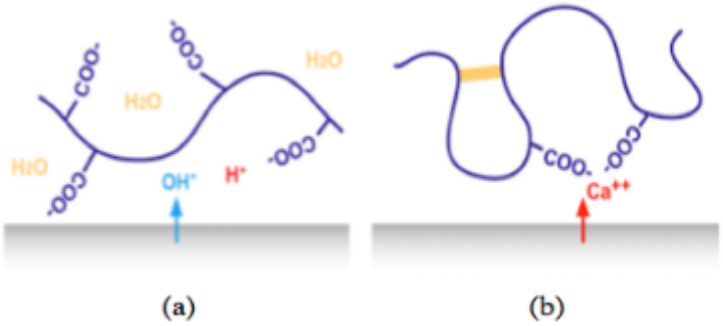

Figure 1.16: Polymer neutralization and syneresis in cement application. (a) hydroxide ions causes the polymer structure to extend (b) divalent calcium cations causes structure to shrink.

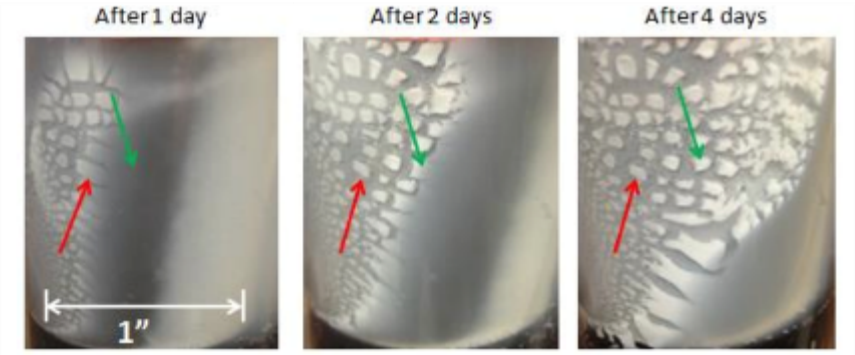

Figure 1.17: Detailed photographs of syneresis forming on cement surface after soaking in 3 wt% Carbopol 934 dispersion; red and green arrows corresponds to identical spatial locations in each photograph (Patterson, 2014).

Previous work (Patterson, 2014) showed that the final gel volume was only a fraction of the initial solution volume and a portion of the sealed leakage pathway was reopened for fluid flow. Detailed photographs of syneresis forming on cement surface after soaking in 3 wt% Carbopol 934 dispersion can be seen in Figure 1.17. In addition, the white precipitation was identified as the product of syneresis and later proved to be calcium-syneresed polymer due to the high concentration of divalent calcium cations on the cement surface (Patterson, 2014). Observations from long period cement soak tests were made and defined the various phases associated with polymer reactions as listed in Table 1.3.

Table 1.3: Polymer phases that appear when polymer dispersion contacts cement for extended periods (Patterson, 2014).

	Color	Viscosity	Location
Polymer Dispersion	White/Opaque	Thin gel	n/a (consumed)
Polymer Gel	Clear	Thick gel	Various
Semisolid	White	Sponge-like solid	On cement surfaces
Water	Clear	Newtonian	Next to semisolid

The flow behavior observed in the polymer injection experiments was interpreted with theoretical equations and serves as a basis for its application to seal cement wells (Patterson, 2014). However, the calcium syneresis that occurred after polymer injection greatly reduces the gel strength. Subsequent gel strength testing of sealed cement cores often result in early breakthrough of fluids and the inconsistency in theoretical yield stresses compared with rheology data obtained from neutralizing polymer with Na(OH) (Shafiei, 2014).

1.10 Research Objectives

The objective of this study is to develop a novel application of a pH-sensitive polymer in sealing fractured cement or micro-annuli in wellbore associated with geological CO_2 storage. This work investigates in a discovery, an effect known as polymer syneresis, which previous work have proven to be detrimental to gel strength and can ultimately compromise the potential sealing capability.

This study focuses on understanding the development of polymer viscosity and identifying the main components of calcium syneresis. Several chemicals are studied and considered as syneresis inhibitors to treat wellbore cement and improve gel stability and

strength. Preliminary tests are designed to find a compatible chemical and an optimal procedure to incorporate into field operations.

The optimal solution is validated against rheology models and field conditions using polymer injection experiments and gel strength tests. In addition, visual observations are made to verify the elimination of syneresis and long-term development of the resulting yield stress gel. The study aims to bring the novel wellbore sealing technology to available field pilot test. Gel strength tests are brought to higher pressure settings and tested with various formation fluids in order to address several possible concerns for field application.

Chapter 2: Experimental Approach[2]

2.1 Injection Fluids

2.1.1 Polymer Dispersion

The polymer dispersion was prepared using Carbopol® 934 purchased from ARC Products Inc. (a product of The Lubrizol Co.). Carbopol 934 is a dry, poly(acrylic) acid that comes as a fine particulate powder with an average particle size of 2-7 microns. These granules of microgel can swell orders of magnitude larger than its original size when dispersed in water and neutralized from its initial acidic state by a basic solution. As pH increases, the swelling of the microgels increases the viscosity of the solution (and provides a fluid yield stress) which contributes to its well-known thickening properties.

---

[2] Ho, J.F., Patterson, J.W., Tavassoli, S., Shafiei, M., Balhoff, M.T., Huh, C., Bommer, P.M., and Bryant, S.L., 2015. The use of a pH-triggered polymer gelant to seal cement fractures in wells. Presented at the Society of Petroleum Engineers (SPE) Annual Technical Conference and Exhibition (ATCE), Houston, Texas, U.S.A., 28-30 September. SPE-174940-MS

Contributions: J.F.Ho and J.W.Patterson were involved in the design and performance of laboratory experiments. M.Shafiei was involved in the acquisition of rheological data. J.F.Ho, J.W.Patterson, M.T.Balhoff, C.Huh, P.M.Bommer, and S.L.Bryant were involved in the conception and analysis of the work. J.F.Ho, J.W.Patterson, and S.Tavassoli were involved in the drafting and revision of the manuscript.

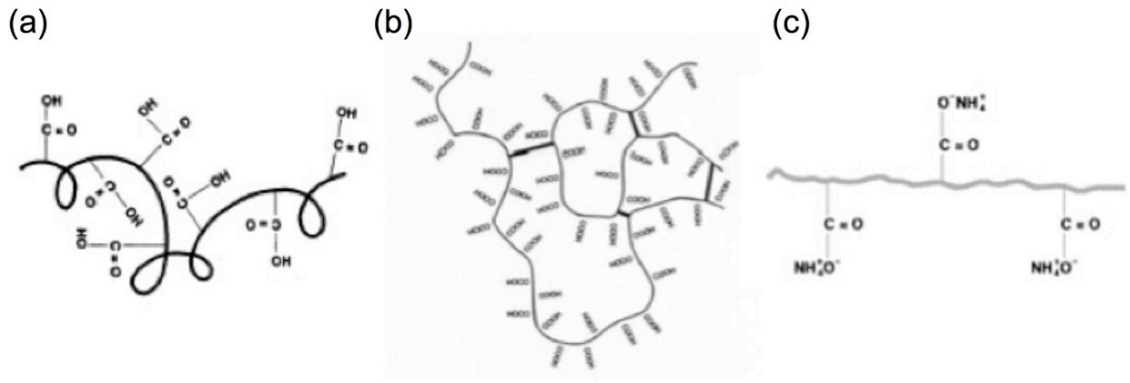

Figure 2.1: Change in molecular structure of poly(acrylic acid) polymer (a) Carbopol in pre-dispersed state, (b) hydrated crosslinked poly-acrylate hydrogel in acidic state, and (c) neutralized carbopol whose chains are expanded (Salamone, 1996).

Dry polymer particles are agglomerates of extremely fine, tightly coiled molecules (Figure 2.1(a)). When hydrated in water, these molecules begin to uncoil and form a cross-linked poly-acrylate hydrogel (Figure 2.1(b)). This results in slightly viscous polymer dispersion with initial pH between 2.5 and 3.0. Thickening gradually occurs once neutralizer, such as sodium hydroxide (NaOH), is added to the dispersion. Neutralization with hydroxide creates negative charges that result in electrostatic repulsion between polymer chains and extension of its structure (Figure 2.1(c)); and this uncoils the molecules and allows polymer gel to swell thereby increasing its viscosity. Maximum thickening can be achieved when the molecule uncoils completely.

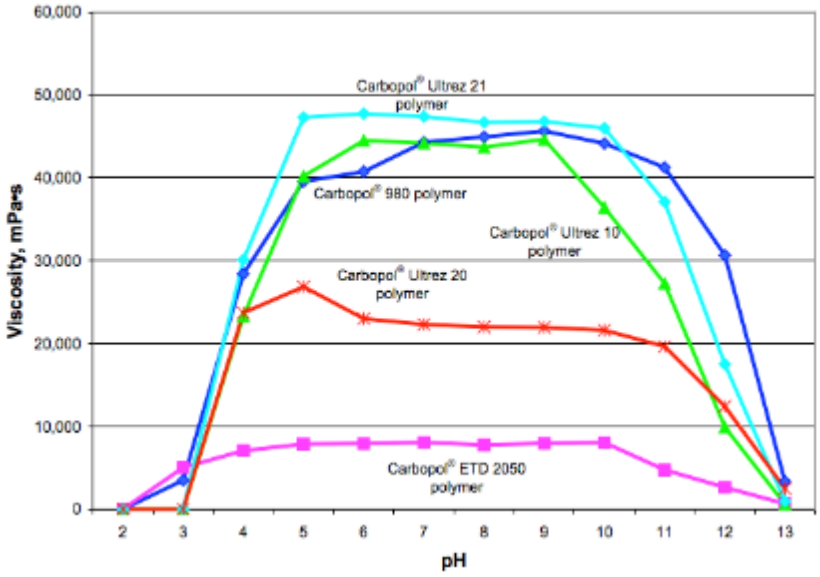

Figure 2-2: Carbopol polymers viscosity versus pH under same polymer concentration (Lubrizol Technical Data Sheet (TDS-237), 2009).

Several commercial grades of pH-sensitive Carbopol polymers (934, 940, 941, Ultrez 20, Ultrez 10 and 1342) were considered and investigated. Carbopol® 934 was chosen based on two desired attributes of the target application: (1) the sealant can be easily injected and remain able to pump for a period of time, and (2) the sealant should develop sufficient yield stress to hold back fluids in high pH condition. The first attribute requirement was met due to the fact that all Carbopol polymers are acidic (pH 2.5-3.0) and have relatively low viscosity when prepared with water as dispersion, as shown on the left side of the viscosity measurements in Figure 2-2. In addition, maximum thickening may take a few minutes to several hours, which allows more time for injection. The second desired attribute can be evaluated with viscosity values on the right side of Figure 2.2 where pH is the highest (pH 11-13). Despite the trend in drastically decreasing viscosity at higher pH, Carbopol 900 series show much better stability in maintaining its viscosity than Carbopol 1342, Ultrez 10 and 20. The same was verified by

rheology tests done on selected Carbopol polymers (Shafiei, 2013), which showed that Carbopol 934 has the highest yield stress among others. Table 2.1 is a comparison of the features of interest for sealing wellbore cement fractures. In this study, the mixture was prepared using 3 wt% Carbopol 934 polymer dispersed in deionized water; this polymer concentration was chosen for its optimization in both polymer injectivity at low pH and resulting gel yield stress at higher pH.

Table 2.1: Comparison of key features suitable for sealing wellbore cement fractures among Carbopol grades compiled based on polymer specification from manufacturer (Lubrizol Technical Data Sheet, 2002).

Carbopol® Grade	934	940	941	1342	Ultrez 10, 20
Ionic resistance				★	★
Thermal stability (up to 60C)	★	★			
Low viscosity at low pH (pH 2-4)	★		★		
Peak viscosity (pH 5-9)	★	★			
High viscosity at high pH (pH 10-12)		★			★
Shear resistance	★	★			
Thickening efficiency	★				

The polymer dispersion is made by slowly dispersing dry Carbopol 934 powder into rapidly agitating DI water. Precautions must be taken because polymer powder tends to form large, partially-wet agglomerates upon contact with water; as a result, microgels will not be fully hydrated. A laboratory overhead stirrer is used to make small batches of polymer dispersion, though a blender can be used to make larger quantities as long as it is kept at moderate agitation (800-1200 rpm). High-shear mixers are not recommended because the agitation could shear open the hydrated polymer and result in permanent

viscosity loss. In addition, undesired bubble formation could be minimized by entirely submerging the mixing blades and by arranging for air bubble release before neutralization.

2.1.2 Syneresis Inhibitors

Rheology tests (Figure 2.3) have been done on 3 wt% Carbopol 934 that show yield stress significantly decreases with the increase of calcium content (Shafiei, 2015). The presence of divalent calcium cations in cement can destabilize gel structure and greatly compromise the gelant's ability to block fluid flow. Therefore two chelating agents, as well as a mineral dispersion, were investigated in order to remove or stabilize divalent calcium ions from the cement surface zone. They were either used as additives in polymer solutions or injected alone as pre-treatment for the subsequent polymer injection.

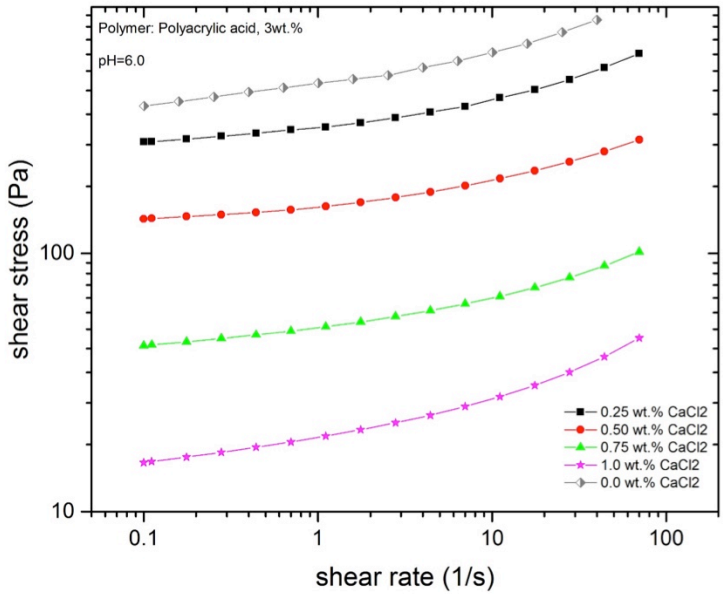

Figure 2.3: Effect of $CaCl_2$ on yield stress of 3 wt% Carbopol 934 (Shafiei, 2015).

Chelating agents are commonly used as syneresis inhibitors for polymer applications in hard formation water (Albonico and Lockhart, 1997). These chemicals can selectively remove metal ions, such as Ca^{2+} and $Mg^{2+,}$ by binding them to its molecule. Once bound, the metals are unable to react in undesirable ways. Detailed information and preparation of the two chelating agent used in this study are summarized below:

- *Ethylenediamine tetra-acetic acid (EDTA)* is one of the most common chelating agents used in chemistry. The aqueous form of EDTA is a clear to slightly yellow solution prepared by dissolving Na_2EDTA2H2O salt in deionized water with NaOH. The EDTA solution used in this was purchased from Fisher Science at its maximum solubility (~10g/100mL water at room temperature) with pH adjusted to 12 and injected as pre-treatment undiluted.
- *Sodium triphosphate (STP)* is another widely used chelating agent. In this study, STP solution was prepared by dissolving white crystal $Na_5P_3O_{10}$ in DI water at its maximum solubility (14.5g/100mL water at room temperature). The prepared STP solution was mostly used for pre-treatment before polymer injection; however, it was also tested as an additive in the polymer dispersion. In addition, it is strongly advised that this procedure be done under a well-ventilated fume hood due to the toxicity of STP at high concentration.

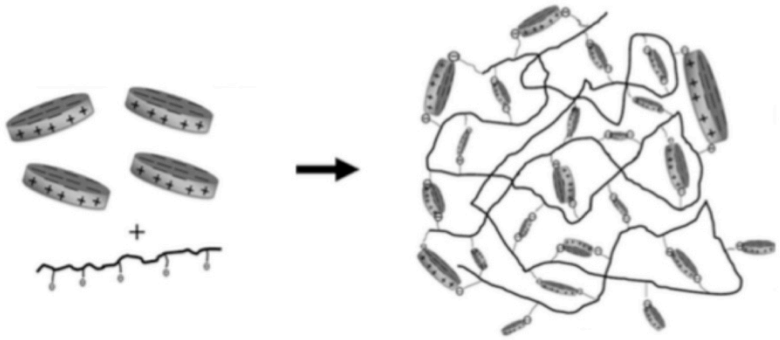

Figure 2.4: Gelation occurs due to electrostatic interaction between anionic polymer and cationic clay surface (Tongwa et al., 2013).

Another way to lessen the effect of polymer syneresis is to incorporate nanomaterial in to the hydrogel to improve the strength of gel structure in presence of divalent calcium ions:

- *Laponite* is a synthetic clay mineral that can be easily dispersed in water. Its disc-shaped clay particles (25-30 nm diameter × 1 nm thickness) develop more negative charges as pH increases, which can be used to attract and lock-in positively-charged calcium ions (Baghdadi et al., 2004). Laponite has positive charges on the edges that can easily attach to the negative charges on the polymer's backbone as illustrated in Figure 2.4. The resulting polymer-clay nanocomposite creates a three dimensional network that causes the mechanical properties of the gelant to increase (Haraguchi and Li, 2006; Schexnailder and Schmidt, 2008).

  Rheology tests (Figure 2.5) have been performed on 3 wt % Carbopol 934 that show yield stress increase when small amounts of Laponite was incorporated (Shafiei, 2015); the yield stress increase was the result of the alkalinity of Laponite. In this study, 0.2 wt% Laponite was used as an additive in 2 wt% Carbopol 934 to form the nanoclay-polymer solution. Since Laponite is highly alkaline, hydrochloric acid

(HCl) was slowly stirred into the solution until pH reaches 2.7 and viscosity was significantly decreased. This allows the solution to be injected into the cement core and tests the improved gel structure's resistance to calcium-induced syneresis.

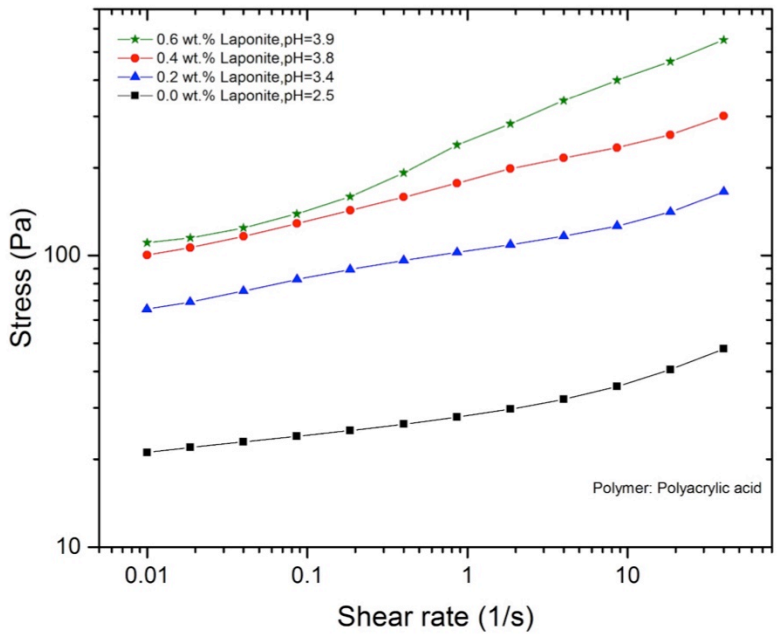

Figure 2.5: Effect of Laponite on yield stress of 3 wt% Carbopol 934 with no calcium content (Shafiei, 2015).

2.2 Core Preparation and Construction

2.2.1 Cement Preparation

Cement cores were created using class H neat cement that is widely used in the oil industry. Standard type cement should be prepared according to API specific water-content ratio to ensure complete hydration of cement compounds. Cement hydration is a major contributor to the resulting strength; it should be noted that excess water that is not hydrated could reduce cement strength and make it more porous and permeable. In this study, all cement was made following a water-content ratio of 38% for the Class H type

(API Spec. 10A, 2002). Measured amount of fresh water is placed in a mixer and mixed at 4000 rpm, and then the measured amount of dry cement was added rapidly and steadily into the agitated water. After dry cement is completely dissolved in water, the mixture is mixed at 12,000 rpm for about 45 seconds to one minute to form a thick cement slurry. The slurry is poured into a mold of specific dimensions and sealed to cure undisturbed for four days in an oven at 50°C and atmospheric pressure. This can speed up the initial cement hydration process, which develops most of its strength, as opposed to curing at room temperature for at least 30 days (long-term strength).

2.2.2 Cement-Cement Construction

Cylindrical cement core (1" diameter × 6" length) cured in a thin plastic tube was removed and sawed in half using a rock saw. The cement half is shown in Figure 2.6(a) has blade marks on the sawed surface that can provide a semi-smooth flow path and a small offset when two halves are re-constructed.

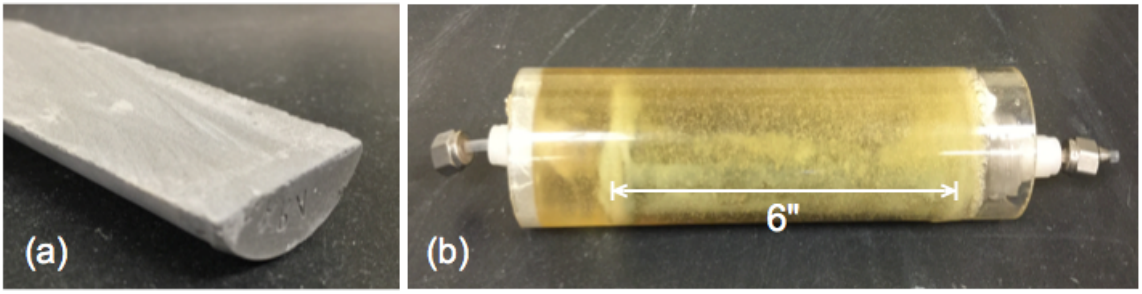

Figure 2.6: Cement-cement core preparation and construction (a) rough sawed cement surface, and (b) two halves epoxied in a polycarbonate tube with ends connected.

Two sawed cement surfaces were placed against each other and placed inside a polycarbonate tube filled with epoxy. The double-surface cement pathway was sealed

inside the tube with ends connected to inlet/outlet for injection as seen in Figure 2.6(b). This type of core allows double cement surface area to be in contact with polymer dispersion mimicking the actual cement fracture at the wellbore (Patterson, 2014).

2.2.3 Cement-Plastic Plate Construction

Smooth-surface cement cores (10" or 6" length × 1" width) were created using a mold made with thin plastic sheets cut to two specific dimensions (1" × 1" and 1" × 10") and constructed to form a rectangular prism with one 1"×10" side left open as illustrated in Figure 2.7(a). Cement slurry was poured and cured in the mold held together by waterproof duct tape; thus a smooth surface can be created upon removal from the mold as seen in Figure 2.8(a).

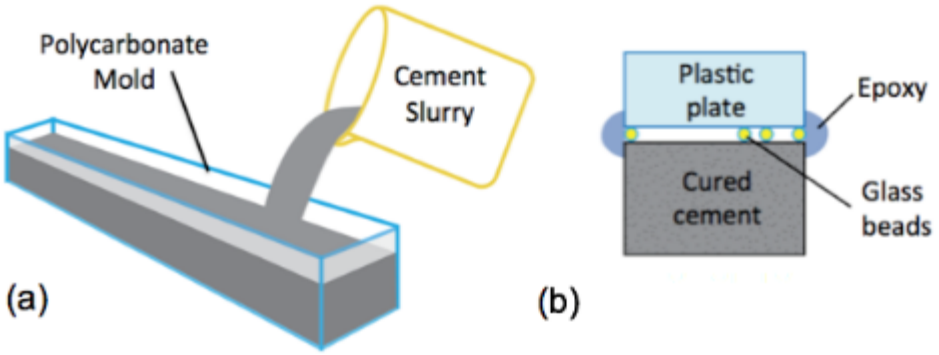

Figure 2.7: Illustrations of (a) plastic mold and (b) the construction of the cement-plastic plate core.

To construct the flow path, a smooth cement surface was placed against a transparent plastic plate with glass beads of known diameter (100-1000 microns) placed between as spacers in attempt to create desired fracture aperture. The fracture created by the cement and plastic plate was then sealed with epoxy around the fracture edges and cement while the front of the transparent plastic plate was left un-epoxied to allow visual

inspection of reactions in the fracture (Figure 2.8(b)). The cement-plastic construction would allow a homogeneous reaction between one cement surface with the polymer dispersion and simplifies the fracture geometry to aid reactive transport simulations.

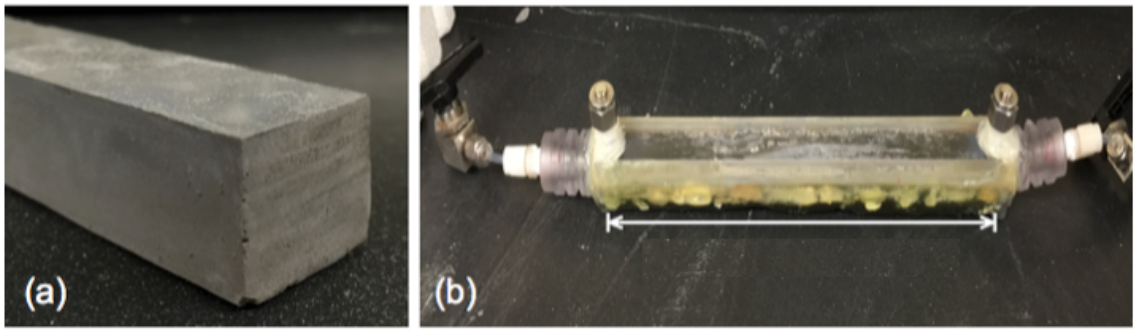

Figure 2.8: Cement-plastic core preparation and construction (a) smooth cement surface with glass beads, and (b) 6" or 10"-length cement with smooth surface placed against a polycarbonate plastic plate with back and sides expoxied.

2.2.4 The Brazilian Fracturing Method

The Brazilian fracturing method used in this study originated from the Brazilian test that is commonly used to determine the tensile strength of rocks (Guo et al., 1993). In the Brazilian test, most cylindrical rock specimens fail in tension, along the length of the core, when subjected to sufficient compressive loads. The same fracturing method is used for cement in attempt to create a tensile fracture mimicking natural formed fractures. The cylindrical cement core is placed laterally in a rock compressor consist of two disc-shaped load frame, and is then subjected to a compressive load large enough to fracture the cement.

Cement cores with diameter greater than 1" typically fractures the core into two halves forming an irregular tensile fracture along the length of the core as seen in Figure 2.9(a). Despite previous successes using the method for cores with larger diameters, all 7/8" cores shattered to pieces and failed to create a tensile fracture along the length of the

cores Figure 2.9(b). There seems to be a lower limit in core diameter for which the method could be used.

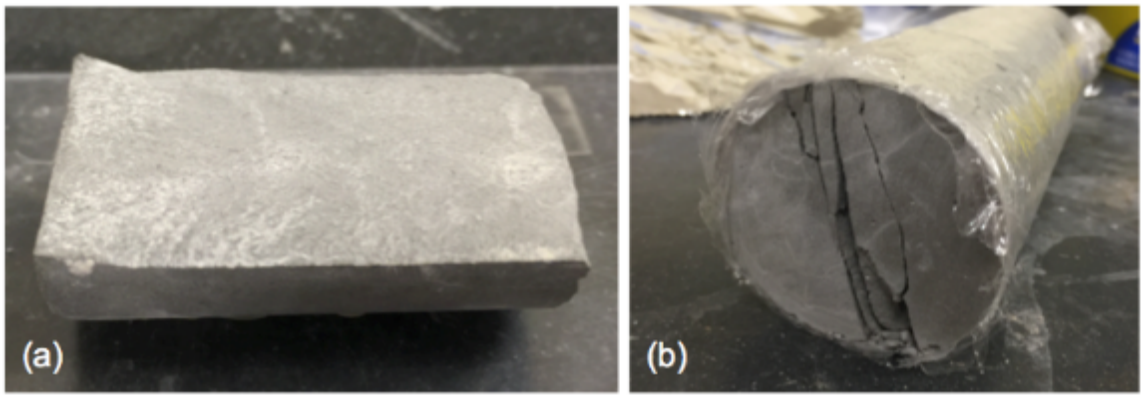

Figure 2.9: The Brazilian fracturing method (a) irregular tensile fracture, and (b) shattered cement core held together by plastic wrap.

2.3 FLOW EXPERIMENTS

2.3.1 Fracture Permeability Test

Sealed cement core is placed under the vacuum pump for at least 12 hours, then saturated with deionized (DI) water for at least 24 hours. A standard permeability test with the injection of DI water is performed at various flow rates while measuring pressure drop in order to determine the effective hydraulic aperture of the slit, B ("effective" because the slit's aperture changes along the length and width of the core),

$$B = \left[\frac{12\mu QL}{W\Delta P}\right]^{1/3}, \tag{2.1}$$

where μ is water viscosity, Q is volumetric flow rate, L is the length and W is the width of the fracture, and ΔP is the pressure drop across the length of the fracture (all units in SI). During DI water injection into the cement fractures, the flow rates 200, 160, 100, 20 mL/min are set by the pump while inlet and outlet pressures are recorded by a differential

pressure transducer. The pressure drops for the different flow rates are averaged and a hydraulic aperture is calculated for each flow rate. These hydraulic apertures are then averaged to obtain the estimated average hydraulic aperture, *B*. An example of the pressure response during a permeability test is shown below in Figure 2.10, with which the average aperture calculated from the four flow rates was 0.489 mm. This aperture can be used to determine the volume of the fracture and the apparent viscosity of the polymer during injection.

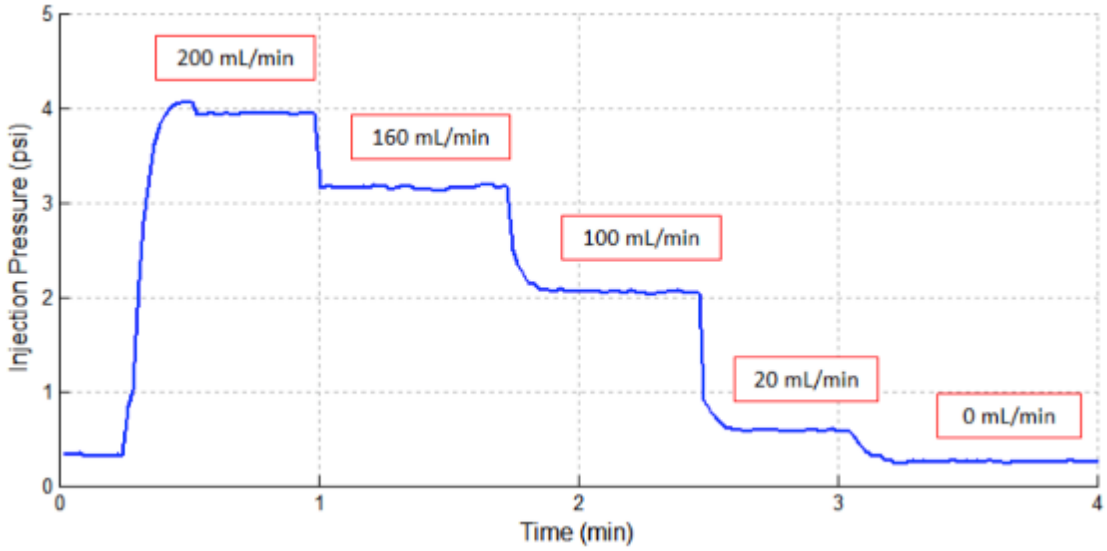

Figure 2.10: Standard permeability tests are performed to estimate the fracture hydraulic aperture (Patterson, 2014).

2.3.2 Pre-treatment and Polymer Placement

Although some experiments were carried out using syneresis inhibitors as additives in the polymer solution during polymer injection, the majority was conducted as separate pre-treatment for cement fractures before polymer injection. Because most syneresis inhibitors are very alkaline, it prematurely increases the pH and viscosity/yield

stress of the polymer when used as additives; thereby injection into cement fractures may be difficult.

Cement pre-treatment is performed by injecting syneresis inhibitors into the fracture volume and allowing time for chemicals to react with calcium ions leaching out from fracture surfaces. The calcium is captured in the reacted chemical then removed by polymer displacement. In some cases, it may be necessary to use DI water to flush out the pre-treatment solution before polymer injection to prevent premature gelling. Figure 2.11 is an illustration of the pre-treatment setup where two Chromaflex glass columns are used to hold and inject fluids. The purpose of placing a volume of mineral oil in between chemical and water from the pump is to prevent mixing as water displaces oil and drive chemicals into the core. In this study, most cores were pre-treated with syneresis inhibitors for durations between 10 minutes to 24 hours before polymer injections.

When polymer injection is performed, the glass columns must be replaced with a steel accumulator that is resistant to pressurized fluids. Pressure drop during polymer injection was recorded for some of the cores, to better characterize reactions in the fracture during injection and to determine polymer injectivity. For most other samples, one fracture volume of 3 wt% Carbopol 934 (dyed blue) was injected and shut for various periods of time to allow gel development.

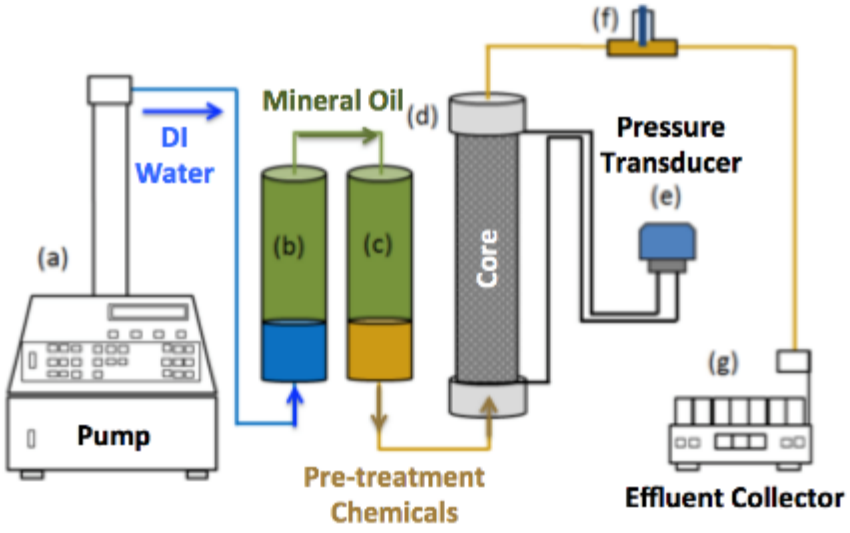

Figure 2.11: The experimental setup for pre-treatment of the cement core sample. (a) ISCO Syringe Pump, (b) Chromaflex glass column of oil (green) above DI water (blue), (c) Chromaflex glass column of oil (green) above pre-treatment solution (orange), (d) cement core sample, (e) differential pressure transducer, (f) pH probe, and (g) effluent collector. The polymer injection experiments are done under similar experimental set up by replacing (b) and (c) with a steel accumulator. In the accumulator, DI water is placed on one side of the piston and polymer dispersion is placed on the other side (Patterson, 2014).

2.4 Gel Strength Testing

2.4.1 Water Breakthrough Test

After the polymer placement and shut-in for different periods of time, water breakthrough tests were performed to obtain holdback pressure over the length of the cores. The test is used to determine the strength of the reacted gel that is formed in cement fracture samples. Both DI water and acidic brine are used as the holdback fluid to test the effect of an acidic environment on gel strength. During the test, pressure drop is increased gradually by pumping the holdback test fluid at a very slow rate (0.25 mL/min) to minimize the disturbance of the reacted gel structure in the fracture in order to mimic an instantaneous constant pressure applied against the placed gel. The maximum pressure

drop before liquid breakthrough occurred is recorded as the maximum holdback pressure and the holdback pressure gradient (psi/ft) was calculated based on the length of the core (either 6" or 10"). Thus, the gel in place is expected to hold back any constant pressure below the maximum holdback pressure. Figure 2.12 is a representation of a typical liquid breakthrough test. As this figure shows the pressure increases steadily until the maximum holdback pressure is reached and pressure drops drastically after the water is broken through the gel.

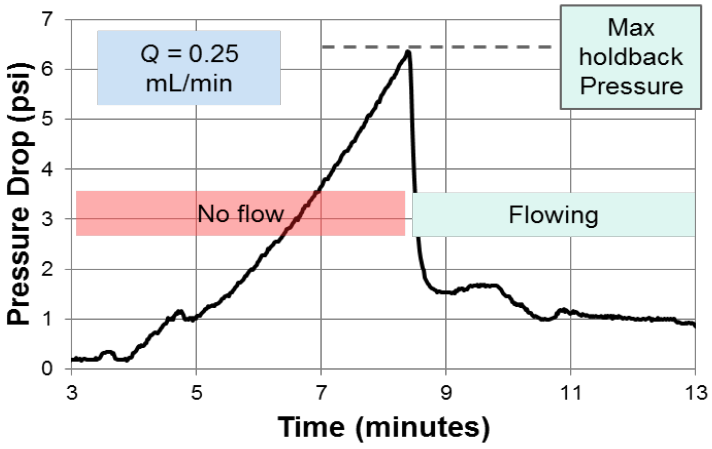

Figure 2.12: An example of gel resistance to pressure buildup in a standard liquid breakthrough test. The test is used to determine the strength of the reacted gel that was placed in the fracture. The holdback pressure gradient is a representation of the gel strength and can be compared to pressure gradients in existing leaky wellbore conditions (Patterson, 2014).

The holdback pressure gradients of the gel were then compared with the theoretical pressure gradients calculated from the gel yield stresses measured in polymer rheology experiments. Theoretical pressure gradients can be calculated by

$$\left(\frac{\Delta P}{\Delta L}\right)_{theoretical} = \frac{2 \cdot \sigma_y}{r_H}, \tag{2.2}$$

where σ_y is the polymer-gel yield stress (psi) and r_H is the hydraulic radius of the aperture calculated by

$$r_H = \frac{A}{P} = \frac{W \cdot B}{2(W + B)}, \tag{2.3}$$

where W is the core width and B is the effective fracture aperture.

In addition to the above gel strength tests with the water injection, the gel strength tests with injection of acidic brine, and also with CO_2 gas plume, were made. Several liquid breakthrough tests were done by injecting acidic brine that was made by adding HCl into 2 wt% NaCl until pH 2 was reached. A flow chart of the standard procedure performed in this study is illustrated in Figure 2.13. The exact details may be slightly different for individual experiments; the procedures are more or less the same.

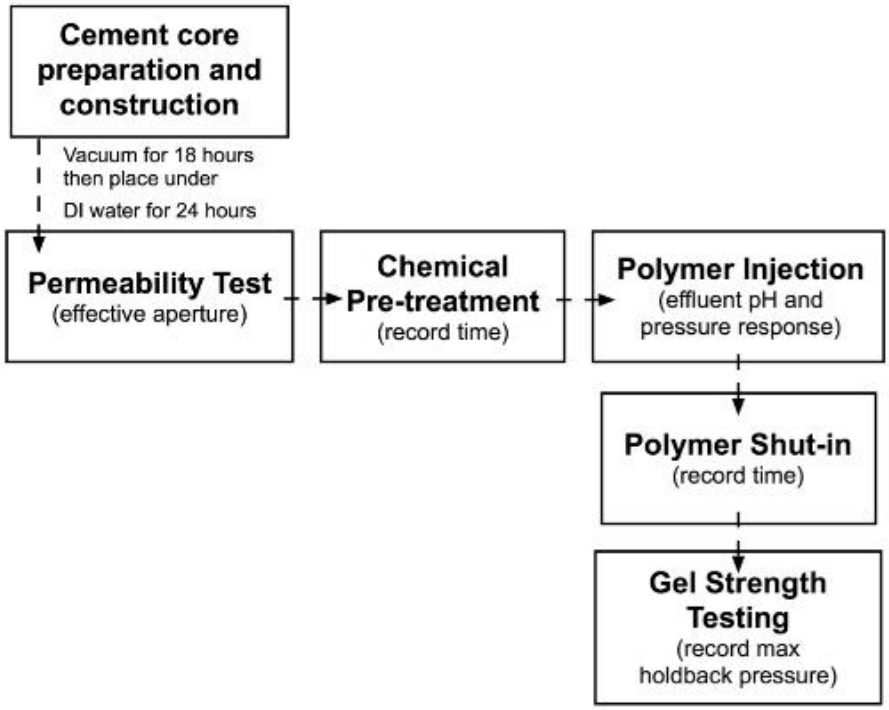

Figure 2.13: Flow chart of standard procedures performed in this study.

2.5 CO_2 Breakthrough Tests

2.5.1 Core Preparation

The 7/8" and 1 7/8" diameters were chosen for the cement core in consideration for the thickness of heatshrink wrapping before fitting into the Hassler coreholders. Heatshrink wrapping is a precautionary procedure as to prevent chemicals or CO_2 from damaging the hydraulic rubber sleeve inside the coreholder. 7/8" diameter × 6" length cylindrical cores are cored from a cured cement block (6"× 6"× 8") and wrapped tightly with one layer of Teflon tape. The wrapped core is then fractured into pieces using the Brazilian method, as previously mentioned, with Teflon wrapping keeping the pieces intact. The resulting cement fracture is not a single tensile fracture and its fracture geometry is unknown. 1 7/8" diameter × 6" length cylindrical cores are cored from the

cured cement block and sawed in half with a rock saw. Table 2.2 lists the dimensions and details of the cement cores used.

Table 2.2: Dimensions and detail of the cement cores prepared for CO_2 breakthrough tests. Heatshrink wraps were purchased from Geophysical Supply Company (Houston, Texas).

Pressure Holdback Test	**Cement Core Dimension** (diameter x length)	**Coreholder Dimension** (diameter x length)	**Fracture Method**	**Heatshrink Wrapping** (diameter)
Low Pressure CO2	7/8" x 6"	1" x 1'	Brazilian	1.5"
High Pressure CO2	7/8" x 6"	1" x 1'	Brazilian	1.5"
High Pressure CO2	1 7/8" x 6	2" x 1'	Sawed	2"

A 6" steel spacer is placed before the 6" Teflon wrapped core to extend total length to 1 ft. Two end connections from the coreholder are placed at both ends of the extended core, then slid into a 1.5" heatshrink wrap tube with length sufficient to wrap at least ½" of each end connections. It is necessary to have heatshrink wrap longer than the length of the inserted core to effectively prevent chemicals or CO_2 from contacting the rubber sleeve inside the coreholder. The entire construction is then placed in an oven set at 50°C for 10-15 minutes until it can be held tightly by heatshrink. The construction with enclosed fractured cement is loaded into the Hassler coreholder, then vacuumed and soaked with DI water under a confining pressure. The Hassler coreholders used in this study were manufactured by Pheonix Instruments with different dimensions and pressure limits as seen in Figure 2.14.

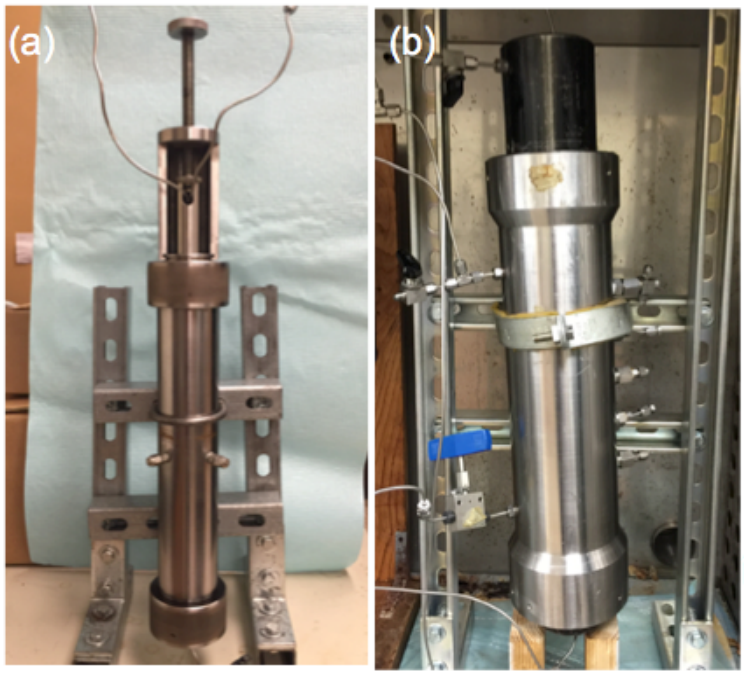

Figure 2.14: Specifications of the 12”-long steel coreholders manufactured by Pheonix Instruments (a) 1” diameter Hassler coreholder (working pressure: 1250 psi), and (b) 2” diameter Hassler coreholder (working pressure: 5000 psi).

The main advantage of using the Hassler coreholder is that tests can be performed at higher pressures (> 100 psi) and remain sealed for longer durations without premature termination due to core material failure. In case of a leak in the wrapped core, selection of the hydraulic rubber sleeve depends on the fluid used in the experiment: Viton tubing is resistant to chemical and most hydrocarbon exposure, while Aflas is good for CO_2 exposure.

2.5.2 Low-Pressure CO_2 Test

A preliminary CO_2 holdback test was carried out in low-pressure setting (under 100 psi) to determine if gel would be weakened when placed in contact with pressurized CO_2 gas for an extended time. The experiment was done in a Hassler

coreholder with a fractured 7/8" × 6" cylindrical cement. A confining pressure set at 100 psi was used throughout the procedures. Figure 2.15 is the experimental setup. The Hassler coreholder was connected to the CO_2 cylinder (full tank at 800 psia) through two pressure regulators to step down the pressure. During the test, the pressure transducer measured and recorded the pressure drop across the length of the core. When the reacted gel in the cement fracture sample was broken through, the pressure drop is expected to drop and the CO_2 will bubble through the outlet, which will be seen in the beaker filled with water. The inlet pressure was initially set at 5 psi and increased by 5 psi over the course of 30 minutes until maximum gauge pressure was reached at 30 psi and left to hold back this constant pressure for two weeks until a second breakthrough test was done with pH 4 acidic brine (2 wt% NaCl).

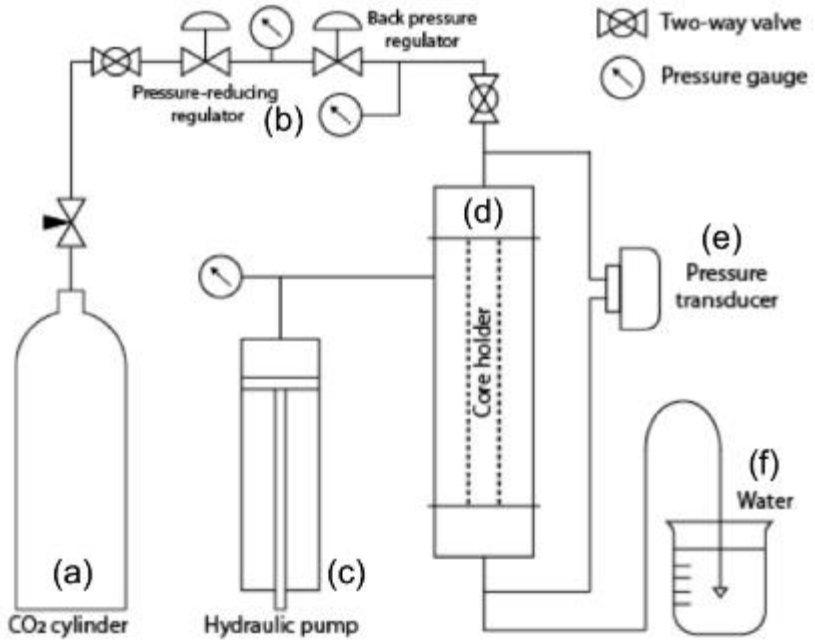

Figure 2.15: The experimental setup for low-pressure CO_2 breakthrough test done at standard conditions: (a) CO_2 cylinder tank (CO_2 > 99% purity) from Matheson Tri-Gas Inc (Basking Ridge, NJ), (b) pressure-reducing and back-pressure regulators from Swagelok Inc., (c) Enerpac P-392 hydraulic hand pump, (d) 1" Hassler coreholder, (e) Rosemount pressure transducers, and (f) beaker filled with water.

2.5.3 High-Pressure CO_2 Test

Two high-pressure CO_2 tests were performed to determine polymer gel's resistance to supercritical CO_2 to mimic geological storage conditions. CO_2 can be compressed to reach supercritical state when both temperature and pressure equal or exceed its critical point of 31°C and 1073 psi.

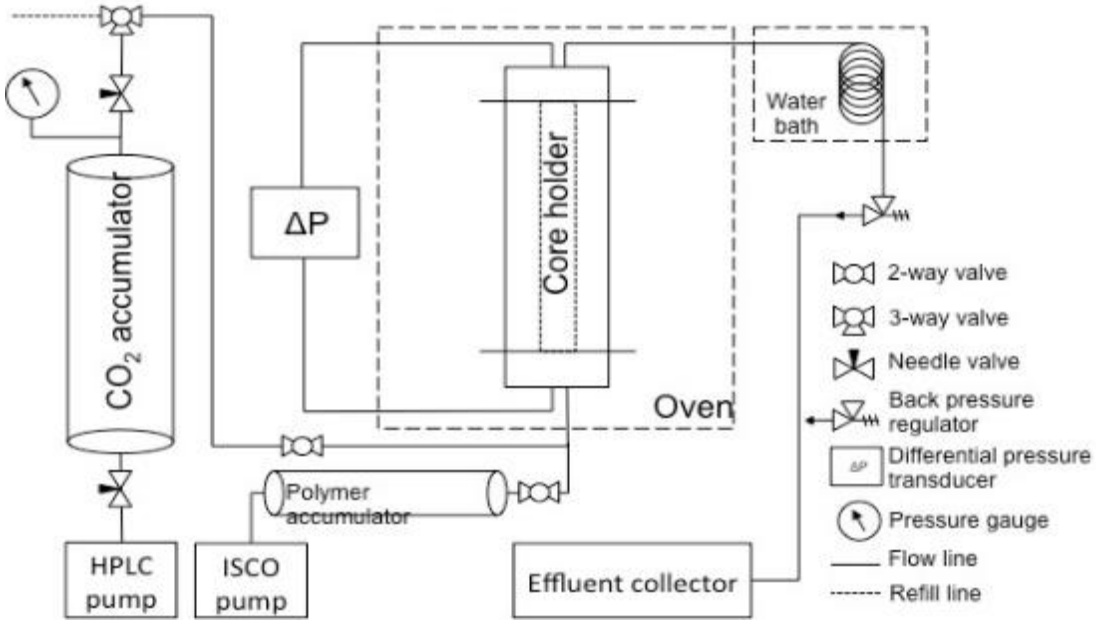

Figure 2.16: Supercritical CO_2 holdback test setup. The fractured cement core is placed into a Hassler coreholder under a fixed temperature in the oven (a). The ISCO pump (b) can be used to pump the pre-treatment fluid and polymer dispersion pre-filled in an accumulator (c). After the polymer placement and shut-in for a period of time to develop yield stress, a separate line can be used to inject supercritical CO_2 from the floating-piston accumulator (d) pressurized by a HPLC dual piston pump (e). Various reasonable pressure gradients will be set across the core with the use of the back-pressure regulator (f) and the pressure transducers (g). The effluent supercritical CO_2 will pass through a heated water bath (h) to prevent the CO_2 from freezing the tubings cause by the sudden pressure drop. Cooled CO_2 effluent is then collected through the effluent collector (i) and redirected to a fume hood.

The coreholder was placed in an oven set at 70°C with inlet connected to the CO_2 accumulator and outlet connected to a back-pressure regulator (BPR). The BPR is pre-set at 1100 psi prior to the start of the experiment to ensure pressure in the coreholder remain above supercritical state unless core is broken through. Pressure transducers connected to the inlet and outlet of the coreholder measures the pressure buildup during the holdback and detects pressure drop when CO_2 breaks through. Once pressure in the CO_2 accumulator reach above 1100 psi, supercritical CO_2 is let into the core and pressure

starts to build up as the HPLC pump continues to pump supercritical CO_2. Once the gel is broken through, effluent CO_2 is cooled down by flowing in the coiled outlet line submerged in a hot water bath set at 70°C to prevent freezing caused by dramatic pressure decrease. Effluent is then redirected to a fume hood.

2.6 CEMENT ANNULUS BENCH TESTS

The setup is analogous to a real cement wellbore in a shallow formation. The cement annulus is created using two pipes that differ in diameter; where the smaller inner pipe mimicking a steel casing, and the larger pipe mimicking an openhole condition in an impermeable formation. Manmade-fractures are created inside the annulus to mimic leakage pathways where the polymer could be inserted and gel strength could be tested under ambient conditions.

2.6.1 Preparation

Two pipes are used to create a cement annulus: the small 1" inner pipe and the large 2.5" outer pipe (with the bottom sealed by a cap). First, a removable PVC cap is used to cap the bottom of the large pipe and 2" of sand is placed at the bottom section. Second, a slightly longer inner pipe is placed in the middle of the large pipe and pushed down into the bottom sand. Cement slurry is poured in slow circular motion into the annulus space to minimize air pockets that can form in the cement annulus; with one inch length from the top of the annulus left unfilled.

To create a long vertical channel, a straightened 1.5 mm metal wired is greased and inserted into the cement annulus. The cement is then left undisturbed for 24 hours before the greased wire is pulled out. The bottom cap is removed and sand is cleaned out. Finally, the removable cap is glued to the bottom with PVC glue. Figure 2.17 is illustration of the construction. To make fractured cement annulus, another bench test

was created using the same method but uses a flexible Tygon tubing as the outer pipe. The cement annulus is set for 24 hours without inserting a wire. The random fractures were later created by hammering the outer Tygon tubing.

.

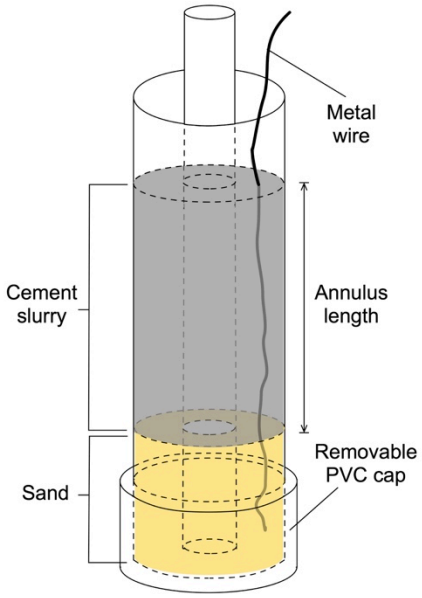

Figure 2.17: Cement annulus bench test construction and setup. The bottom of the large pipe is capped with a PVC cap. Sand is placed in the pipe at the bottom with the inner tube pushed into the sand. Cement slurry is poured into the annulus space and a metal wire is inserted all the way to the bottom of the cement to create a leakage channel. After the cement sets, the bottom cap and wire are removed and sand is cleaned out. Finally, the PVC cap is glued to the bottom of the large pipe ready for chemical pre-treatment and polymer injection.

2.6.2 Procedure

Both types of cement annulus bench tests are pre-treated with sodium triphosphate for 24 hours, then injected with polymer until polymer immerge from the top of the annulus. Subsequently, the top of the annulus is added with some water and sealed up with parafilm to prevent dehydration. The injected polymer in cement annulus is left to shut-in for more than 24 hours. After polymer shut-in, top of the hollow inner tubing is

connected to compressed air so that a constant pressure can be applied to the bottom of the sealed annulus as seen in Figure 2.18. The constant pressure applied is set according to a reasonable static holdback pressure gradient of around 15 psi/ft. This constant pressure gradient is monitored for one week before moving on to higher pressure gradients for testing maximum holdback pressure for breakthrough.

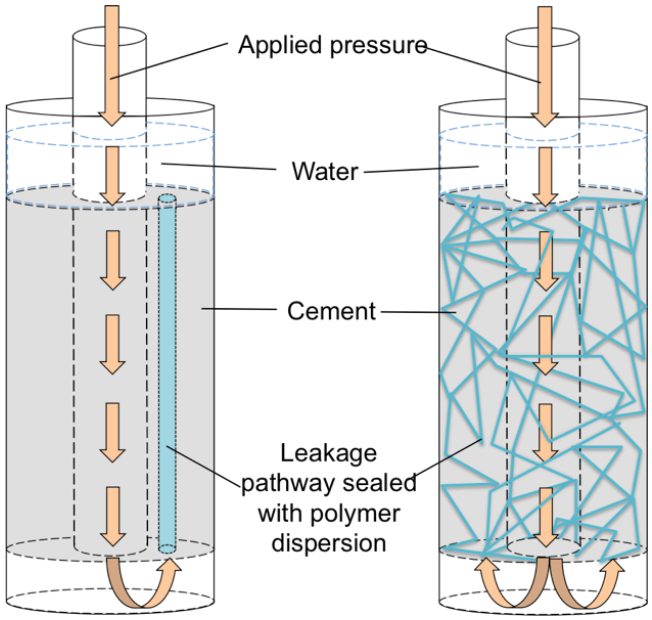

Figure 2.18: Cement annulus bench test with channel pathway PVC-1 (left) and fractured pathway TYG-1 (right), then applied with a constant pressure at the bottom by hooking the top of the inner pipe to stream of compressed air for a period of time. If the seal held over time, a gel strength testing with higher pressure can be done with the increase of compressed air pressure until the gel is broken through.

Chapter 3: Results and Discussion[3]

3.1 Polymer Injection and Results

This section lists the 18 cement corefloods and 2 cement annulus bench tests done in this study. Labeling of each coreflood is based on the cement length, core construction and the order the experiment was performed. The label starts by using numbers to specify the length (in inches) of the core (e.g., 6FP-34 is 6" and 10FP-36 is 10"); then followed by letters to indicate the type of core construction (e.g., 6CF-36 is a cement-cement fracture core, 10FP-36 is a cement-plastic plate core and 6CHass-1 is a cement coreflood performed in a Hassler coreholder). Lastly, the number following the dash indicates the sequence in which the coreflood was performed.

In this section, the pressure data, effluent pH, and visual observations from all the corefloods and cement annulus tests are presented first. The comparison of the results to understand the sealing mechanisms and the parameters that control the sealing behavior is then provided in the subsequent sections.

---

[3] Ho, J.F., Patterson, J.W., Tavassoli, S., Shafiei, M., Balhoff, M.T., Huh, C., Bommer, P.M., and Bryant, S.L., 2015. The use of a pH-triggered polymer gelant to seal cement fractures in wells. Presented at the Society of Petroleum Engineers (SPE) Annual Technical Conference and Exhibition (ATCE), Houston, Texas, U.S.A., 28-30 September. SPE-174940-MS

Contributions: J.F.Ho and J.W.Patterson were involved in the design and performance of laboratory experiments. M.Shafiei was involved in the acquisition of rheological data. J.F.Ho, J.W.Patterson, M.T.Balhoff, C.Huh, P.M.Bommer, and S.L.Bryant were involved in the conception and analysis of the work. J.F.Ho, J.W.Patterson, and S.Tavassoli were involved in the drafting and revision of the manuscript.

3.1.1 Cement-Cement Fractures

3.1.1.1 Core 6CF-36

Experiments 6CF-36 and 6CF-39 are constructed using two cylindrical halves cement which doubles the cement surface area when reacting with polymer gel. Both cores have similar apertures and were shut-in for 2 weeks followed by water breakthrough test using pH 4 acidic brine (2 wt% NaCl pH lowered by HCl). 6CF-36 had a longer $Na_5P_3O_{10}$ pre-treatment time of 24 hours, while 6CF-39 was treated for only 10 minutes.

Core	Fracture Type	Aperture	Pretreatment Fluid and Time	Injected Solution	Volume Injected
6CF-36	Cement-Plastic Smooth	0.436 mm	12 wt% $Na_5P_3O_{10}$ 24 hours	3 wt% Carbopol 934	1 FV

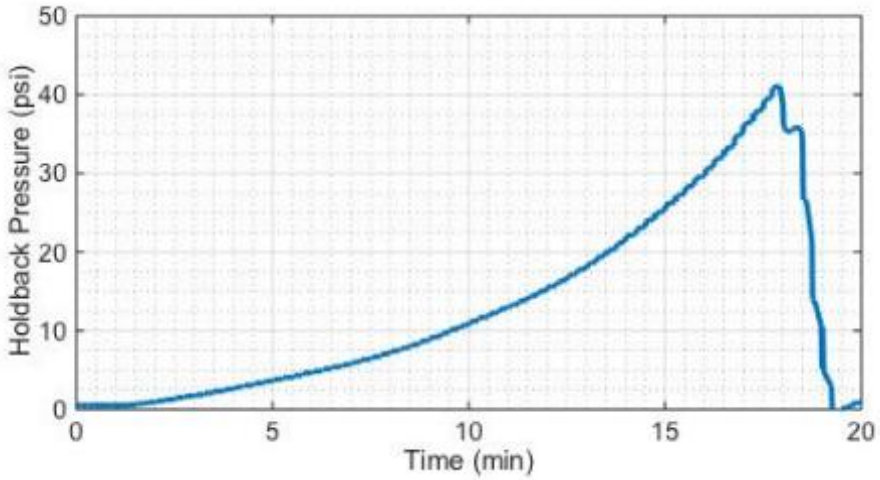

Figure 3.1: Pressure response during gel strength testing of 6CF-36 after 2 weeks polymer shut-in (24-hr $Na_5P_3O_{10}$ pre-treated core). Core dimensions: effective aperture 436 microns × 6 inch in core length.

Core 6CF-36 was pre-treated with 12 wt% $Na_5P_3O_{10}$ for 24 hours before being injected with 3 wt% Carbopol 934. The gel-in-place was able to hold back a pressure gradient of 82.3 psi/ft as seen in Figure 3.1.

3.1.1.2 Core 6CF-39

Core 6CF-39 was pre-treated with 12 wt% $Na_5P_3O_{10}$ for only 10 minutes before being injected with 3 wt% Carbopol 934. The gel-in-place was able to hold back a pressure gradient of 104.1 psi/ft as seen in Figure 3.2. The result of a higher holdback pressure gradient for only 10 minutes of pre-treatment, although close to the 82.3 psi/ft for 24 hour pre-treatment (6CF-36), indicates that gel strength and stability may not have a strong dependency on the pre-treatment time.

Core	Fracture Type	Aperture	Pretreatment Fluid and Time	Injected Solution	Volume Injected
6CF-39	Cement-Plastic Smooth	0.463 mm	12 wt% $Na_5P_3O_{10}$ 10 minutes	3 wt% Carbopol 934	1 FV

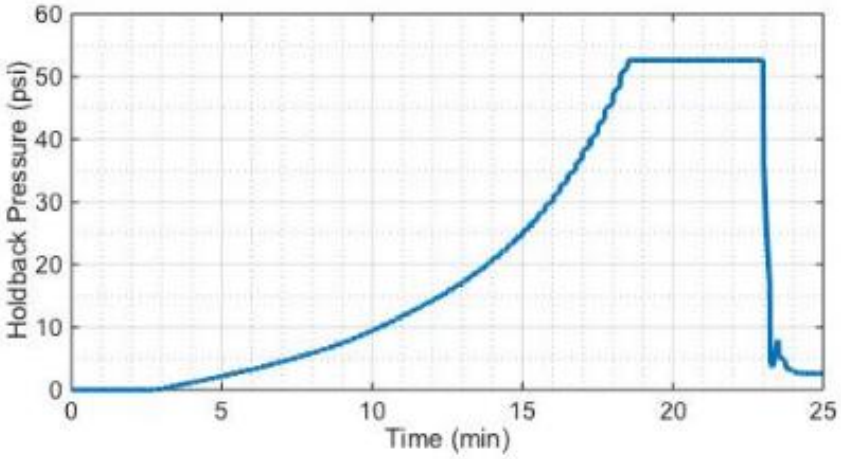

Figure 3.2: Pressure response during gel strength testing of 6CF-39 after 2 weeks polymer shut-in (10-min $Na_5P_3O_{10}$ pre-treated core). Core dimensions: effective aperture 463 microns × 6 inch in core length.

3.1.2 Cement-Plastic Fractures

3.1.2.1 Core 6FP-29

Injection experiment 6FP-29 tested the addition of Laponite in the injected polymer solution. Since the Laponite is alkaline, hydrochloric acid was added to the

solution to lower the pH to 2.7, which lowers the viscosity of the polymer solution for injection. The purpose of adding Laponite into the polymer dispersion was to prevent high concentration of calcium cations in the cement from collapsing the polymer gel and promoting syneresis.

Core	Fracture Type	Aperture	Injected Solution	Injection Rate	Volume Injected
6FP-29	Cement-Plastic Sawed	0.1624 mm	2 wt% Carbopol 934 0.2 wt% Laponite, HCl (pH starting at 2.7)	1.00 mL/min	172 FV

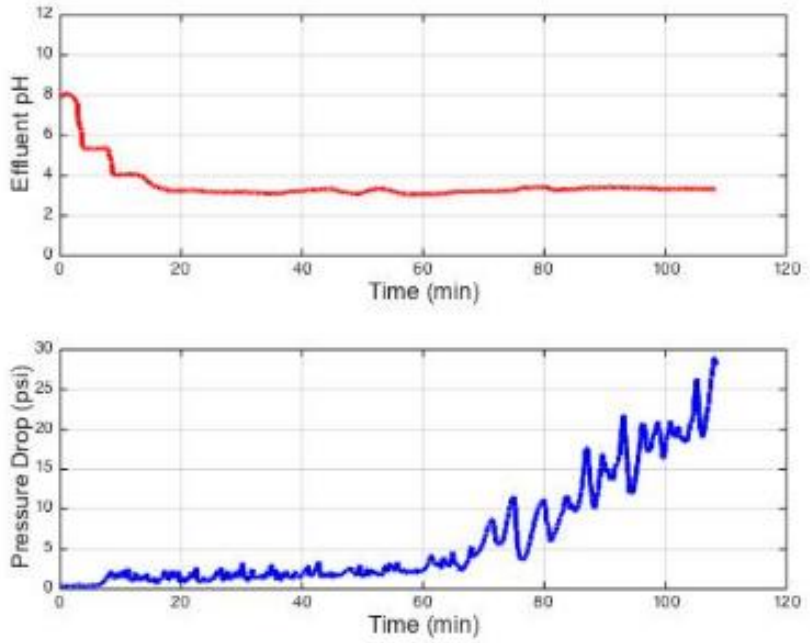

Figure 3.3: Effluent pH and pressure response during (2 wt% Carbopol 934, 0.2 wt% Laponite mixture) polymer injection of EDTA pre-treated core (6FP-29, effective aperture 162 microns) at 1 mL/min.

The pressure drop remained steady during the first hour of injection while a flow path was forming in the core as seen in Figure 3.3. After the first hour, the pressure started to increase at about 0.45 psi/min. The effluent pH remained steady at around pH

3.25 after injecting 16 FV. The injection was terminated when the pressure drop reached 30 psi due to the pressure limitation of the pump.

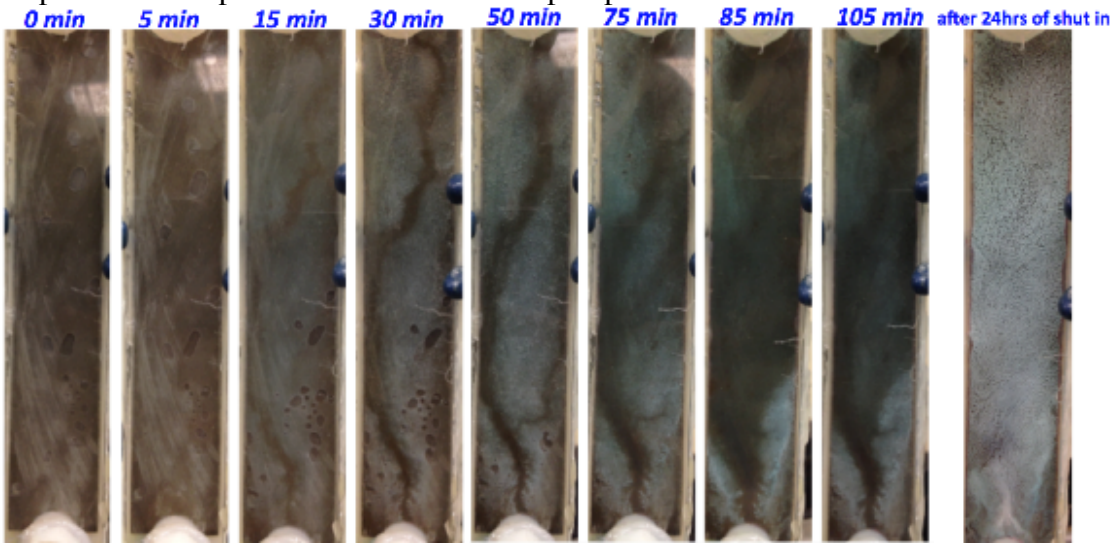

Figure 3.4: Visual inspection of polymer-cement reaction on sawed fracture surface during polymer injection (polymer flow from bottom to top) and after 24-hour polymer shut-in (6FP-29).

Core 6FP-29 was shut-in for 24 hours after polymer injection. Grainy-white precipitation formed evenly on the fracture surface (Figure 3.4). The core was then placed under a 2.6 psi/ft pressure holdback with 2 weight percent NaCl solution. At first, it was assumed that the white precipitation was calcified gel from syneresis, however, the white precipitation started to disappear and became transparent over the course of a week (Figure 3.5). This indicates that the precipitation may not be calcified gel as we know syneresis is not reversible. The core held a pressure gradient of 2.6 psi/ft for several months.

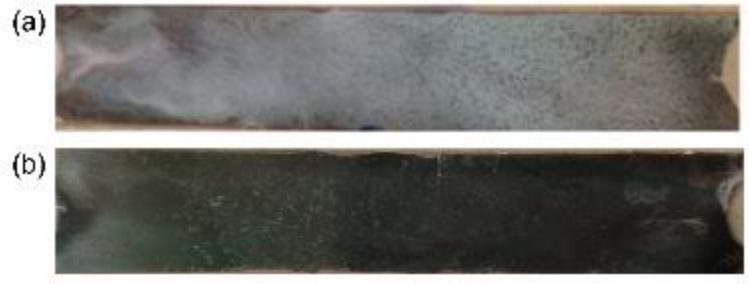

Figure 3.5: Visual inspection of core 6FP-29 (a) after 24-hour polymer shut-in and (b) after 1 week polymer shut-in.

3.1.2.2 Core 6FP-30

Core 6FP-30 was pre-flushed with EDTA tetrasodium salt (activity at 40%) for an hour, then shut in for 24 hours before the polymer injection experiment. Polymer dispersion was injected following the EDTA shut in (without DI water pre-flush), which resulted in the polymer solution immediate reaction with the highly alkaline EDTA inside the fracture causing the pH and the viscosity to increase rapidly. The pressure drop reached 15 psi over the first 12 minutes and caused core holder to leak, thus experiment was terminated (Figure 3.6).

Core	Fracture Type	Aperture	Injected Solution	Injection Rate	Volume Injected
6FP-30	Cement-Plastic Sawed	0.2437 mm	2 wt% Carbopol 934	1.00 mL/min	36 FV

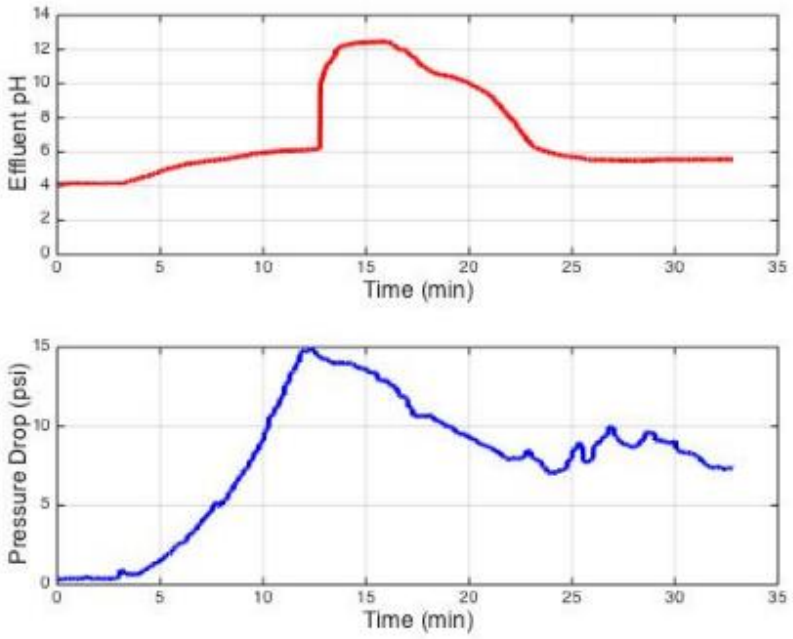

Figure 3.6: Effluent pH and pressure response during 2 wt% Carbopol 934 polymer injection of EDTA pre-treated core (6FP-30, effective aperture 244 microns) at 1 mL/min. The core was not pre-flushed with DI water before polymer injection. Resulted in early termination.

3.1.2.3 Core 6FP-31

Core 6FP-31 was pre-treated with hydrochloric acid at pH 1.15 for 36 hours to dissolve unwanted minerals near the fracture surface without allowing iron precipitation to form on the surface. The core was then pre-treated with EDTA tetrasodium salt (activity at 40%) as a chelating agent for 24 hours. The core was pre-flushed with DI water before polymer injection to clear out the EDTA in the fracture to prevent rapid gelling of the polymer solution.

Core	Fracture Type	Aperture	Injected Solution	Injection Rate	Volume Injected
6FP-31	Cement-Plastic Sawed	0.2153 mm	2 wt% Carbopol 934	1.00 mL/min	96 FV

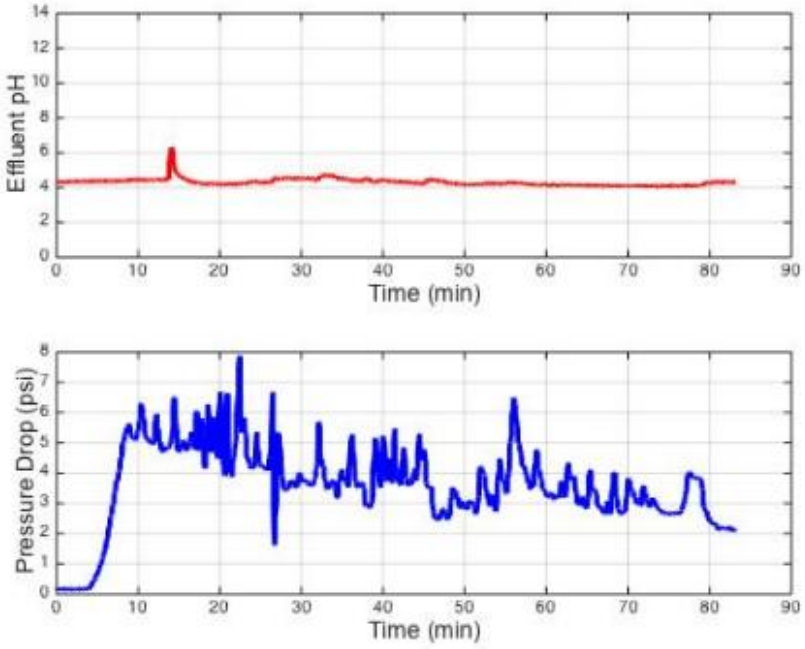

Figure 3.7: Effluent pH and pressure response during 2 wt% Carbopol 934 polymer injection of EDTA pre-treated core (6FP-31, effective aperture 215 microns) at 1 mL/min. The core was pre-flushed with DI water before polymer injection.

Figure 3.7 shows effluent pH remained fairly constant at about pH 4.2 during the injection. The pressure drop increased to about 5.5 psi during the first 10 minutes then gradually decreased at about 0.04 psi/min. Sections of gel rearrangement were observed during injection causing temporary blockage and breakthroughs in the fracture and sudden changes in pressure drop. Core 6FP-31 was then shut in for one week during which no white precipitation was formed in the fracture.

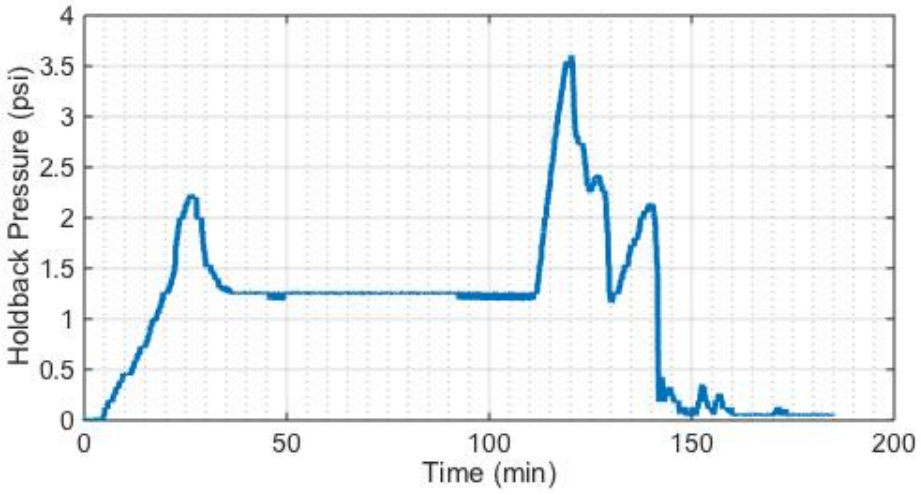

Figure 3.8: Pressure response during gel strength testing of 6FP-31 after one week of polymer shut-in (EDTA pre-treated core injected with 2 wt% Carbopol 934). Core dimensions: effective aperture 215 microns × 6 inch in core length.

Flow initiation pressure test (red DI water injected at 0.1 ml/min) was performed after the one-week shut-in (Figure 3.8). After the first 30 minutes of injection, a small breakthrough was seen at the inlet while gel continued to hold pressure at 1.3 psi. Injected DI water completely broke through the gel in the core after 120 minutes of injection at 3.6 psi and a distinct flow path can be seen in the fracture (Figure 3.9). The gel was able to hold back a pressure gradient of 7.2 psi/ft during flow initiation pressure injection.

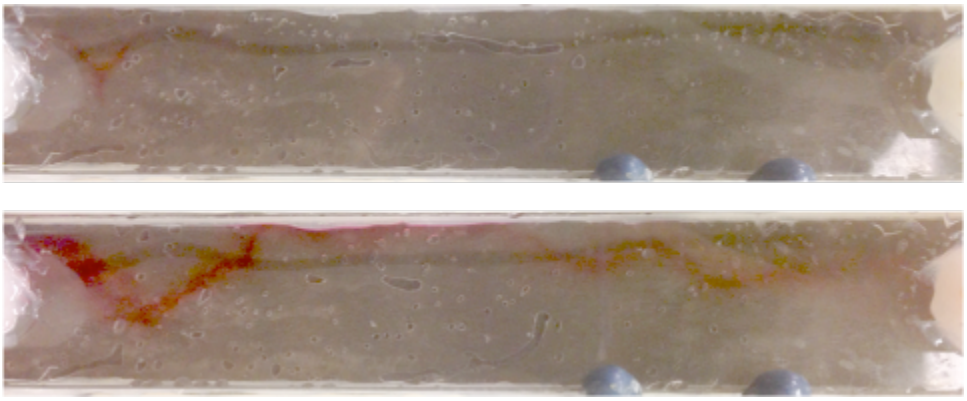

Figure 3.9: Visual observation during gel strength testing of 6FP-31 after one week polymer shut-in (a) small breakthrough after 30 minutes (left) and (b) complete breakthroght after 120 minutes. (EDTA pre-treated core injected with 2 wt% Carbopol 934). Core dimensions: effective aperture 215 microns × 6 inch in core length.

3.1.2.4 Core 6FP-33

Sodium triphosphate, 4 wt% $Na_5P_3O_{10}$ was mixed in to the polymer dispersion, and the mixture was injected into core 6FP-33 without any pre-treatment. Figure 3.10 and Figure 3.11 show the effluent pH, pressure response and visual inspection during polymer injection. Flow initiation pressure test was preformed after injecting 112 fracture volumes of the mixture followed by a 24-hour shut in. The reacted gel was able to hold back a pressure gradient of 58 psi/ft during flow initiation pressure injection as seen in Figure 3.12.

Core	Fracture Type	Aperture	Injected Solution	Injection Rate	Volume Injected
6FP-33	Cement-Plastic Sawed	0.1379 mm	3 wt% Carbopol 934 4 wt% $Na_5P_3O_{10}$	1.00 mL/min	112.4 FV

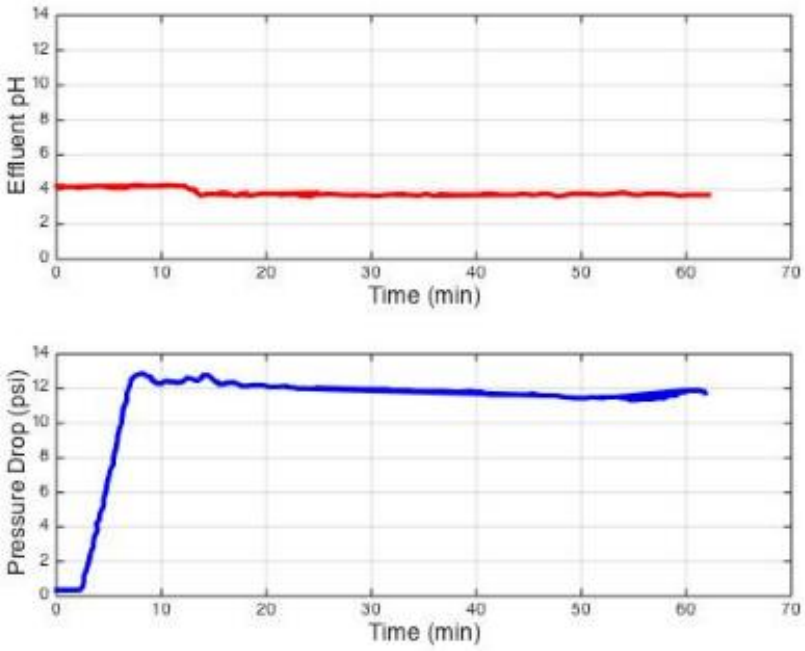

Figure 3.10: Effluent pH and pressure response during (3 wt% Carbopol 934, 4 wt% $Na_5P_3O_{10}$ mixture) polymer injection of core 6FP-33 (effective aperture 138 microns) at 1 mL/min.

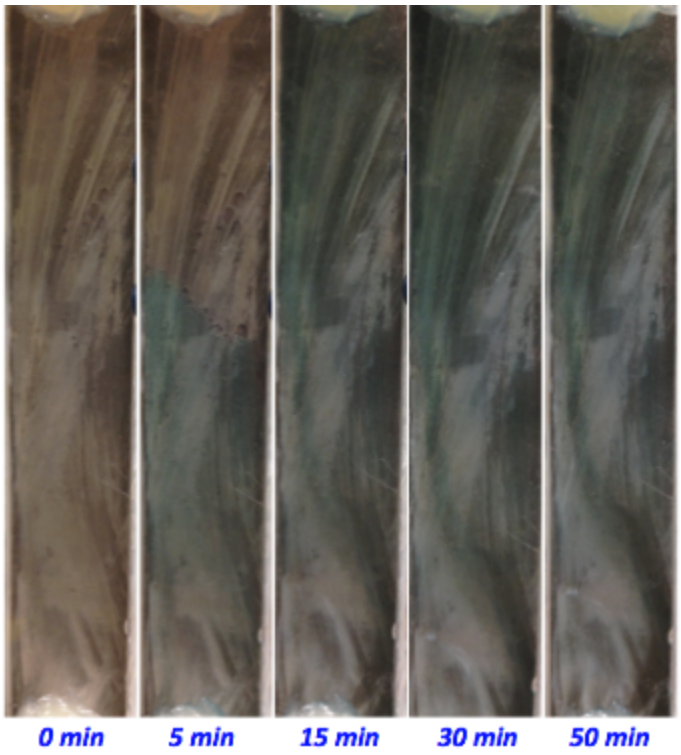

Figure 3.11: Visual inspection of polymer-cement reaction on sawed fracture surface during polymer injection 6FP-33 (polymer flow from bottom to top).

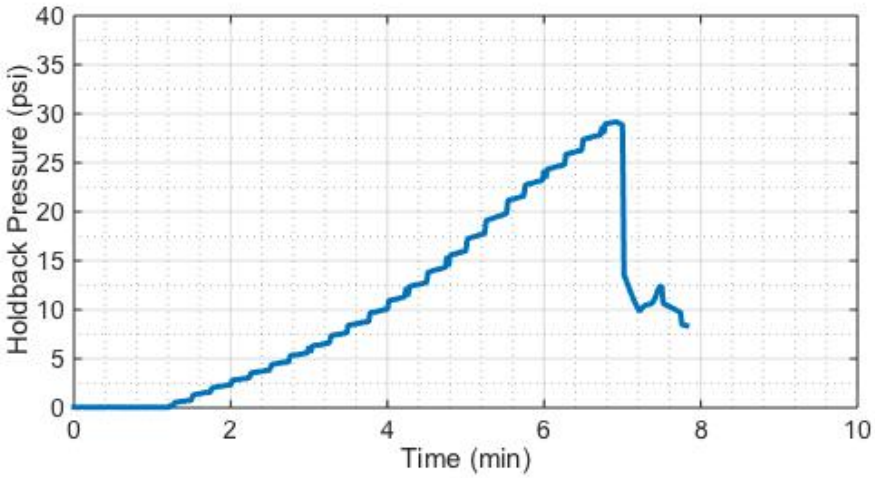

Figure 3.12: Pressure response during gel strength testing of 6FP-33 after 24-hour polymer shut-in (core injected with 3 wt% Carbopol 934, 4 wt% $Na_5P_3O_{10}$ mixture). Core dimensions: effective aperture 138 microns × 6 inch in core length.

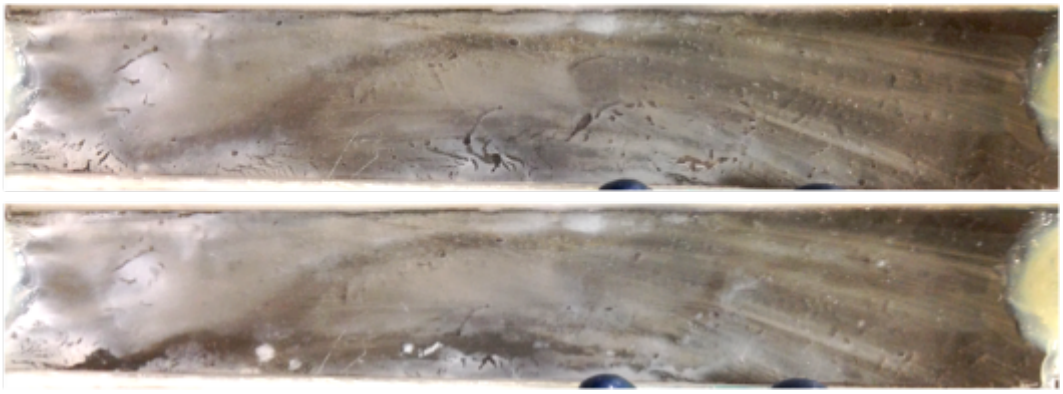

Figure 3.13: Visual inspection of 6FP-33 (a) after 24-hour polymer shut-in (b) during gel strength testing (holdback fluid injected from left to right). The fluid broke through from the most syneresed region where gel shrinkage and expelled water can be seen.

An apparent flow path, where the fracture had wider aperture, was observed during injection; reacted gel remained clear during injection and after 24 hour shut in. However, area with narrow aperture showed syneresis very early after the injection most likely due to relatively less calcium removal by $Na_5P_3O_{10}$ in the mixture. These areas have weak gel strength that initiated water breakthrough observed during the flow initiation pressure test (Figure 3.13).

3.1.2.5 Core 6FP-34

Core 6FP-34 was pre-treated with 12 weight percent $Na_5P_3O_{10}$ for 24 hours, and then was injected with 98 fracture volumes of polymer dispersion. Figure 3.14 and Figure 3.15 show the effluent pH, pressure response and visual inspection during polymer injection. Two water breakthrough tests were done on 6FP-34 over different shut-in times.

Core	Fracture Type	Aperture	Injected Solution	Injection Rate	Volume Injected
6FP-34	Cement-Plastic Sawed	0.1583 mm	3 wt% Carbopol 934	1.00 mL/min	98 FV
Pre-soaked with $Na_5P_3O_{10}$ for 24 hours before polymer injection					

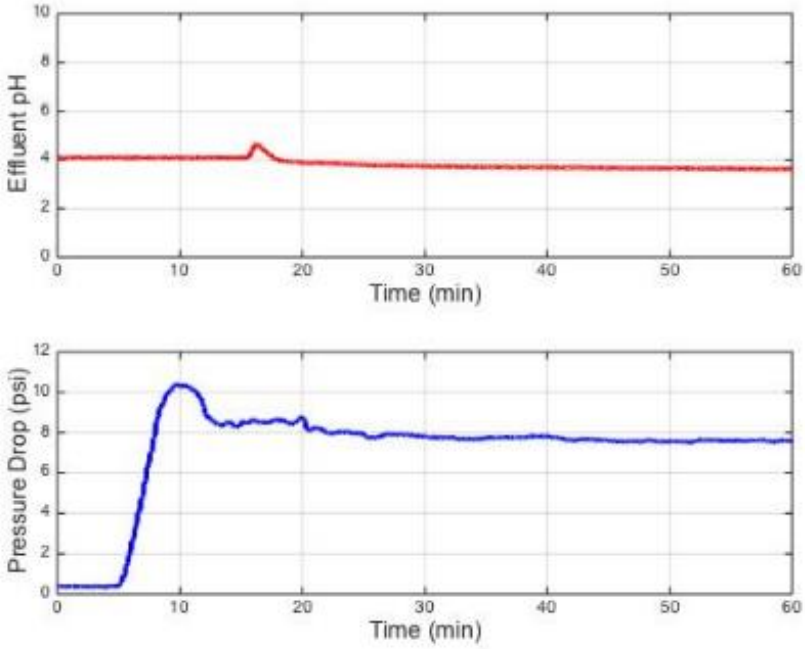

Figure 3.14: Effluent pH and pressure response during 3 wt% Carbopol 934 polymer injection of 24-hour $Na_5P_3O_{10}$ pre-treated core (6FP-34, effective aperture 159 microns) at 1 mL/min.

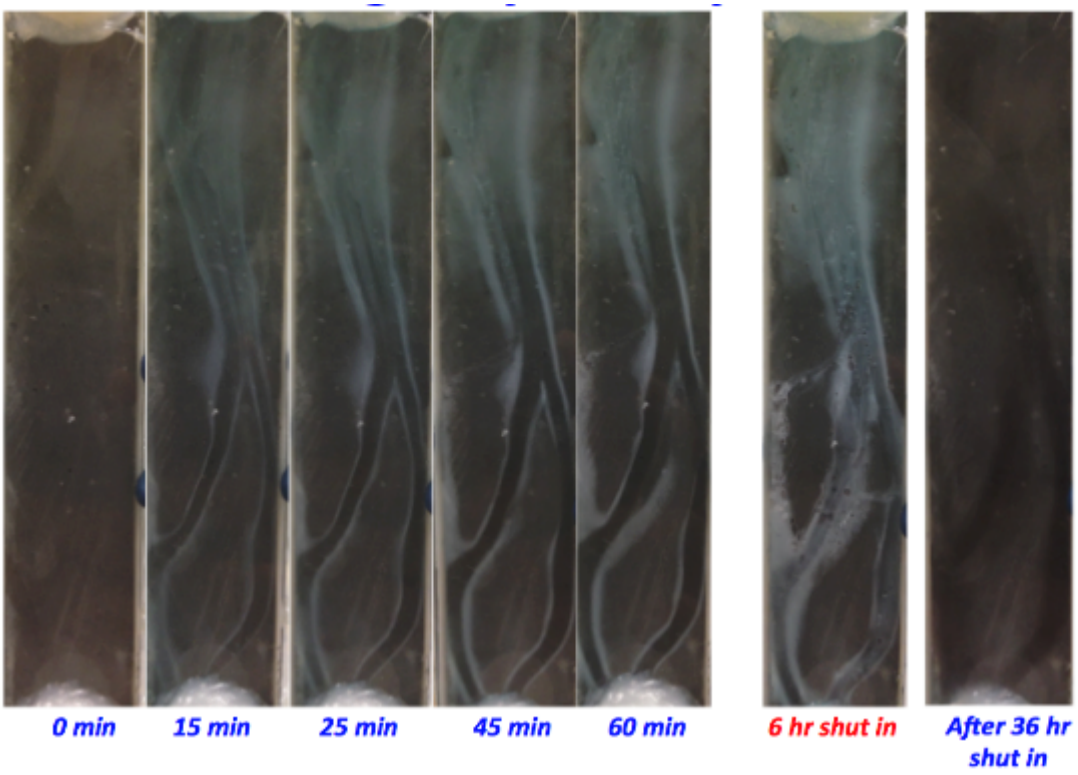

Figure 3.15: Visual inspection of polymer-cement reaction on sawed fracture surface during polymer injection and after 6-hr and 36-hr polymer shut in of core 6FP-34 (polymer flow from bottom to top). 24-hour $Na_5P_3O_{10}$ pre-treated core.

The first water breakthough test was performed after 36-hour shut-in. Clear gel formed throughout the fracture surface and was able to hold back a pressure gradient of 72 psi/ft during the water breakthrough test as seen in Figure 3.16. A second water breakthough test was performed 10 weeks after the first breakthrough, and surprisingly, the leakage pathway in the gel was healed and held back 80 psi/ft as seen in Figure 3.17. Syneresis did not occur throughout and after both polymer shut-in.

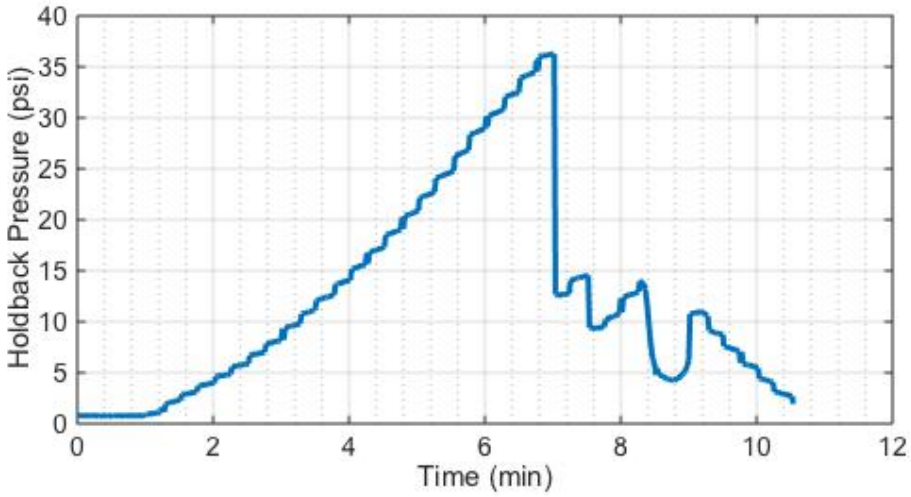

Figure 3.16: Pressure response during gel strength testing of 6FP-34 after 24-hour polymer shut-in (24-hr $Na_5P_3O_{10}$ pre-treated core). Core dimensions: effective aperture 159 microns × 6 inch in core length.

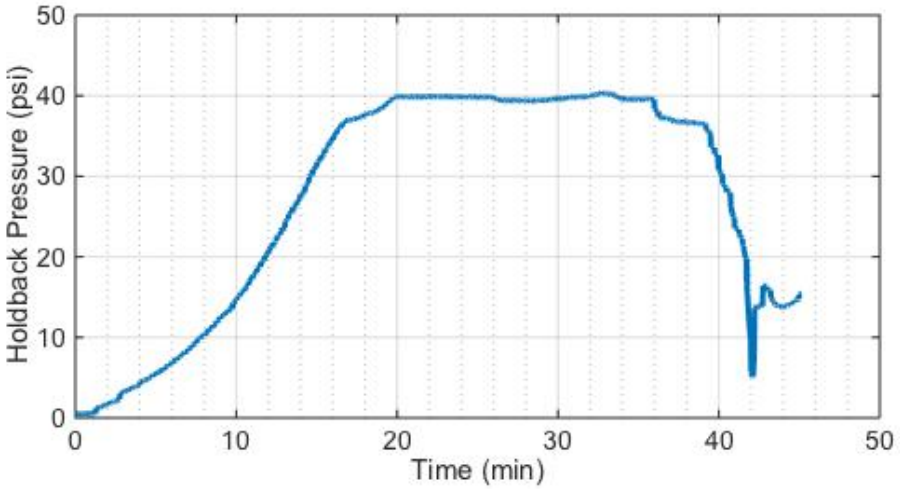

Figure 3.17: Pressure response during gel strength testing of 6FP-34 after 10 weeks polymer shut-in (24-hr $Na_5P_3O_{10}$ pre-treated core). Core dimensions: effective aperture 159 microns × 6 inch in core length.

3.1.2.6 Core 10FP-36

Core 10FP-36 was pre-treated with 12 wt% $Na_5P_3O_{10}$ for 24 hours. After the pre-treatment, only one fracture volume of 3 wt% Carbopol 934 was injected into the core for a 24-hour shut-in to primarily focus on the calcium removal effect of chemical reaction using chelating agents. During the water breakthrough test, the reacted gel in core 10FP-36 (10" in length) was able to hold back a pressure gradient of 65 psi/ft over 6.8 inches of the fracture before the epoxy coreholder was broken through (at 8 min water injection) at 3.2 inches from the inlet as seen in Figure 3.18. Syneresis did not occur before or after the water breakthrough.

Core	Fracture Type	Aperture	Pretreatment Fluid and Time	Injected Solution	Volume Injected
10FP-36	Cement-Plastic Smooth	0.255 mm	12 wt% $Na_5P_5O_{10}$ 24 hours	3 wt% Carbopol 934	1 FV

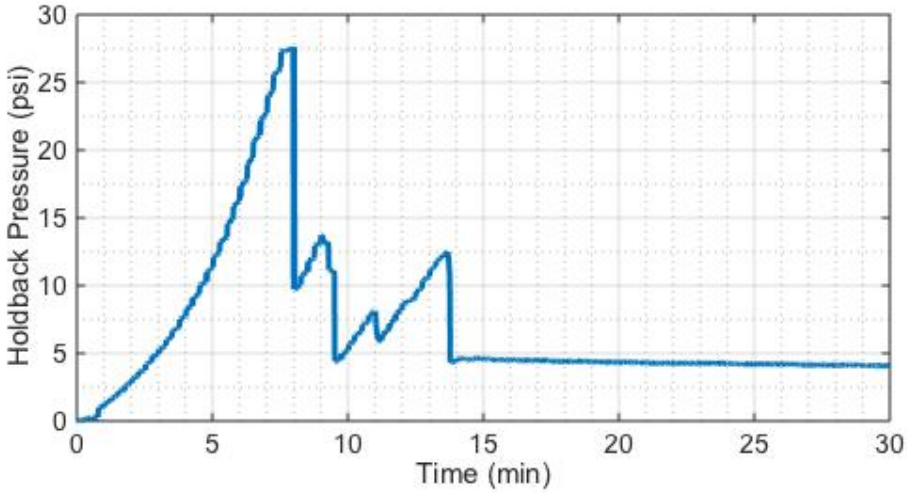

Figure 3.18: Pressure response during gel strength testing of 10FP-36 after 24-hour polymer shut-in (24-hr $Na_5P_3O_{10}$ pre-treated core). Core dimensions: effective aperture 255 microns × 10 inch in core length.

3.1.2.7 Core 10FP-38

Core 10FP-38 was pre-treated with 12 wt% $Na_5P_3O_{10}$ for 6 hours. After the pre-treatment, only one fracture volume of 3 wt% Carbopol 934 was injected into the core for a 24-hour shut in to primarily focus on the calcium removal effect of chemical reaction using chelating agents. The reacted gel in core 10FP-38 was able to successfully hold back a pressure gradient of 62.4 psi/ft. The pH of a sample of polymer gel that was flushed out during the test was measured at pH 5.51. Syneresis did not occur before or after the water breakthrough.

Core	Fracture Type	Aperture	Pretreatment Fluid and Time	Injected Solution	Volume Injected
10FP-38	Cement-Plastic Smooth	0.228 mm	12 wt% $Na_5P_3O_{10}$ 6 hours	3 wt% Carbopol 934	1 FV

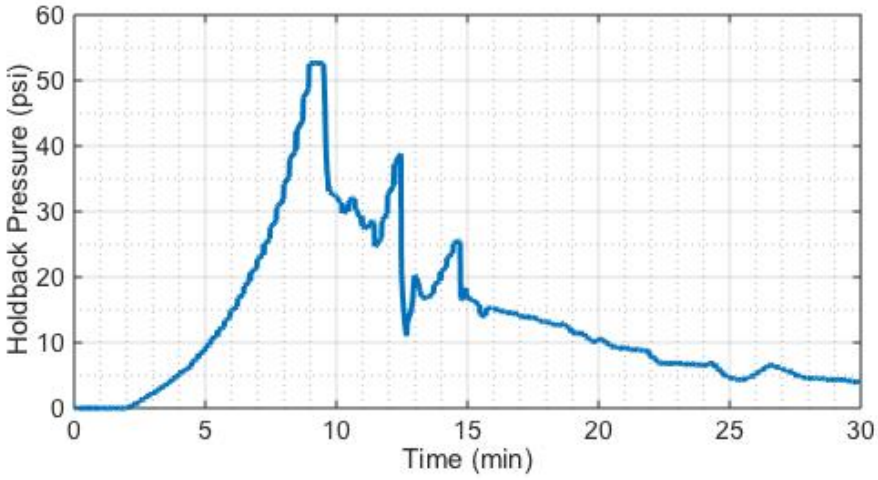

Figure 3.19: Pressure response during gel strength testing of 10FP-38 after 24-hour polymer shut-in (6-hr $Na_5P_3O_{10}$ pre-treated core). Core dimensions: effective aperture 228 microns × 10 inch in core length.

A second water breakthrough test was performed 5 weeks after the first breakthrough and the healed leakage pathway in the gel held a pressure gradient of 39.6 psi/ft before water breakthrough as seen in Figure 3.20.

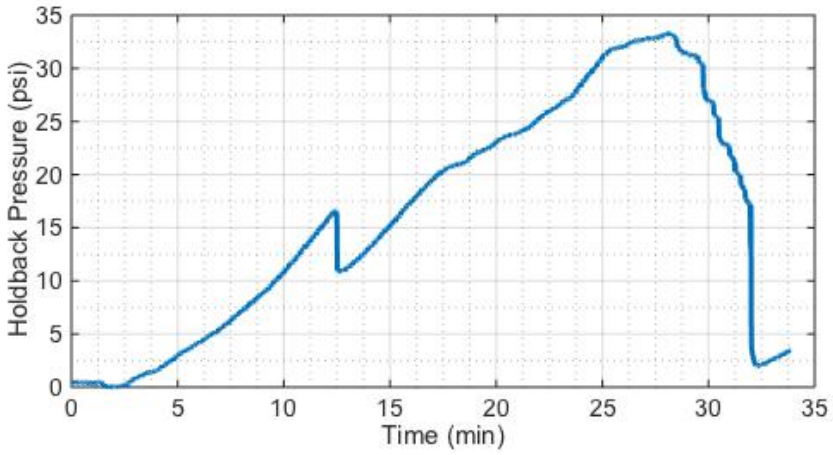

Figure 3.20: Pressure response during gel strength testing of 10FP-38* after 5 weeks polymer shut-in (6-hr $Na_5P_3O_{10}$ pre-treated core). Core dimensions: effective aperture 228 microns × 10 inch in core length.

3.1.2.8 Core 10FP-35

Experiments 10FP-37 and 10FP-35 were designed to investigate polymer gel strengths using both $Na_5P_3O_{10}$ pre-treated and untreated cores while allowing the polymer gel to be shut-in for one week. Core 10FP-35 was not treated with any pre-treatment chemical prior to the injection of 3 wt % Carbopol 934. The resulting gel held a pressure gradient of 22 psi/ft one week during the water breakthrough test (Figure 3.21) despite the formation of white-syneresed polymer. Syneresis was seen throughout 10FP-35, hence a second water breakthough test was not considered.

Core	Fracture Type	Aperture	Pretreatment Fluid and Time	Injected Solution	Volume Injected
10FP-35	Cement-Plastic Smooth	0.218 mm	-----	3 wt% Carbopol 934	1 FV

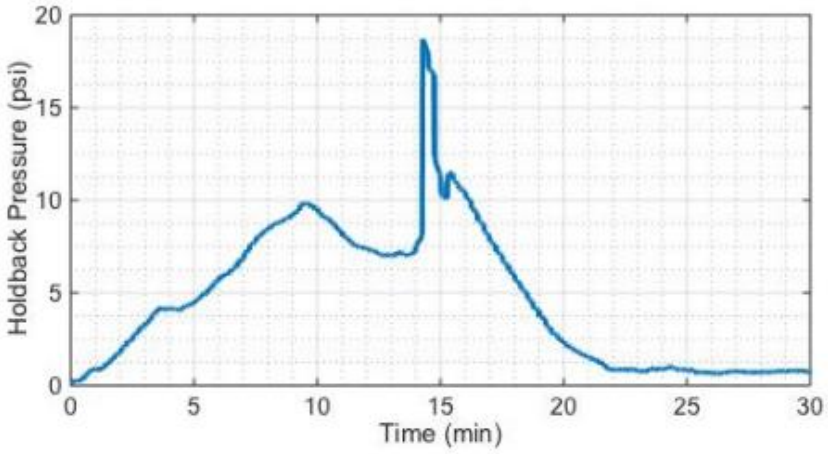

Figure 3.21: Pressure response during gel strength testing of 10FP-35 after 1 week polymer shut-in (core was injected with 3 wt% Carbopol 934 with no pretreatment). Core dimensions: effective aperture 218 microns × 10 inch in core length.

3.1.2.9 Core 10FP-37

Core 10FP-37 was pre-treated with 12 wt% $Na_5P_3O_{10}$ prior to the injection of 3 wt % Carbopol 934. After one week of polymer shut-in, water breakthrough test was performed and the core held a pressure gradient of 27.6 psi/ft as seen in Figure 3.22. Syneresis was not seen before or after the water breakthrough.

Core	Fracture Type	Aperture	Pretreatment Fluid and Time	Injected Solution	Volume Injected
10FP-37	Cement-Plastic Smooth	0.209 mm	12 wt% $Na_5P_3O_{10}$ 12 hours	3 wt% Carbopol 934	1 FV

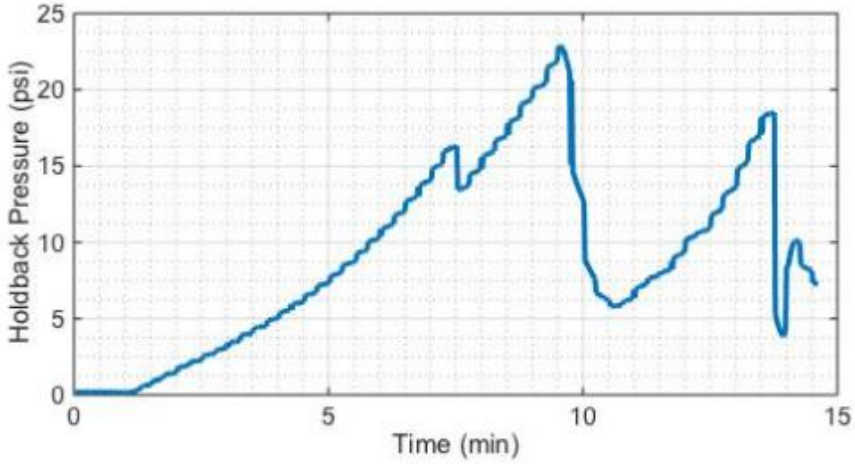

Figure 3.22: Pressure response during gel strength testing of 10FP-37 after one week of polymer shut-in (core was injected with 3 wt% Carbopol 934 with 12-hr $Na_5P_3O_{10}$ pretreatment). Core dimensions: effective aperture 209 microns × 10 inch in core length.

The result of the water breakthrough test for 10FP-35 and 10FP-37, as expected, were significantly lower than previous experiments. The formation of bubbles was observed in 10FP-37 during the polymer shut-in period. However, the results show that even with the presence of bubbles in the fracture, the pre-treated core still maintained a large gel strength indicating that the effect of bubble formation may not be as detrimental as syneresis. More tests are may be required to investigate the effect of air bubbles on gel strength.

3.1.2.10 Core 10FP-39

Core 10FP-39 was conducted to verify the effectiveness of $Na_5P_3O_{10}$ pre-treatment as bubbles develop in the gel over time. The core was pre-treated with $Na_5P_3O_{10}$ for 6 hours (same as 10FP-38) but polymer gel was shut in for 5 weeks before performing the water breakthrough test for the first time. Air bubbles were larger than seen in 10FP-37. Figure 3.23 shows that 10FP-39 held a pressure gradient of 50 psi/ft during water breakthrough test. Compared to 10FP-37 (one week shut-in), the result of 10FP-39 suggests that the gel strength may have increased as the air/gas in the bubbles gradually dries up the gel inside the fracture.

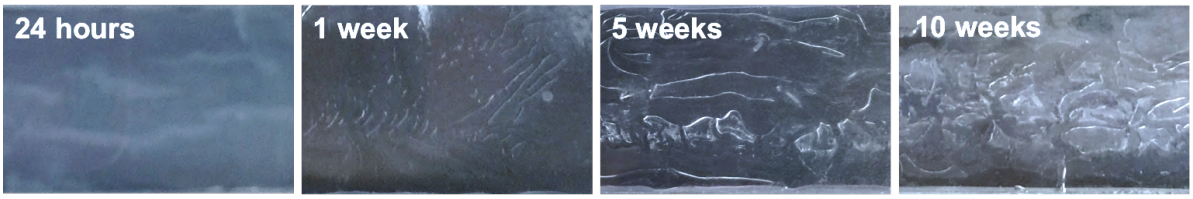

Figure 3.23: The formation of air bubbles one week after polymer placement and dehydration of gel in $Na_5P_3O_{10}$ pre-treated cement fractures over various polymer shut-in time. This is due to slower reaction between the residual $Na_5P_3O_{10}$ and reacted gel that occurs for weeks after polymer placement. Holdback pressure gradients from liquid breakthrough tests done on these cores have shown to be higher as the bubbles dehydrate the reacted gel in the fracture. In addition, polymer syneresis was successfully inhibited for over 10 weeks with the use of $Na_5P_3O_{10}$.

3.1.2.11 Core 10FP-40

Sodium triphosphate pre-treatment time of 24 hours, 12 hours and 6 hours were used in the previous experiments, and in all cases, there were no traces of syneresis. However, there were also no correlation between the length of pre-treatment time with the resulting gel strength. Since $Na_5P_3O_{10}$ is known as an efficient chelating agent in

many applications, experiment 10FP-40 was designed to evaluate the pre-treatment time dependency of gel strength compared to other longer periods.

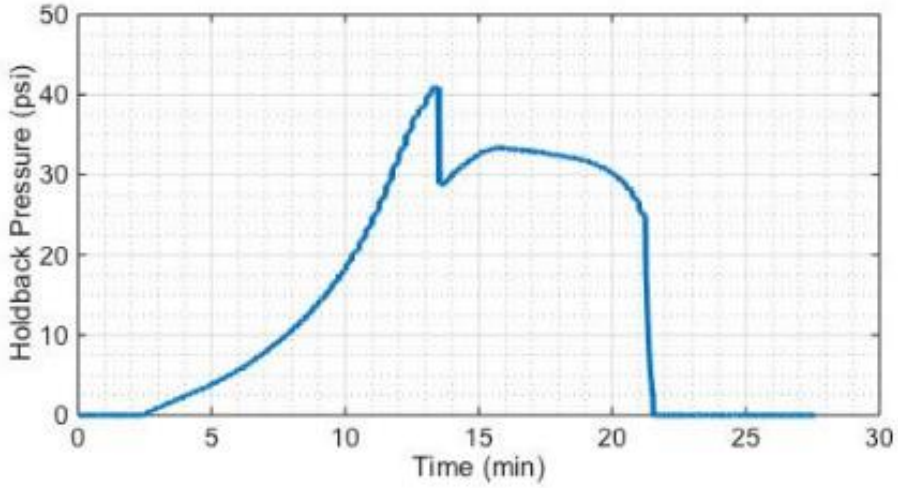

Figure 3.24: Pressure response during gel strength testing of 10FP-40 after one week of polymer shut-in (core was injected with 3 wt% Carbopol 934 with 10-min $Na_5P_3O_{10}$ pretreatment). Core dimensions: effective aperture 547 microns × 10 inch in core length.

Core 10FP-40 was pre-treated with 12 wt% $Na_5P_3O_{10}$ for only 10 minutes before injecting 3 wt% Carbopol 934. The gel was shut in for one week before performing a water breakthough test using acidic brine (2 wt% NaCl pH lowered to 4 using HCl). The resulting gel held a pressure gradient of 48.4 psi/ft as seen in Figure 3.24. Compared to 10FP-37 that was pre-treated for 12 hours, the 10-minute pre-treatment showed a better result even though acidic brine was used as holdback fluid. This prompted the investigation into whether a more corrosive fluid would dissolve the gel-in place and result in weaker gel strength during breakthrough.

3.1.2.12 Core 10FP-41

With similar apertures, core 10FP-41 and 10FP-42 were designed to explore the effectiveness of the gelling mechanism under shorter processing times (continuous

process). The tests focus on short pre-treatment time, short polymer shut-in time followed by an immediate water breakthrough test with DI water (for 10FP-41) and acidic brine (for 10FP-42). Both cores were pre-treated with 12 wt% $Na_5P_3O_{10}$ solution for only 10 minutes, then were injected with 3 wt% Carbopol 934 (dyed blue) until pressure drop in the core was stabilized before being shut-in for only one hour.

Figure 3.25 shows the pressure drop and pH effluent for the Core 10FP-41 during polymer injection. The spike in effluent pH corresponds to the spike in pressure drop indicating that the neutralization reaction has reached its limit at injection rate of 1FV/min.

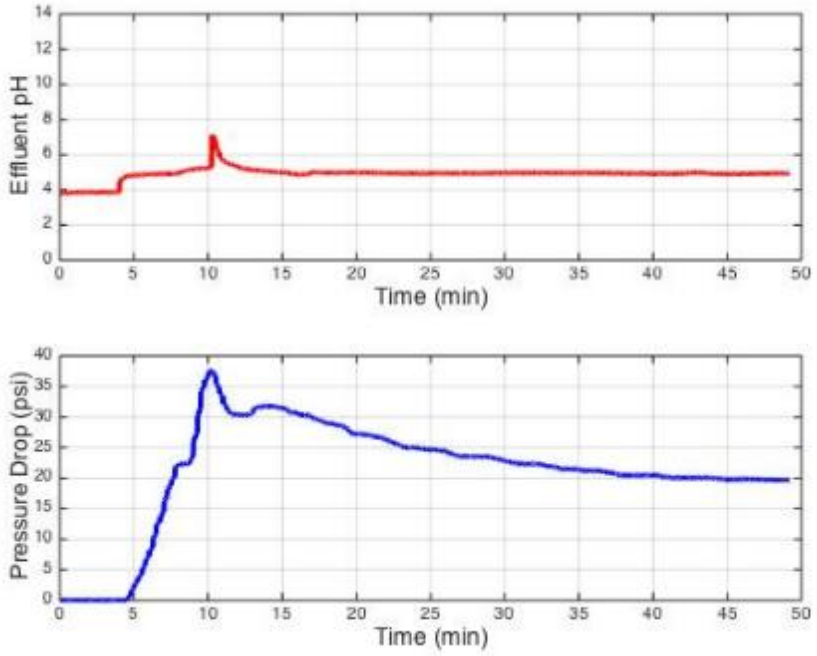

Figure 3.25: Effluent pH and pressure response during (3 wt% Carbopol 934) polymer injection of 10-min $Na_5P_3O_{10}$ pre-treated core (10FP-41, effective aperture 530 microns) at 3.42 mL/min (~1 FV/min).

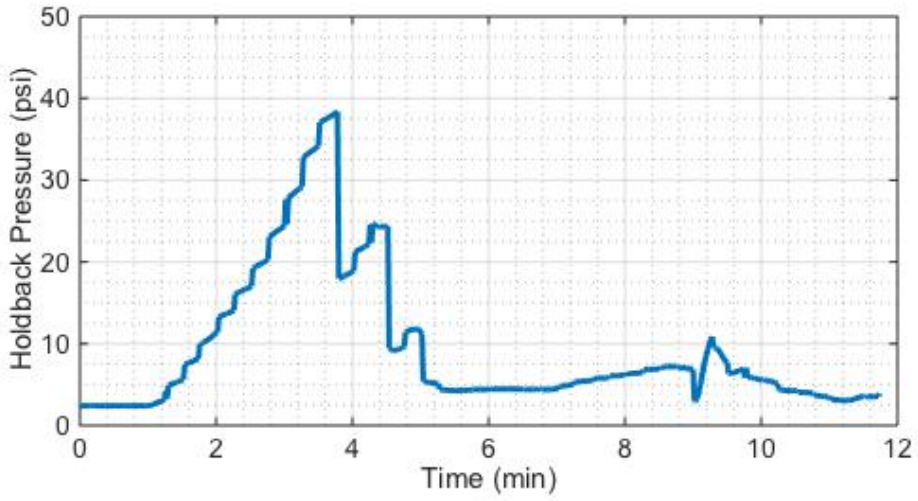

Figure 3.26: Pressure response during gel strength testing of 10FP-41 after 1-hour polymer shut-in (core was injected with 3 wt% Carbopol 934 with 10-min $Na_5P_3O_{10}$ pretreatment). Core dimensions: effective aperture 530 microns × 10 inch in core length.

Despite that unreacted polymer (opaque gel that was dyed blue) remained visible, as to clear reacted gel, after only one hour of polymer shut-in, a water breakthrough test was done using DI water (Figure 3.26). 10FP-41 held back a pressure gradient of 15 psi/ft before DI water broke through the unreacted polymer region.

3.1.2.13 Core 10FP-42

Core 10FP-42 followed the same quick 10-minute pre-treatment, one hour shut-in procedure as the previous 10FP-41. Figure 3.27 shows a similar effluent pH and pressure response as the pressure drop stabilized. The core was shut-in for only one hour, not allowing the gel to completely react like 10FP-41, and a water breakthrough test was performed using pH 4 acidic brine (2 wt% NaCl).

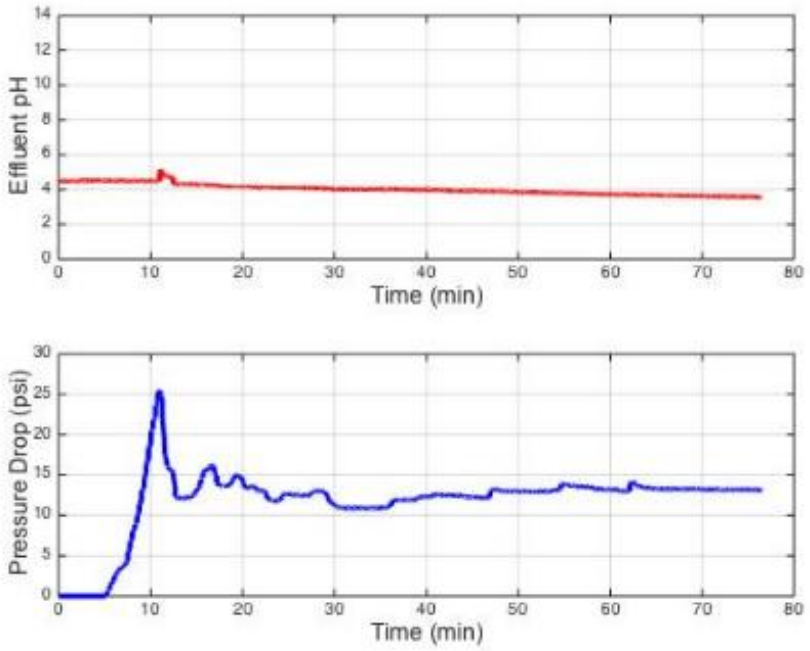

Figure 3.27: Effluent pH and pressure response during (3 wt% Carbopol 934) polymer injection of 10-min $Na_5P_3O_{10}$ pre-treated core (10FP-42, effective aperture 525 microns) at 3.40 mL/min (~1 FV/min).

The resulting gel held a pressure gradient of 15.4 psi/ft of acidic brine (Figure 3.28) that is about the same pressure gradient as the previous core broken through with water. This indicates that the property of the holdback fluid has little effect on the ability of the gel to hold back pressure due to its limited contact with the fluid at such small fracture apertures. However once broken through, the gel in core 10FP-42 was dissolved rather quickly by the acidic brine as seen in Figure 3.29 due to increase contact of fluids with gel.

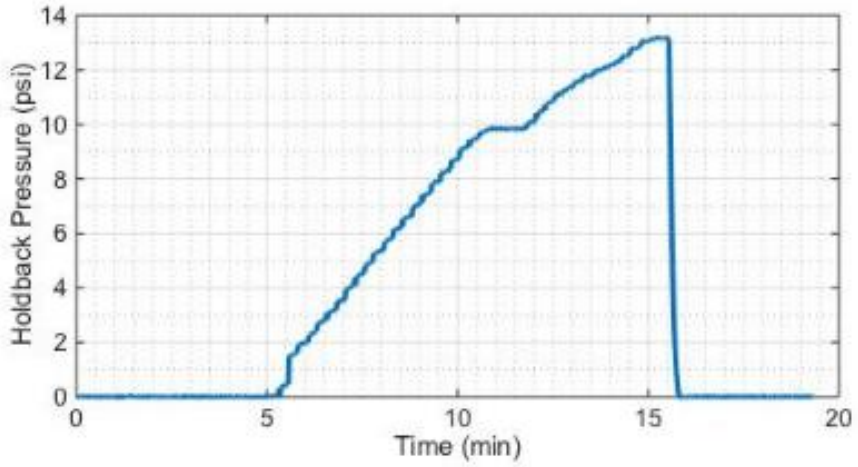

Figure 3.28: Pressure response during gel strength testing of 10FP-42 after 1-hour polymer shut-in (core was injected with 3 wt% Carbopol 934 with 10-min $Na_5P_3O_{10}$ pretreatment). Core dimensions: effective aperture 525 microns × 10 inch in core length.

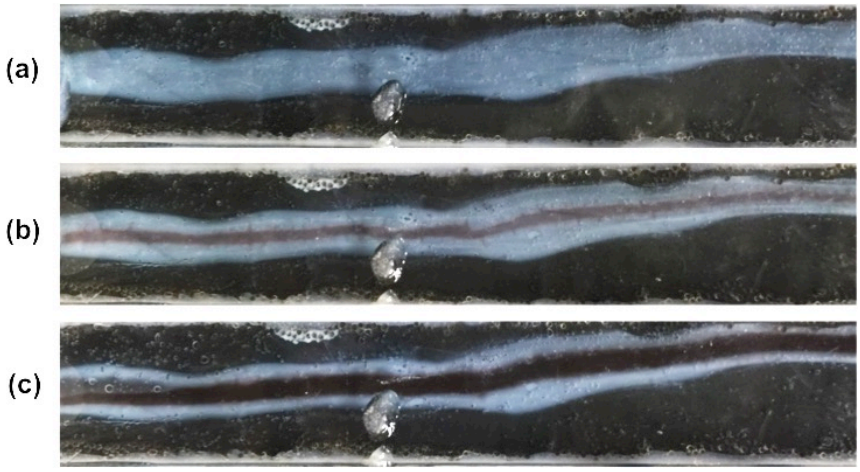

Figure 3.29: Breakthrough of polymer gel in the continuous injection test (10FP-42): (a) polymer injection flow path (opaque, dyed-blue polymer) within gel deposit in fracture (clear, immobile strong gel) during polymer injection; (b) initial breakthrough of pH 4 acidic brine (dyed red) after one-hour polymer shut-in; and (c) increased dissolution of polymer gel by acidic brine sometime after breakthrough.

3.1.3 CO_2 Pressure Holdback Tests

3.1.3.1 6CHass-1

Experiment 6CHass-1 was done using a Hassler coreholder. The first gel strength test was done after 24 hours of polymer shut-in with holdback CO_2 gas under constant pressure at 30 psi, the core was not broken through for 8 weeks until the second gel strength test was done. 6CHass-1 held a pressure gradient of 60 psi/ft of gas state CO_2, and was expected to hold more pressure gradient. However, gel strength test for 6CHass-1 was not pressurized further with CO_2 gas to cause a breakthrough.

The second gel strength test was done using 2 wt% NaCl, acidic brine (pH 2). The pressure drop was increased gradually by pumping the acidic brine at a very slow rate (0.5 mL/min) to minimize the disturbance of the reacted gel structure inside the fracture. Figure 3.30 shows the result of the acidic brine breakthrough test.

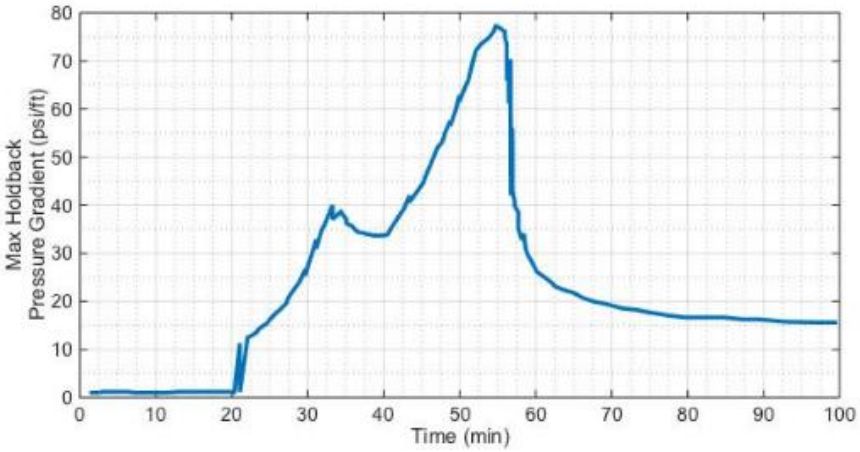

Figure 3.30: Pressure response during gel strength testing of 6CHass-1 after 8 weeks polymer shut-in (core was injected with 3 wt% Carbopol 934 with 10-min $Na_5P_3O_{10}$ pretreatment). Core dimensions: effective aperture 423 microns, 7/8" diameter × 6" in core length. (Confining pressure was 100 psi)

3.1.3.2 6CHass-2

Cylindrical cement sample in 7/8" diameter, 6" in length was wrapped in heat-shrink tubing, then fractured using the Brazilian method, allowing the fractured cement to be successfully contained in the wrap. The fractured core was placed in a 1" diameter Hassler coreholder (1250 psi pressure limit) with confining pressure set at 1500 psi. The core was saturated with DI water overnight, then proceeded to pre-treatment with $Na_5P_3O_{10}$ for 10 minutes followed by injection of one fracture volume of 3 wt% Carbopol 934. After the injection, polymer gel was shut in the cement for 24 hours to allow the polymer to develop gel strength.

After polymer shut-in, the core was placed in an oven set at 70°C with inlet connected to the CO_2 accumulator and outlet connected to a back pressure regulator (BPR) set at 1100 psi. Once the pressure in the CO_2 accumulator reached supercritical condition (1100 psi), the CO_2 inlet was opened while the HPLC pump continues to pump supercritical CO_2 into the core allowing pressure to buildup. Pressure transducers

connected to the inlet and outlet of the coreholder measures the pressure buildup during the holdback and detects pressure drop once supercritical CO_2 breaks through.

The supercritical CO_2 breakthrough test represents using the pH-triggered polymer at higher depths and supercritical conditions. The gel-in-cement over the 6" fracture was able to holdback 146 psi/ft of supercritical CO_2 (Figure 3.31). This is due to the high confining pressure (1500 psi) that provided a smaller aperture, as this is where the gel system works best, and limited contact of gel and supercritical CO_2 at inlet before the breakthrough, which does not allow the dissolution of yield stress gel.

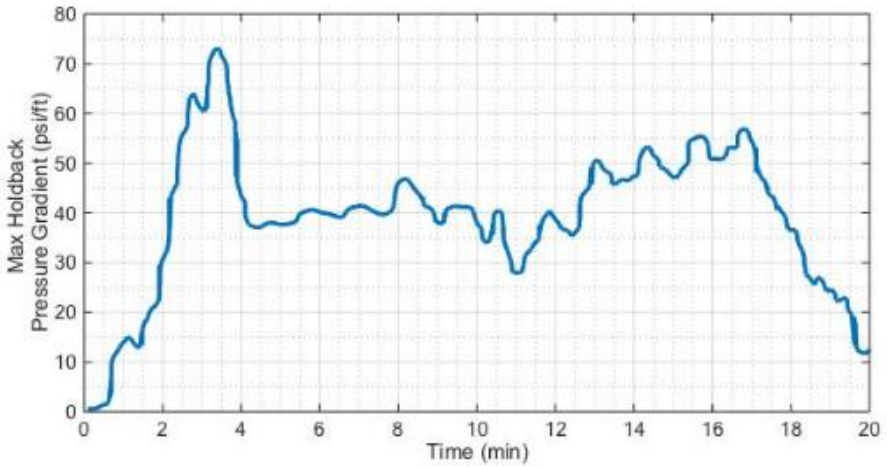

Figure 3.31: Pressure response during gel strength testing of 6CHass-2 after 24-hour polymer shut-in (core was injected with 3 wt% Carbopol 934 with 10-min $Na_5P_3O_{10}$ pretreatment). Core dimensions: effective aperture 213 microns, 7/8" diameter × 6" in core length. (Confining pressure was 1500 psi) Max operating pressure 1200 psi

3.1.3.3 6CHass-3

A larger cement sample of 1 7/8" diameter, 6" in length was sawed in half with a rock saw, placed back together and wrapped in heat-shrink tubing. The core was placed in a 2" diameter Hassler coreholder (5000 psi pressure limit) with confining pressure set

at 3000 psi to create a small aperture of 181 microns. After it was saturated with DI water overnight, the core was pre-treatment with $Na_5P_3O_{10}$ for 10 minutes followed by injection of one fracture volume of 3 wt% Carbopol 934. Polymer gel was then shut in the cement for 24 hours to allow the polymer to develop gel strength.

After polymer shut-in, the core was placed in an oven set at 70°C with inlet connected to the CO_2 accumulator and outlet connected to a back-pressure regulator (BPR) set at 1100 psi. Once the pressure in the CO_2 accumulator reached supercritical condition (1100 psi), the inlet was opened allowing pressure to buildup. The gel-in-cement over the 6" fracture was able to hold back a pressure gradient of 3000 psi/ft before supercritical CO_2 broke through as seen in Figure 3.32.

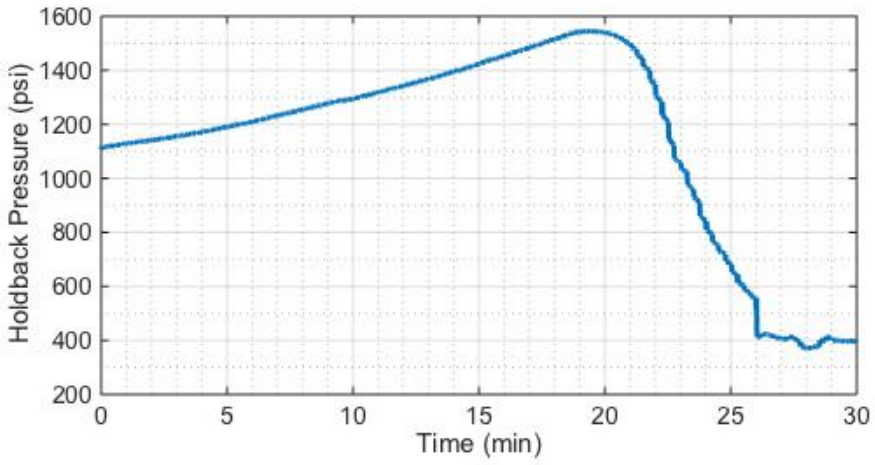

Figure 3.32: Pressure response during gel strength testing of 6CHass-3 after 24-hour polymer shut-in (core was injected with 3 wt% Carbopol 934 with 10-min $Na_5P_3O_{10}$ pretreatment). Core dimensions: effective aperture 181 microns, 1 7/8" diameter × 6" in core length. (Confining pressure was 3000 psi)

3.1.4 Cement Annulus Bench Tests

The cement annulus bench test injection of polymer in cement pathway is a practical approach in demonstrating the application of pH-triggered polymer sealant in a

cement annulus (Figure 3.33). Experiment PVC-1 (coat hanger channel, 1.167 ft in length) was able to hold back constant pressure gradient, 15 psi/ft, for one week without any breakthrough. Then a breakthrough test was done on PVC-1 by slowly increasing inlet pressure of compressed air until the bench test was broken through at 62 psi, which is around 63 psi/ft. This holdback pressure gradient of the bench test PVC-1 is in the expected range of gel's sealing performance at shallow reservoir depths. Previous corefloods, that had a polymer shut-in time of more than one week under standard condition, have shown to have an average holdback pressure gradient very close to PVC-1.

Figure 3.33: Experiment PVC-1 (left) and TYG-1 (right) successfully held 15 psi/ft constant pressure for one week. During pressure breakthrough test, PVC-1 had maximum breakthrough at 63 psi/ft and TYG-1 (right) had maximum breakthrough at 25.6 psi/ft.

Experiment TYG-1 (fractured cement in Tygon tubing, 1.25 ft in length) was also able to hold back constant pressure gradient, 15 psi/ft, for one week without any

breakthrough. The same breakthrough test was done on TYG-1 and it held a pressure gradient of 25.6 psi/ft before compressed air broke through. This pressure gradient is sufficient for the requirement of holding back a few psi/ft for rising buoyant CO_2; however, the lower holdback pressure may be the result of the tubing material's expansion response to the pressure increase, which can create gaps between tube wall and cement for compressed air to breakthrough.

3.2 KEY SUMMARY OF THE EXPERIMENTS

Several syneresis inhibitors were tested in search of an effective solution to eliminate calcium syneresis. Different procedures were used with these syneresis inhibitors depending on the nature of the chemical and its pH condition. Table 3.1 and Table 3.2 are the summary of the tests done in this study, varying the parameters of interest.

Table 3.1: A summary of syneresis inhibitors, Laponite and EDTA, tested in this study and their gel strength results. All cores were injected with 2 wt% Carbopol 934. Test 6FP-29 used Laponite as an additive to the polymer solution; the procedure was designed without pre-treatment to test Laponite's ability to stabilize gel structure in the presence of calcium. Laponite enhanced gel was able to hold a static pressure gradient of 2.6 psi/ft (acidic brine) for several months. Test 6FP-30 and 6FP-31 were designed to use EDTA pre-treatment to remove calcium ions in the cement before subsequent polymer injection. However, 6FP-30 was terminated during polymer injection due to rapid pressure increase caused by the neutralization reaction of residual EDTA with polymer; hence test 6FP-31 included a water pre-flush in between EDTA and polymer injection. Individual core lengths are marked in the number at beginning of the test number.

Core Type	Test	Fracture Aperture (mm)	Syneresis Inhibitor	Shut-in Time	Max Holdback Pressure Gradient (psi/ft)	Static Holdback Pressure Gradient (psi/ft)
Cement-Plastic	6FP-29	0.162	Laponite	24 hours	--	2.6 psi/ft
	6FP-30	0.244	EDTA	--	--	--
	6FP-31	0.215	EDTA	1 week	7.2	--

Table 3.2: A summary of sodium triphosphate ($Na_5P_3O_{10}$) pre-treatment and gel strength testing results. Cement cores in this table were pre-treated with 14.5 g/100 mL $Na_5P_3O_{10}$ from 10 minutes up to 24 hours, then injected with 3 wt% Carbopol 934 polymer dispersion and allowed polymer shut-in from 1 hour up to 10 weeks. Various holdback fluids were used in the liquid holdback test to obtain the maximum holdback pressure gradient (psi/ft); the acidic brine was made by adding HCl acid into 2 wt% NaCl until the solution reached pH 4 measured by a pH meter. For 6Hass-1, CO_2 gas was injected at room temperature and held above 60 psi/ft constant pressure for 8 weeks and was followed by a gel strength test using acidic brine. Individual core lengths are marked in the number at beginning of the test number.

Core Type	Test	Fracture Aperture (mm)	Pretreatment Time	Shut-in Time	Max Holdback Pressure Gradient (psi/ft)	Holdback Fluid
Cement-cement	6CF-36	0.436	24 hours	2 weeks	82.3	pH 4 brine
	6CF-39	0.463	10 minutes	2 weeks	104.1	pH 4 brine
Cement-Plastic	6FP-33	0.138	As an additive	24 hours	56	DI water
	6FP-34	0.159	24 hours	24 hours	72	DI water
				10 weeks	80	DI water
	10FP-35	0.218	--	1 week	21	DI water
	10FP-37	0.209	12 hours	1 week	27.6	DI water
	10FP-36	0.255	24 hours	24 hours	65	DI water
	10FP-38	0.228	6 hours	24 hours	62.4	DI water
				5 weeks	39.6	DI water
	10FP-39	0.277	6 hours	5 weeks	50.4	DI water
	10FP-40	0.547	10 minutes	1 week	48.4	pH 4 brine
	10FP-41	0.530	10 minutes	1 hour	15	DI water
	10FP-42	0.525	10 minutes	1 hour	15.4	pH 4 brine
Hassler coreholder	6Hass-1	0.423	10 minutes	24 hours	> 60	CO_2 gas
			10 minutes	8 weeks	160	pH 4 brine
	6Hass-2	0.213	10 minutes	24 hours	150	Supercritical CO_2
	6Hass-3	0.181	10 minutes	24 hours	3000	Supercritical CO_2

The following sections will discuss how the parameters that were varied for different experiments affect the strength and stability of the resulting polymer gel.

Section 3.3 is a discussion on the effect of calcium syneresis by identifying the important stages of syneresis, predicting the patterns of syneresis in a fracture through convective-diffusion, and explaining the inconsistent behavior of syneresis for blocking flow. Section 3.4 focuses on the effect of surface geometry and fracture aperture in the development of gelant yield stress. Section 3.5 describes the effect of fluid reactions between cement and syneresis inhibitors, as well as, between gelant and formation fluids. Section 3.6 discusses the effect of reaction time in each experimental step as to optimize the design of procedures. Lastly, section 3.7 summarizes the key features and findings for the pH-sensitive polymer application in sealing cement fractures.

3.3 Effect of Syneresis

Polymer gels undergoing syneresis have difficulty of maintaining gel stability. The presence of divalent cations in cement destabilizes gel structure and greatly compromises the gelant's mechanical strength to block fluid flow in the application of sealing cement fractures. This section explains the formation of calcium syneresis and its detrimental effects on the gel used as sealant.

3.3.1 Stages of Calcium Syneresis

Three types of polymer gel formation were visually distinguished as polymer reacted with the cement fractures. These gel types exhibit different behavior and form in a sequence under the influence of hydroxide and calcium cations. The stages of polymer syneresis can be identified in a static dunk test as described here:

1. Slightly opaque polymer solution is the unswollen microgel solid dispersion that is first observed passing through the fracture gap. This acidic dispersion is slightly viscous, nevertheless flows quickly and easily on the cement surface.

2. *Clear solid-like gel* is the swollen microgel deposited on the fracture surface, as the pH of the dispersion is increased, in immediate reaction with the OH^- leaching out from the cement. This clear microgel deposit is a rather short transition stage but exhibits large yield stress that can greatly reduce flow during injection.

3. *White-syneresed polymer* begins to form after the clear gel formation, due to the subsequent Ca^{++} leaching out from the cement. Reaction with Ca^{++} collapses of the structure of the swollen microgel and yields a white-calcium precipitation starting from the cement surface. Continuous supply of calcium ions can happen gradually over time and are seen to cause the remaining clear gel to expel all of its water until separate layers of water and syneresed-polymer is formed.

It is important to distinguish the above three states, as the key to maintaining effective seal depends on maximizing the deposition of clear swollen gel and minimizing the formation of syneresed Ca-polymer complex.

3.3.2 Convective-Diffusion Controlled Syneresis

The rate of syneresis formation depends on pH, fracture geometry and geochemistry. Although at a slower rate, reaction of calcium ions and swollen mircogel particles is much like that of OH^- in the flowing polymer solution. During injection of polymer dispersion into the fracture two factors are coupled that influences the formation of white-calcium syneresis: convection in flowing fluid and diffusion in the gel deposit. These two phenomena can be seen simultaneously controlling the rate of syneresis in a fracture during polymer injection:

1. *Convection dominated flow channel:* The main path of the flowing polymer will form where the aperture is the widest, in other words, path of least resistance as seen in Figure 3.34(a) during polymer inection. In the flow channel, the calcium ions will be

stripped away, along with some swollen gel, from the cement surface by the high shear induced concentration gradient. After polymer injection, this pathway generally has the lowest calcium content and consequently less syneresis.

2. *Diffusion dominated gel deposition region:* The areas of narrow apertures form the low velocity region where gel deposits. During polymer injection, calcium ions will diffuse into deposit gel layer and have sufficient time to react with the swollen gel. The clear gel stage only occurs briefly as white syneresis starts to form; these areas generally result in the weakest points in the gel during water breakthrough tests as seen in Figure 3.34(c).

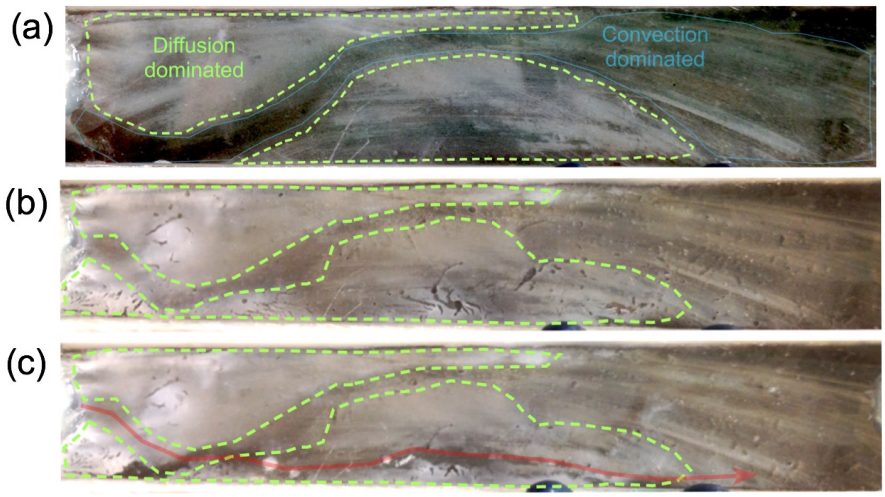

Figure 3.34: Core 6FP-33 (4 wt % $Na_5P_3O_{10}$ as additive in 3 wt% Carbopol 934) polymer syneresis progression (a) flow channel and gel deposition formed at steady-state (80 min) during polymer injection (b) white-calcium syneresis expulsion of water after 24 hr shut-in (c) gel broken through syneresed region during water breakthrough test (flow direction left to right).

3.3.3 Effects on Gel Strength and Stability

The gradual syneresis on the surface of the untreated cement can happen over the course of time as the reaction reaches completion. It is an unstable form of polymer gel,

and can easily detach on its own or is stripped away by fluid flow in the fracture. This behavior can be explained with the cement-cement fractures, as illustrated in Figure 3.35 (Patterson, 2014).

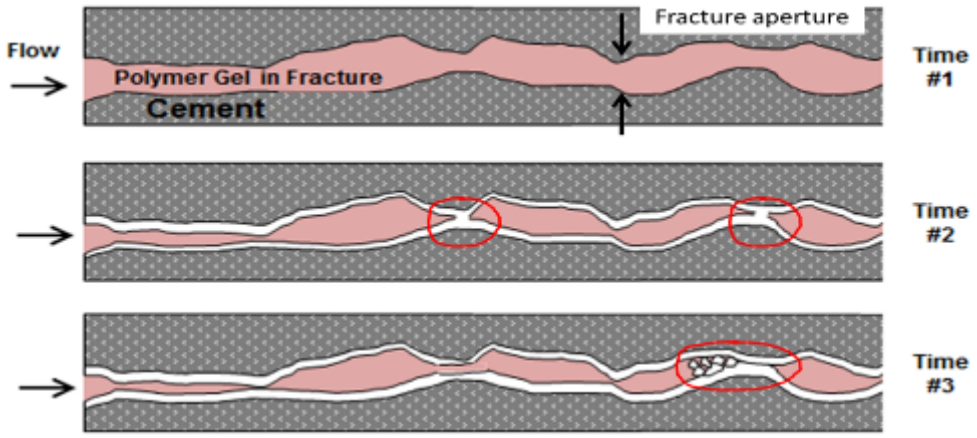

Figure 3.35: An illustration of the polymer syneresis reaction in the cement fracture over time. The syneresed polymer (white precipitation) starts depositing as soon as polymer dispersion (red) is in contact with untreated cement. Syneresed polymer is an unstable semi-solid that contracts over time, and can easily detach on its own or be stripped away by fluid flow in the fracture. Cyclical blockage and fluid breakthrough were often observed during polymer injections in the untreated cores. Early blockage by syneresised polymer during polymer injection may prevent the polymer from reaching all of the pathways that require proper seal; in addition, the detachment of syneresed polymer from time to time may re-open pathways for fluid flow (Patterson, 2014).

Early blockage by syneresed polymer during polymer injection may prevent the polymer from reaching all of the pathways that require proper seal; in addition, the detachment of syneresed polymer from time to time may re-open pathways for fluid flow. Due to the irregularity of the flow channels formed in these rough-walled fractures (both in sawed and Brazilian fracture), cyclical blockage and fluid breakthrough occurred during polymer injections. As a result, polymer injectivity was poor. Furthermore, cores

exhibiting the syneresis effect typically were not able to hold back pressurized fluid over long periods of time, which easily broken through at lower pressure gradients.

Table 3.3: Maximum holdback pressure gradients recorded in liquid breakthrough tests (DI water) for untreated cement cores (F-9, F-12 and F-14) and HCl (pH 2.2) pre-treated cement cores (FP-26 and FP-27). These cores had relatively successful polymer placements, despite syneresis observed in all of them, and the fracture remained blocked before performing the breakthrough test. While core F-14 was able to hold back 40 psi/ft due to its higher polymer concentration at 4.5 wt%, most untreated cement cores injected with 3 wt% Carbopol 934 were only able to hold back a few psi/ft. Cores pre-treated with HCl had similar holdback pressure gradients as the untreated cores. HCl was unsuccessful in inhibiting syneresis and has shown to increase fracture aperture, also, leaving behind large amounts of oxidized iron precipitation (Patterson, 2014).

Core Type	Experiment	Aperture (mm)	Injected Solution		Shut-in Time	Holdback Pressure Gradient (psi/ft)
			Polymer (wt%)	NaCl (wt%)		
Cement-cement	F-9	0.336	3	0.5	4 days	6.5
	F-12	0.271	3	0.5	4 days	7.2
	F-14	0.359	4.5	0.5	4 days	40
Cement-Plastic	FP-26	0.314	3	--	24 hours	2.6
	FP-27	0.229	3	--	24 hours	8

Table 3.3 lists the results of several liquid breakthrough tests that were carried out with the polymer placement in untreated cores. Even when successfully placed, the gel was only able to hold back a few psi/ft (F-9, F-12, FP-26 and FP-27) while most cores experienced liquid breakthrough immediately due to the presence of unstable syneresed polymer inside the fracture.

3.4 Effect of Fracture Geometry

The depositional pattern of swollen gel and the resulting yield stress can be affected by fracture geometry in cement, namely the fracture surface and aperture. This

section discusses their effects on gel strength that were identified in flow experiments and verified through subsequent water breakthrough tests.

3.4.1 Cement Surface Type

The surface geometry determines how microgel dispersions are transported and swollen microgels are deposited in a cement fracture. Rough surfaces create irregular channels that make the polymer flow field and neutralization reaction relatively complicated. The effective aperture of these cores calculated from permeability test only represent the overall fracture permeability and does not account for local irregularities that may or may not aid the formation of uniform strong gel. Two distinct flow patterns were observed during polymer injection in smooth and sawed fracture geometries. In Figure 3.36(a), tortuous conduits separating and joining in the direction of flow effected by variations in cross-section of a rough surface. From a modeling point of view, this phenomenon may be difficult to characterize compared to a simple smooth fracture; where reacted swollen gel deposit uniformly from the sides towards the middle to create a single straight flow path, as seen in Figure 3.36(b). Polymer flow and reaction in smooth cement geometry is very useful for studying gel deposition kinetics.

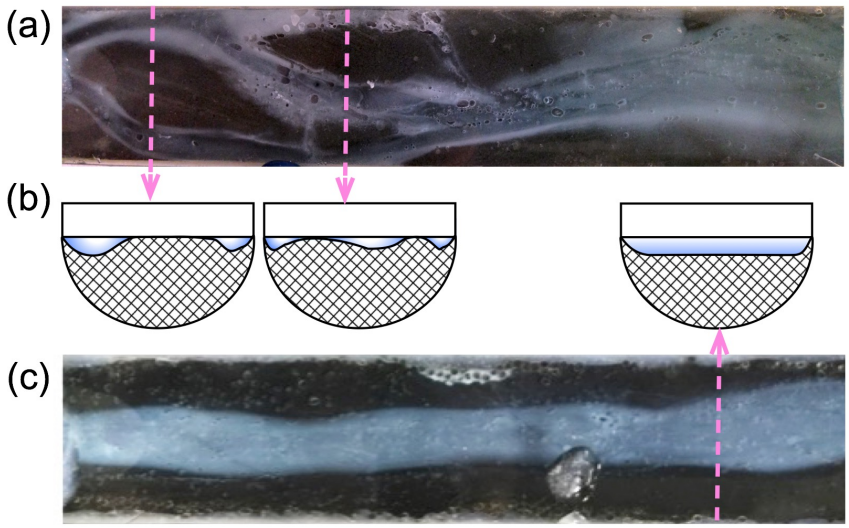

Figure 3.36: The effect of surface geometry on polymer gel reaction in cement fractures: (a) polymer flow in sawed cement fracture (6FP-34), (b) heterogeneity of surface geometry seen in the cross-sectional view of the two different surface geometry, and (c) polymer flow in simple smooth cement fracture (10FP-42).

Many natural fracture in wellbore cement are most likely to have complicated fracture geometry and flow patterns, nevertheless results from gel strength tests indicate that such irregularity will not have much effect on the ultimate gel strength. This is because the clear gel deposits form stable large networks that can rearrange between each other to maintain seal upon increasing pressure gradient, which is different from the coincidental flow and blockage of the syneresed polymer materials.

3.4.2 Fracture Aperture

The theoretical maximum holdback pressure gradient is a function of yield stress of the gel and effective aperture of the sealed fracture. In theory, as fracture apertures decrease the maximum pressure gradient is expected to increase. There is only a weak correlation between the two from the overall gel testing results, because variables such as

pre-treatment time and shut-in time are not held constant. The gel strength and effective aperture relationship can be seen in a few similar tests where other variables are held constant; Table 3.4 contains the gel strength testing results selected for 8 cores pre-treated with sodium triphosphate and injected with 3 wt% Carbopol 934.

Table 3.4: Relationship between effective fracture aperture and maximum holdback pressure gradient for cement cores with similar $Na_5P_3O_{10}$ pre-treatment and polymer shut-in time.

Test	Pretreatment Time	Shut-in Time	Fracture Aperture (microns)	Pressure Gradient (psi/ft)
6CHass-3	10 minutes	24 hours	181	3000
6CHass-2	10 minutes	24 hours	213	150
6FP-34	24 hours	24 hours	159	72
10FP-36	24 hours	24 hours	255	65
10FP-38*	6 hours	5 weeks	228	40
10FP-39	6 hours	5 weeks	277	50
10FP-42	10 minutes	1 hour	525	15.4
10FP-41	10 minutes	1 hour	530	15

The maximum holdback pressure gradients are plotted in log-scale for those selected cores to compare with their effective apertures in Figure 3.37. The trend indicates holdback pressure gradients tend to increases exponentially as aperture decreases, however the data also suggest that there may be a range where effective fracture aperture start to contribute significantly to the maximum holdback pressure.

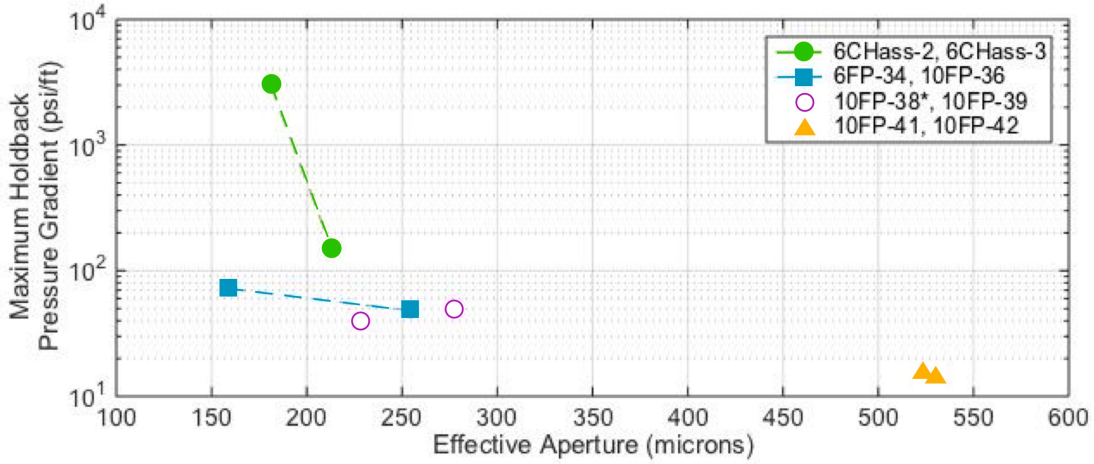

Figure 3.37: Relationship between effective fracture aperture and maximum holdback pressure gradient for cement cores pre-treated with $Na_5P_3O_{10}$ and sealed with 3 wt% Carbopol 934 (not including 6FP-35 and 6FP-33 where $Na_5P_3O_{10}$ was not used as pre-treatment).

These micro-apertures can be especially difficult to create in the lab and maintain throughout the multiple tests, though attempts had been made to use glass beads of known diameter to keep apertures constant. One reason may be that all the cement-plastic cores were hand-made, and mechanical strength of the epoxy used to seal cement and plastic plates were simply insufficient in keeping apertures constant at higher pressures. It is possible for some fractures to be wider than what was originally measured from the permeability tests. Recent tests (6CHass-2, 6CHass-3) performed with the use of steel coreholder were effective in aperture control due to the presence of confining pressure.

3.5 Effect of Fluids

The chemical reactions between syneresis inhibitors and cement, as well as between polymer gel and formation fluids have a significant influence on the design of procedures. This section discusses the application and effectiveness of each syneresis

inhibitors, and the effect of acidic formation fluid once the gel is placed, to understand their effect on polymer injection and resulting gel-in-place.

3.5.1 Syneresis Inhibitors

In order to prevent syneresis, several chemicals were sought and tested to remove the calcium content from the cement and stabilize gel strength. The following discusses each of their performances:

1. Laponite as polymer additive:

The addition of Laponite into polymer dispersion while adding acid to reduce the final pH exhibited much potential during polymer injection seen in Figure 3.38. The pH 2.7 nanocomposite microgel mixture can be seen to be developing some viscosity as it reacts with cement while maintaining only a relatively small pressure drop of a few psi over the course of almost an hour. This indicates that reaction between cement and mixture occurs rather gradually and uniformly because gel slowly deposits causing pressure drop to increase slightly as flow area is reduced. Photos taken during injection show no sign of calcium syneresis and correspond to the start of rapid pressure buildup (at 60 minutes) when polymer dispersion can be seen to have transformed in to clear gel that occupied the entire fracture Figure 3.4. The injection of the mixture ended at 110 minutes showing no sign of syneresis.

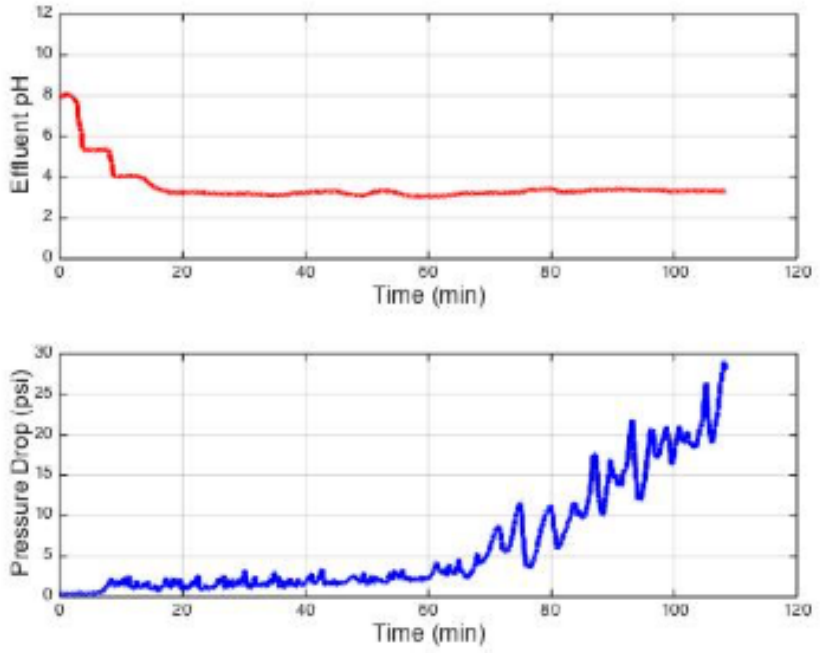

Figure 3.38: Effluent pH and pressure drop recorded during polymer injection in core 6FP-29 (2 wt% Carbopol 934 and 0.2 wt% Laponite)

After 24 hours of polymer shut-in, white-precipitation can be seen covering the entire cement surface. Upon closer inspection, the precipitation had a grainy texture that was very different from usual rubbery syneresis texture and gradually faded over the course of a week. This indicates that the precipitation may not be calcified gel as syneresis is not reversible. The core was able to hold a static pressure gradient of 2.7 psi/ft over several months without the appearance of syneresis.

The result agrees with another rheology study that showed the strong polymer-clay reaction produced a dense hydrogel network and result in remarkable mechanical performance (Tongwa et al., 2013). This explains why the final product of a clear gel, dense Carbopol 934 and Laponite network, was able to prevent calcium from causing syneresis and maintain seal for a long period of time. Although there are no further tests performed to test the limitations of the Laponite-Carbopol mixture beyond the small

static pressure gradient, the addition of the nano-clay is believed to have potential as a stable sealant for blocking buoyant CO_2; and perhaps applications at high temperature conditions (Tongwa et al., 2013).

2. EDTA as pre-treatment:

Cement cores treated with EDTA tetrasodium salt showed good result in removal of calcium and prevention of syneresis after polymer placement; however, polymer injection into EDTA treated cores had unstable pressure response due to the fact that EDTA is highly alkaline.

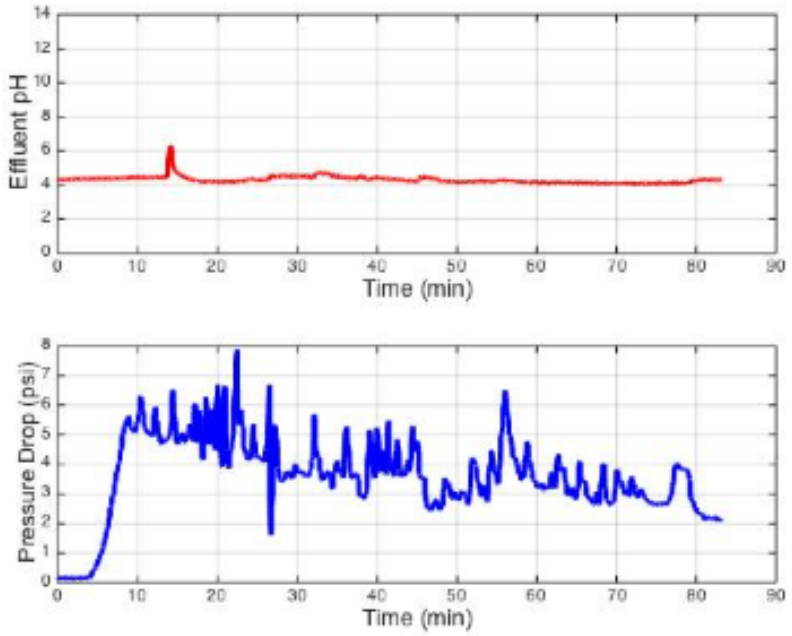

Figure 3.39: The effluent pH and pressure drop recorded during polymer injection of 6FP-31 (3 wt% Carbopol 934 after EDTA pre-treatment).

Figure 3.39 shows that despite the water pre-flush before polymer injection, the residual EDTA caused a rapid increase in pressure drop upon contact with polymer. The pressure response remained erratic throughout the polymer injection over the course of 80

minutes, meaning that the reactivity of EDTA is still strong. This may become a problem for sealing leakages in a wellbore since pathways are generally longer than that of in lab scale and injectivity may be compromised before polymer reaches the target zone.

3. Sodium triphosphate ($Na_5P_3O_{10}$*) pre-treatment:*

Use of sodium triphosphate ($Na_5P_3O_{10}$) for pre-treatment provided effective calcium control and inhibited the formation of syneresed polymer. Cement fractures pre-treated with $Na_5P_3O_{10}$ maintained good polymer injectivity and greatly improved the long-term strength and stability of the gel in place. During polymer injection in $Na_5P_3O_{10}$ pre-treated cores, the effluent pH steadily decreases. The pressure drop also decreases as shown in Figure 3.40. This indicates that the decreasing viscosification of the polymer dispersion with time is reducing the pressure drop more than the pressure drop increase by flow channel constriction.

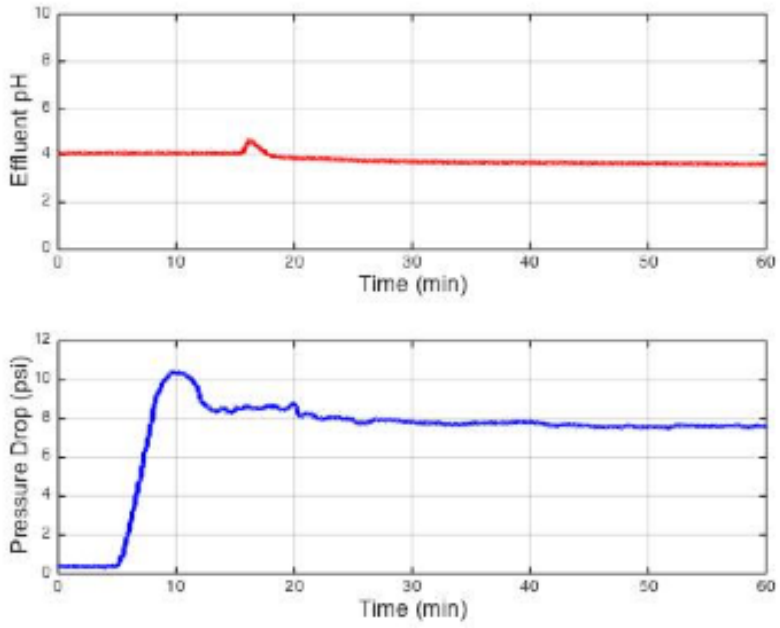

Figure 3.40: The effluent pH and pressure drop recorded during polymer injection of 6FP-34 (3 wt% Carbopol 934 after 24 hr $Na_5P_3O_{10}$ pre-treatment).

Table 3.2 is a detailed summary of the experiments using $Na_5P_3O_{10}$ under various pre-treatment times, polymer shut-in time and the holdback fluid employed. The gel strength tests after 24 hours of shut-in for the $Na_5P_3O_{10}$ pre-treated cement cores held back an average of 60 psi/ft of water under standard conditions and held back 150-3000 psi/ft under supercritical conditions. This is compared to the cores without pre-treatment (6FP-35 and cores in Table) held back an average of 14.2 psi/ft. Cores pre-treated with $Na_5P_3O_{10}$ showed no signs of polymer syneresis later in long periods of shut-in.

4. Hydrochloric acid pre-flush:

Preliminary hydrochloric acid pre-flush had been tested in attempt to remove calcium ions from fracture surface (Patterson, 2014). In his study, cores pre-flushed with acid generally result in aperture enlargement and the formation of rust-colored iron precipitation. In some cases, the injection of acid can reduce aperture by dissolving

calcium content in cement and transporting it further into the fracture to form calcite precipitation. However, his experiments have proven that hydrochloric acid pre-flush only partially reduced calcium syneresis which has relatively limited improvement in maintaining polymer gel strength and stability Figure 3.41.

Figure 3.41: Hydrochloric acid (pH 2.29) pre-flushed cement core (6FP-27) after 24 hours polymer shut-in. White calcium precipitation with rust-colored precipitate (Patterson, 2014).

3.5.2 Pressurized Holdback Fluids

The acidity and salinity of CO_2 saturated brine in storage formations are considered detrimental to pH-sensitive polymer and could potentially reverse the yield stress developed by the gel in place. Core 10FP-41 and 10FP-42 were carried out under the same pre-treatment and in similar apertures, but injected with different holdback fluids to test gel strength after just one hour of shut-in. After gel strength testing of gel-in place, both cores yield desirable holdback pressure gradients at around 15 psi/ft regardless of the composition of the fluids. It was found that the gel strength mainly depends on the pressure applied to the gel in fracture due to limited contact of the fluid and gel at the inlet (very narrow fracture aperture).

However, holdback fluid composition can have a significant effect on gel stability once the gel is broken through by pressure. The yield stress of gel greatly decreases as acidic brine flows through the broken gel system; the pH-gelling mechanism can be

reversed as the contact and reaction of fluid and gel increases. This behavior was observed in the acidic brine breakthrough in core 10FP-42. Figure 3.42 shows the fast dissolution of polymer gel in the previous flow path (weaker area in fracture) by the pH 4 brine (dyed red). The extended duration of the acidic environment can potentially reverse the gel back to its original Newtonian fluid state, thus leakage pathway will be re-established.

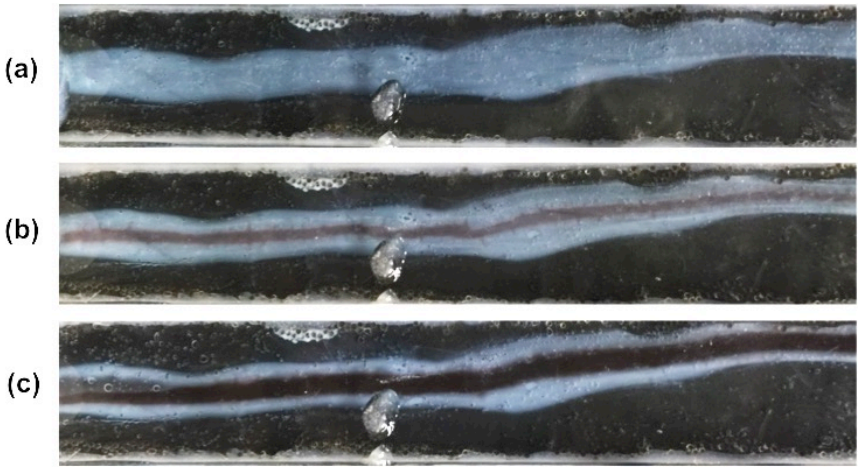

Figure 3.42: Breakthrough of polymer gel (injecting from left to right) in the continuous injection test (experiment 10FP-42): (a) polymer injection flow path (opaque, dyed-blue polymer) within gel deposit in fracture (clear, immobile strong gel) during polymer injection; (b) initial breakthrough of acidic brine (dyed red) after one-hour polymer shut-in; and (c) increased dissolution of polymer gel by acidic brine sometime after breakthrough.

3.5.3 Dehydration of Gel Deposit

Air bubbles in reacted gel deposit were observed over time in completely sealed reacted cement cores. Gel strength tests were carried out on cores at different stages of shut-in time as the presence of air bubbles has the potential to link and re-introduce leakage pathways; however, the results from the tests show the opposite as seen in Table 3.2.

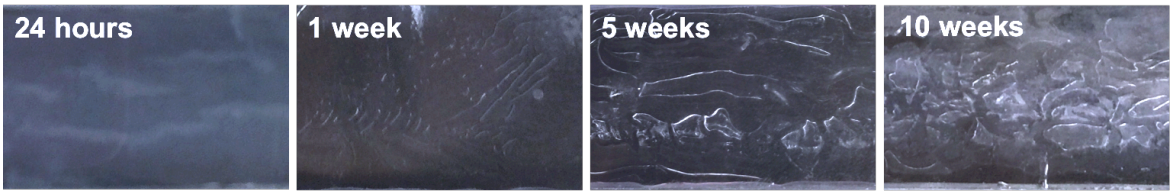

Figure 3.43: The formation of air bubbles one week after polymer placement and dehydration of gel in $Na_5P_3O_{10}$ pre-treated cement fractures over various polymer shut-in times. Holdback pressure gradients from liquid breakthrough tests done on these cores have shown to be higher as the bubbles dehydrate the reacted gel in the fracture. In addition, polymer syneresis was successfully inhibited for over 10 weeks with the use of $Na_5P_3O_{10}$.

Figure 3.43 shows the reacted gel inside a sealed cement fracture actually undergoes a dehydration process that is caused by air bubbles formed from residual chemical reaction. The air bubbles generally start to appear around one week of polymer shut-in and continues to grow over the course of several weeks. As the gel is dehydrated, the polymer concentration is increased locally and the formation of solid-stiff gel stops the growth of the bubbles creating air pockets that cannot be move around easily.

3.6 Effect of Reaction Time

In order to design application, it is necessary to investigate in the optimal reaction time in each procedure. This section discusses the optimization for the pre-treatment time and the estimation for polymer shut-in time to achieve sufficient gel strength and longevity.

3.6.1 Pre-treatment Time

Cores pre-treated with sodium triphosphate ($Na_5P_3O_{10}$) have proven to be effective at inhibiting syneresis and improving gel strength by both visual observation and gel strength tests (Table 3.2) compared to untreated cores (Table 3.3). It was originally

thought that the cement cores pre-treated for longer durations would result in higher gel strength. Some of the earlier cores were all subjected to a standard 24-hour pre-treatment.

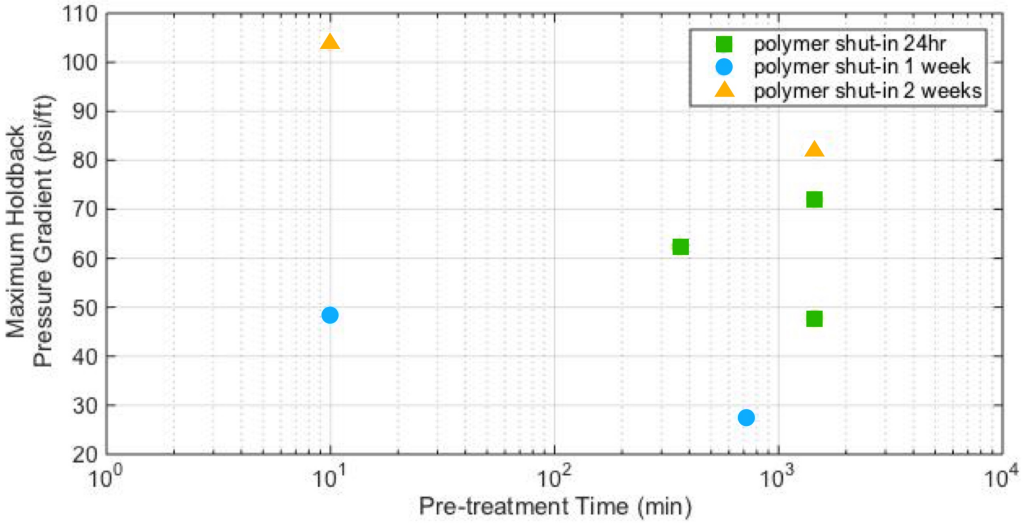

Figure 3.44: Sodium triphosphate ($Na_5P_3O_{10}$) pre-treatment time shows no correlation in the improvement of resulting maximum holdback pressure for subsequent 24-hour, 1-week, and 2-week polymer shut-in.

In order to improve the procedure efficiency, the optimal pre-treatment time was sought. Later experiments were designed to pre-treat cement cores for 12 hours, 6 hours and 10 minutes. Several subsequent gel strength tests were not affected by the longer treatment time, in fact, some results show that pre-treating cores as less as 10 minutes were sufficient to inhibit syneresis. Figure 3.44 are the results from gel strength tests were subjected to the same polymer shut-in times showed that there is perhaps no correlation between pre-treatment time and gel strength. This suggests that $Na_5P_3O_{10}$ pre-treatment reacts fast with the calcium ions close to the cement surface. Quick procedures using shorter $Na_5P_3O_{10}$ pre-treatment time is ideal and allows for faster leak repairs and better-cost efficiency.

3.6.2 Polymer Shut-in Time

The dehydration of gel deposit was observed in many cores that had polymer shut-in time over a course of weeks. Subsequent gel strength test revealed that dehydrated gel poses no harm to gel strength and long-term stability. Most tests have shown that the gel-in-place can develop a much stronger as the gel matures. Two sets of experiments under 10-minute and 24-hour pre-treatment time are compared in Figure 3.45. Both sets of data showed an increase in maximum holdback pressure as polymer shut-in time is increased. This result is very suitable and desirable for sealing purposes since the ultimate goal is for the gel in cement fractures to remain stable and strong long after the injection procedure.

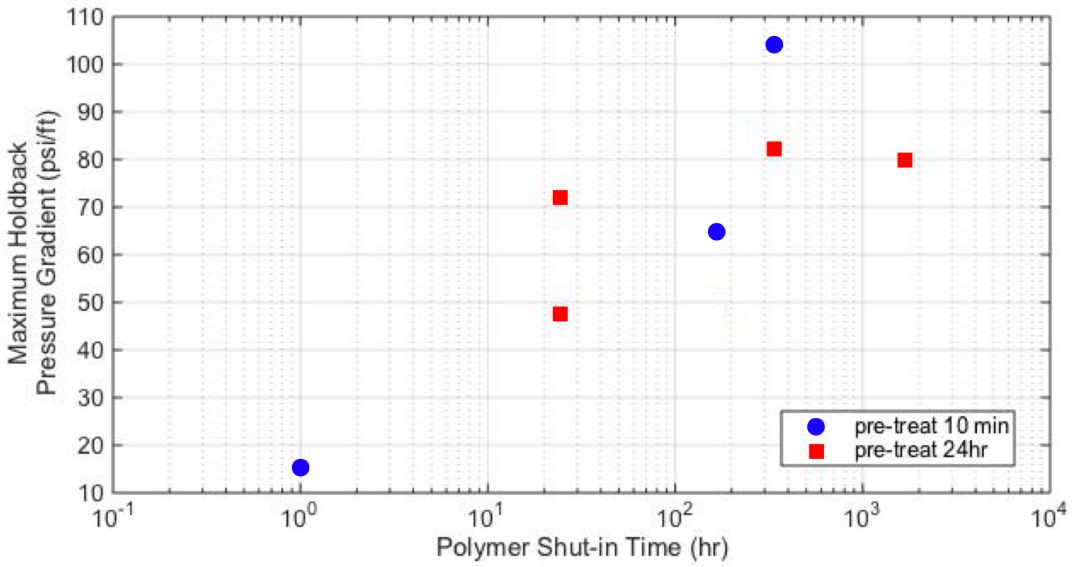

Figure 3.45: Maximum holdback pressure increases as a function of polymer shut-in time for cores pre-treated with STP for 10 minutes (6CF-39, 10FP-40, 10FP-41, 10FP-42) and cores pre-treated with STP for 24 hours (6FP-34, 6CF-36, 10FP-36).

3.7 TECHNICAL FEATURES

- The pH-sensitive polymer dispersion is suitable for repairing leaks in wellbore cement due to its ability in developing considerable yield stress in-situ. Here are some of the key features found in this study:
- Acidic polymer dispersion has little viscosity and can be injected very easily without requiring much pressure.
- Solid to swollen microgel particles are less than 100 nm in size and can be ideal for sealing cement micro-apertures that are potentially hard to penetrate.
- Highly alkaline environment in cement fractures aid the development of yield stress and can prevent the deswelling of microgels.
- Swollen microgel particles can block considerable amount of flow-induced pressure gradient orders of magnitude higher than required for an uprising buoyant CO_2 plume.
- A quick cement pre-treatment using sodium triphosphate can effectively remove calcium ions and inhibit polymer syneresis.
- Polymer thickening and gel deposition is controlled via the reactive transport in cement fractures; therefore, injection rate can be used to time the pH-gelling as polymer solution reaches target zone.
- The maturation of injected gel can provide long-term stability and robust seal for small cement fractures.
- The reaction between formation fluids and gel is assumed to be minor due to limited contact in small fractures.

Chapter 4: Conclusions and Future Work[4]

4.1 CONCLUSIONS

The novel sealant technology uses a pH-triggered mechanism well suited for wellbore cement in which polymer viscosification happens naturally and locally. The alkaline cement causes the increase in polymer pH and contributes to the effective transition of polymer solution into a yield stress gel. Compared to other applications (water shut-off, or conformance control), this wellbore sealant eliminates the need to account for a crosslinking agent and can develop significant gel strength at low relatively low concentrations. The injection of poly(acrylic acid) dispersion into an experimental cement fracture at ambient conditions have shown to successfully react with alkaline cement. Based on the well integrity application, experimental work done in this study can concludes several key findings:

- Although many rheology tests have confirmed the ability of the polymer in developing significant yield stresses, an unexpected reaction occurred when tests were done with cement. Calcium ions contained in the cement leached out into the fracture and reacted with the polymer dispersion to form calcium precipitates. This reaction causes polymer syneresis in which water is expelled from the gel structure

[4] Ho, J.F., Patterson, J.W., Tavassoli, S., Shafiei, M., Balhoff, M.T., Huh, C., Bommer, P.M., and Bryant, S.L., 2015. The use of a pH-triggered polymer gelant to seal cement fractures in wells. Presented at the Society of Petroleum Engineers (SPE) Annual Technical Conference and Exhibition (ATCE), Houston, Texas, U.S.A., 28-30 September. SPE-174940-MS

Contributions: J.F.Ho and J.W.Patterson were involved in the design and performance of laboratory experiments. M.Shafiei was involved in the acquisition of rheological data. J.F.Ho, J.W.Patterson, M.T.Balhoff, C.Huh, P.M.Bommer, and S.L.Bryant were involved in the conception and analysis of the work. J.F.Ho, J.W.Patterson, and S.Tavassoli were involved in the drafting and revision of the manuscript.

causing an irreversible shrinkage in volume. Syneresed gel is shown to be detrimental to the strength and long-term stability of the gel placement.

- The key to avoid the polymer syneresis is to inhibit the calcium ions in cement from reacting with the gel-in-place. It was found that a nano-clay particle known as Laponite could be mixed in polymer dispersion to desensitize ionic attractions and stabilize gel structure. This nano-composite hydrogel application was able to inhibit calcium syneresis and provide at least several months of effective seal; therefore, Laponite is considered to have potential for improving gel longevity.
- Other chelating agents, such as EDTA and sodium triphosphate, were also used as syneresis inhibitors and are found to be effective at removing calcium by binding the ion to its structure before polymer injection. Despite the effectiveness of EDTA during visual observation of syneresis, the rapid reaction of polymer and EDTA during injection often resulted in irregular fluctuations in pressure and failed to maintain good polymer injectivity. In addition, hydrochloric acid was found to have little effect on calcium but have strong reaction with the iron content in cement, which often resulted in the appearance of both calcium syneresis and iron precipitation.
- Among the several syneresis inhibitors tested, it was determined that sodium triphosphate ($Na_5P_3O_{10}$) had the best performance when used as a pre-treatment for cement cores. Cement cores pre-treated with $Na_5P_3O_{10}$ not only inhibited polymer syneresis but also showed good injectivity and promising gel strength. The resulting holdback pressure gradients for pre-treated cores were orders of magnitude higher than the few psi/ft measured for untreated cores and yielded better safety margin for the sealant design based on the 0.2-0.4 psi/ft required for a rising CO_2 leakage.

- In addition, multiple experiments showed that the calcium removal reaction of $Na_5P_3O_{10}$ and cement surface is very quick. This allowed pre-treatment procedures to shortened from 24 hours to as brief as 10 minutes while maintaining desirable gel strengths; hence use of $Na_5P_3O_{10}$ can greatly improve operational efficiency and result in less rig time.
- The development of gel strength is directly related to the static polymer shut-in time and the dehydration of reacted gel, as air bubbles form inside the fracture due to the slow reaction between residual $Na_5P_3O_{10}$ and the polymer. While the polymer gel could holdback as much as 15 psi/ft pressure gradient after only one hour of reaction, the matured/aged gel that has been shut-in for more than 5 weeks have a greater average gel holdback gradient of over 70 psi/ft.
- As expected, performance of the polymer gel system improves significantly as the effective fracture aperture gets smaller. A cement core subjected to high confining pressure to create a small fracture held as much as 3000 psi/ft in pressure gradient when performed under supercritical CO_2 conditions. The result of gel strength was seen to improve exponentially as effective apertures were less than 300 microns, while there was less correlation in larger aperture ranges.
- Contrary to what had been expected, the effect of the type of holdback fluid used is negligible on the initial breakthrough from multiple tests. This is due to the nature of the small fractures where the contact (reaction surface area) of the holdback fluid with reacted gel is extremely small; the fluid breakthrough is mainly caused by the pressure gradient increase. However, once the gel is broken through by pressure, the effect of holdback fluid type was apparent. The acidic (lower pH) fluid that is contacting more surface area of gel was then able to reverse the pH-triggered gelling mechanism and quickly dissolve the gel in place.

- Multiple experiments done in ambient conditions have proven that the pH-sensitive polymer gel system has sufficient gel strength to block 10-100 psi/ft of pressurized fluids. This can conclude the effectiveness of its application for sealing leakage pathways in shallow formation (up to 70°C in subsurface temperature). Furthermore, the result from the CO_2 breakthrough tests in small fracture apertures show that the injected polymer gel can hold 100-1000 psi/ft of pressure gradients under supercritical condition and will be more than sufficient to hold the required few psi/ft for an uprising, buoyant CO_2 plume from a leaky storage well.

4.2 FUTURE WORK

pH-sensitive polymer-gel systems have been well-studied for various enhanced oil recovery applications; however, little is known or discussed about its novel application in enhancing wellbore integrity. More work is necessary to improve the performance and feasibility of this sealant technology. It is highly recommended for future studies to focus on the following:

1. *Pore-scale reactive transport model:* A practical model is needed to capture the pH-trigger mechanism during polymer injection into micro-fractures with respect to time. The time-dependency requires the development of a diffusion model for polymer and a kinetic relationship for gel deposition. Combined with available rheology data and previous corefloods, the model should predict changes in pH and the deposition of gel for a simple fracture geometry. The modeling of some key concentrations is currently underway, but may require additional laboratory experiments for more information.
2. *Lab-scale corefloods at reservoir conditions:* Some corefloods performed in this study have indicated the potential use of the polymer sealant above ambient conditions. However, supercritical CO_2 and many other fluids are likely stored in

deeper formations under high pressure, high temperature conditions. Additional polymer corefloods should be conducted in Hassler coreholders to evaluate the thermal stability (above 70°C), pressure-induced shrinkage, and the aging of gel at higher pressure and temperature settings.

3. *Field-scale applications in shallow wells*: The polymer-gel sealant is presumably ready for field-scale tests in shallow wells. Preparation work should be carried out to thoroughly investigate in leakage conditions and fracture patterns in the cement wellbore. There will most likely be technical risks that require concern; hence, new laboratory experiments should be specifically designed to evaluate those problems.

References

API (American Petroleum Institute), 2011. Specification for cements and materials for well cementing.

Albonico, P., and Lockhart, T.P., 1997. Stabilization of polymer gels against divalent ion-induced syneresis. *Journal of Petroleum Science and Engineering* **18**(1) 61-71.

A-sasutjarit, R., Sirivat, A., and Vayumhasuwan, P., 2005. Viscoelastic properties of Carbopol 940 gels and their relationships to Pirocam diffusion coefficients in gel bases. *Pharmaceutical Research* **22**(12): 2134-2140.

Bachu, S. and Bennion, D.B. 2009. Experimental assessment ofbrine and/or CO2 leakage through well cements at reservoir conditions. *Int.J. Greenhouse Gas Control* **3** (4): 494-501.

Baghdadi, H.A., Sardinha, H., and Bhatia, S.R., 2004. Rheology and gelation kinetics in Laponite dispersions containing poly(ethylene oxide). *Journal of Polymer Science*, Part B: Polymer Physics **43**: 233-240.

Balhoff, M.T., Lake, L.W., Bommer, P.M., Lewis, R.E., Weber, M.J. and Calderin, J.M. 2011. Rheological and yield stress measurements of non-Newtonian fluids using a Marsh Funnel. *Journal of Petroleum Science and Engineering* **77**(3-4): 393-402.

Barnes, H.A. 1999. A brief history of yield stress. *Appl. Rheol.* **9**: 262-266.

Barnes, H.A. 1999. The yield stress—a review—everything flows? J. *Non-Newtonian Fluid Mech.* **81**: 133–178.

Bird, R.B., Armstrong, R.C., and Hassager, O., 1987a. Dynamics of Polymeric Liquids. Volume 1: Fluid Mechanics. Wiley Intersci., New York.

Bird, R.B., Curtiss, C.F., Armstrong, R.C., and Hassager, O., 1987b. Dynamics of Polymeric Liquids. Volume 2: Kinetic Theory. Wiley Intersci., New York.

Brannon-Peppas, L., and Peppas, N.A., 1988. Structural analysis of charged polymeric networks. *Polymer Bulletin* **20**: 285-289.

Bruant, R.G., Guswa, A.J., Celia, M.A., and Peters, C.A., 2002. Peer review: Safe storage of CO2 in deep saline aquifers. *Environmental Science and Technology* **36**A: 240-245.

Bryant, S.L., Rabaioli, M.R., and Lockhart, T.P., 1996. Influence of syneresis on permeability reduction by polymer gels. Presented at the 1996 SPE/DOE Symposium on Improved Oil Recovery held in Tulsa, OK, 21–24 April. SPE-35446.

Choi, S.K., Mee Ermel, Y., Bryant, S.L., Huh, C., and Sharma, M.M., 2006. Transport of a pH-Sensitive Polymer in Porous Media for Novel Mobility-Control Applications. Presented at SPE/DOE Symposium on Improved Oil Recovery, Tulsa, Oklahoma, U.S.A., 22-26 April. SPE-99656.

Cloitre, M., Borrega, R., Monti, F., and Leibler, L. 2003. Structure and flow of polyelectrolyte microgels: from suspensions to glasses. *C. R. Physique* **4**: 221-230.

Davies, R.J., Almond, S., Ward, R.S., Jackson, R.B., Adams, C., Worrall, F., Herringshaw, L.G., Gluyas, J.G., and Whitehead, M.A. 2014. Oil and gas wells and their integrity: Implications for shale and unconventional resource exploitation. *Marine and Petroleum Geology* **56**: 239-254.

Dusseault, M.B., Gray, M.N., and Nawrocki, P.A. 2000. Why Oilwells Leak: Cement Behavior and Long-Term Consequences. Presented at the SPE International Oil and Gas Conference and Exhibition, Beijing, China, 7-10 November. SPE-64733.

EPA (Environmental Protection Agency), 2012. Inventory of U.S. greenhouse gas emmisions and sinks: 1990-2010. U.S. Environmental Protection Agency, Office of Atmospheric Programs, EPA 430-R-12-001.

Goodwin, K.J., 1984. Principles of squeeze cementing. Presented at the Permian Basin Oil & Gas Recovery Conference, Midland, Texas, U.S.A., 8-9 March. SPE-12603.

Guo, H., Aziz, N.I., and Schmidt, L.C., 1993. Rock fracture-toughness determination by the Brazilian test. *Engineering Geology* **33**(3):177-188.

Gutowski, I.A., Lee, D., de Bruyn, J.R., and Frisken, B.J. 2012. Scaling and mesostructure of Carbopol dispersions. *Rheol. Acta* **51**(5): 441-450.

Haraguchi, K., and Li, H.J., 2006. Mechanical Properties and Structure of Polymer–Clay Nanocomposite Gels with High Clay Content. *Macromolecules* **39**(5):1898–1905.

Helfrich, K.R. 1995. Thermo-viscous fingering of flow in a thin gap: a model of magma flow in dikes and fissures. *J. Fluid Mechanics* **305**: 219-238.

Hepple, R., and Benson, S., 2002. Implications of surface seepage on the effectiveness of geologic storage of carbon dioxide as a climate change mitigation strategy. Lawrence Berkley National Laboratory, LBNL-51267.

Huerta, N.J., Bryant, S.L., Strazisar, B.R., Kutchko, B.G., and Conrad, L.C. 2009. The influence of confining stress and chemical alteration on conductive pathways within wellbore cement. *Energy Procedia* **1** (1): 3571-3578.

Huh, C., Choi, S.K., and Sharma, M.M. 2005. A Rheological Model for pH Sensitive Ionic Polymer Solutions for Optimal Mobility. Presented at the SPE Annual Technical Conference and Exhibition held in Dallas, Texas, U.S.A., 9 – 12 October. SPE-96914.

IPCC (Intergovernmental Panel on Climate Change), 2005. IPCC Special Report on Carbon Dioxide Capture and Storage. Prepared by Working Group III of IPCC/WMO/UNEP, Cambridge University Press.

Lalehrokh, F., Bryant, S.L., Huh, C. and Sharma, M.M., 2008. Application of pH-triggered polymers in fractured reservoirs to increase sweep efficiency. Presented at the SPE/DOE Improved Oil Recovery Symposium, Tulsa, Oklahoma, U.S.A., 19 - 23 April. SPE-113800.

Lalehrokh, F., Bryant, S.L., 2009. Application of pH-triggered polymers for deep conformace control in fractured reservoirs. Presented at the SPE Annual Technical Conference and Exhibition, New Orleans, Louisiana, U.S.A., 4 - 7 October. SPE-124773.

Milanovic, D., Smith, L., Intetech Ltd. 2005. A Case History of Sustainable Annulus Pressure in Sour Wells – Prevention, Evaluation and Remediation. Prepared for presentation at the SPE High Pressure/High Temperature Sour Well Design Applied Technology Workshop, The Woodlands, Texas, U.S.A., 17 - 19 May. SPE-97597.

Morris, K.A., Deville, J.P., and Jones, P.J. 2012. Resin-Based Cement Alternatives for Deepwater Well Construction. Presented at the SPE Deepwater Drilling and Completions Conference, Galveston, Texas, U.S.A., 20 – 21 June. SPE-155613.

NRC (National Research Council), 2010. Advancing the science of climate change, report in brief. NRC, The National Academies Press, Washington D.C., U.S.A.

Nordbotten, J.M., Celia, M.A., Bachu, S., and Dahle, H.K., 2005. Semianalytical solutions for leakage through an abandoned well. *Environ. Sci. Technol.* **39**:602-611.

Patterson, J.W. 2014. *Placement and performance of pH-triggered polyacrylic acid in cement fractures*. MS thesis, The University of Texas at Austin, Austin, Texas, U.S.A. (May 2014).

Radonjic, M., Yalcinkaya, T., and C.S., W. 2010. Conductivity of Fractures in Oilwell Cement upon Contact with Sequestered CO2. Presented at the 3rd International Conference on Porous Media and its Applications in Science and Engineering, Montecatini Terme, Italy, 20-25 June.

Ravi, K., Bosma, M., and Gastebled, O. 2002. Improve the Economics of Oil and Gas Wells by Reducing the Risk of Cement Failure. Presented at the IADC/SPE Drilling Conference, Dallas, Texas, U.S.A., 26 - 28 February. SPE-74497.

Roberts, G.P., and Barnes, H.A. 2001. New measurements of the flow curves for carbopol dispersions without slip artifacts. *Rheol. Acta* **40** (5): 499–503.

Salamone, J.C., 1996. Polymeric Materials Encyclopedia, Twelve Volume Set. CRC Press, 23 July 1996.

Schexnailder and Schmidt, 2009. Nanocomposite polymer hydrogels. *Colloid. Polym. Sci*. **287**: 1-11.

Shafiei, M., 2013. Unpublished communications. University of Texas at Austin, Austin, Texas, U.S.A.

Shafiei, M., 2014. Unpublished communications. University of Texas at Austin, Austin, Texas, U.S.A.

Shafiei, M., Bryant, S.L., Balhoff, M.T., Huh, C., and Bonnecaze, R., 2015. Optimizing Hydrogel Formulation for Sealing Cracked Wellbores for CO_2 Storage. *Journal of Rheology* (paper in preparation).

Sydansk, R.D. 1993. Acrylamide-Polymer/Chromium (III)-Carboxylate Gels for Near Wellbore Matrix Treatments. *SPE Advanced Technology Series*, Volume 1, Issue 1. SPE-20214.

Tongwa, P., Nygaard, R., and Baojun, B., 2013. Evaluation of a nanocomposite hydrogel for water shut-off in enhanced oil recovery applications: Design, synthesis, and characterization. *Journal of Applied Polymer Science* **128**(1): 787-794.

Toor, I.A.,1983. Problems in Squeeze Cementing. Presented at the Middle East Oil Technical Conference and Exhibition, Manama, Bahrain, 14-17 March. SPE-11499.

Um, W., Jung, H.B., Kabilan, S., Suh, D.M., and Fernandez, C.A. 2014. Geochemical and Geomechanical Effects on Wellbore Cement Fractures: Data Information for Wellbore Reduced Order Model. Prepared for the U.S. Department of Energy under Contract DE-AC05-76RL01830. Pacific Northwest National Laboratory, January.

van der Tuuk Opedal, N., Torsæter, M., Vrålstad, T., and Cerasi, P. 2013. Potential Leakage Paths along Cement-formation Interfaces in Wellbores; Implications for CO_2 Storage. *Energy Procedia* **51**: 56-64.

Watson, T.L., and Bachu, S. 2007. Evaluation of the Potential for Gas and CO2 Leakage Along Wellbores. Presented at the E&P Environmental and Safety Conference, Galveston, Texas, U.S.A., 5-7 March. SPE-106817.

Watson, T.L., Bachu, S., 2008. Identification of wells with high CO2-leakage potential in mature oil fields developed for CO2-enhanced oil recovery. SPE/DOE Improved Oil Recovery Symposium, Tulsa, Oklahoma, U.S.A., 19-23 April. SPE-112924.

Watson, T.L., and Bachu, S. 2009. Review of failures for wells used for CO2 and acid gas injection in Alberta, Canada. *Energy Procedia* **1**(1): 3531-3537.

Zhang, M., and Bachu, S., 2010. Review of integrity of existing wells in reaction to CO2 geological storage: What do we know? *International Journal of Greenhouse Gas Control* **5**: 826–840.